UNITED STATES, DEPARTMENT OF THE INTERIOR

GEOLOGICAL SURVEY.



# ORIGIN AND CHEMICAL COMPOSITION OF EVAPORITE DEPOSITS

By

George W. Moore





A Dissertation Presented to the Faculty of the
Graduate School of Yale University in
Candidacy for the Degree of Doctor of Philosophy

1960



This report is preliminary and has not been edited or reviewed for conformity with U. S. Geological Survey standards and nomenclature.

## ILLUSTRATIONS

ILLUSTRATIONS--continued

ILLUSTRATIONS--continued

TABLES

# ORIGIN AND CHEMICAL COMPOSITION OF EVAPORITE DEPOSITS

By George W. Moore

## ABSTRACT

A comparative study of marine evaporite deposits forming at the present time along the Pacific coast of central Mexico and evaporite formations of Permian age in West Texas Basin was made in order to determine if the modern sediments provide a basis for understanding environmental conditions that existed during deposition of the older deposits. The field work was supplemented by investigations of artificial evaporite minerals precipitated in the laboratory and by study of the chemical composition of halite rock of different geologic ages.

The environment of deposition of contemporaneous marine salt deposits in Mexico is acidic, is strongly reducing a few centimeters below the surface, and teems with microscopic life. Deposition of salt, unlike that of many other sediments, is not wholly a constructional phenomenon. Permanent deposits result only if a favorable balance exists between deposition in the dry season and dissolution in the wet season.

Evaporite formations chosen for special study in the West Texas Basin are, in ascending order, the Castile, Salado, and Rustler formations, which have a combined thickness of 1200 meters. The Castile formation is largely composed of gypsum rock, the Salado, halite rock, and the Rustler, quartz and carbonate sandstone. The lower part of the Castile formation is bituminous and contains limestone laminae. The Castile and Rustler formations thicken to the south at the expense of salt of the intervening Salado formation.

The clastic rocks of the Rustler formation are interpreted as the deposits of a series of barrier islands north of which halite rock of the Salado was deposited. The salt is believed to have formed in shallow water of uniform density that was mixed by the wind. Where water depth exceeded the depth of wind mixing, density stratification developed, and gypsum was deposited. Dense water of high salinity below the density discontinuity was overlain by less dense, more normally saline water which was derived from the sea to the south. Mixing of the two water layers at their interface diluted the lower layer so as to prevent halite formation, but at the same time the depressed solubility of calcium sulfate in the mixture at the interface caused precipitation of gypsum.

The upper water layer is believed to have supported a flourishing microscopic biota whose remains descended into semisterile brine below where reducing conditions prevailed. This environment generated the bituminous gypsum rock. At times, microcrystalline calcium carbonate of probable biochemical origin formed in the upper layer and settled below to form limestone laminae such as those of the lower part of the Castile formation.

Chemical analyses of Permian and present-day salt were compared with analyses of marine salt as old as Cambrian age to determine if evaporite deposits can contribute information on the geologic history of sea water. The results contain uncertainties that cannot be fully resolved, but they suggest that the ratio between ions in sea water has been approximately constant since Precambrian time. In addition, the abrupt initial appearance of rock salt deposits in Cambrian time suggests that the Precambrian ocean may have been rather dilute, but this apparent relationship also could have been caused by other factors.

# INTRODUCTION

A correct appraisal of the origin of a series of sedimentary rocks is aided by an accurate knowledge of the conditions of deposition of analogous sediments forming today. In the case of relatively rare rocks such as evaporite deposits, whose present-day counterparts have received little previous study, comparison with recent sediments is especially valuable.

The classic view has been that thick sequences of rock salt were formed by the desiccation of sea water in areas separated from the sea by a partial barrier. Most modern investigators have also favored a marine origin for such deposits. The marine hypotheses propose that a rock sequence is deposited which follows the sequence of minerals precipitated from sea water when it is evaporated in the laboratory--namely, carbonate minerals, then sulfate minerals, and finally chloride minerals. This sequence may exist vertically upward in the evaporite basin, and it may extend inward toward the basin from the source of sea water. Where the horizontal sequence is present, the relationship may be employed to compile a paleogeographic reconstruction of conditions at the time of deposition.

In order to evaluate these hypotheses, and apply them if they are valid, modern and ancient deposits of salt were examined in this investigation. A locality on the west coast of Mexico was selected for the study of present-day deposition of evaporite minerals, and Permian evaporite formations of West Texas Basin were chosen as examples of typical evaporite rocks.

The Permian deposits exhibit a complex interfingering relationship between thin beds containing nonclastic carbonate minerals and those composed of halite and gypsum. Redbeds interfinger with the evaporite rocks at the north edge of the basin, and quartz sandstone and bioclastic carbonate rocks interfinger with them near the top of the sequence at the south edge. It was the plan of this investigation to examine these formations, especially their shore facies, and compare them with the evaporite deposits forming today under known conditions.

Owing to the larger role played by chemical processes in the formation of evaporite deposits than in most other sedimentary rocks, special consideration was given to the chemical characteristics of the environments of deposition of the salt deposits, both present-day and Permian. The work on evaporite chemistry suggested that the chemical composition of rock salt might be employed to reflect the chemistry of sea water through geologic time. New analyses of samples of halite rock as old as Cambrian age were obtained and allow an evaluation of the potential of this method in interpreting the geologic history of sea water since Precambrian time.

## Field and Laboratory Work

Field work in the West Texas Basin was done during six months in the summer and winter of 1958-59. Special emphasis was given to the study of outcropping equivalents of the salt-bearing formations which have received scant attention in the past. It was found that distinctive beds can be traced and mapped at the surface even in

units that have been reduced by leaching to a tenth their thickness in the subsurface. Beds of gypsum rock or limestone more than 10 meters thick commonly show only slight tilting and faulting and are easily mapped, even though more than 300 meters of salt has been dissolved from rocks underlying them. Beds 5 meters thick are usually broken and discontinuous but can commonly be traced for great distances. Beds less than 5 meters thick are brecciated and mixed, but, if a formation containing such beds has a distinctive overall lithology, the brecciated zone itself can be mapped on the surface as a lithologic unit.

A result of the present work is a map of the outcrop of the Salado formation of Permian age. The Salado has long been recognized in the subsurface where it is 500 meters thick, but surface mapping had not been attempted before.

The study of present-day evaporite sedimentation was undertaken near Los Mochis, Sinaloa, on the Pacific coast of central Mexico. Approximately two weeks were spent on this work during the rainy season in August 1957 and one week during the dry season in May 1959. Information was obtained on the physical and chemical characteristics of the environment and on facies relations between the clastic and evaporite deposits.

The chemical aspects of salt and gypsum deposition were investigated in laboratory experiments. The studies provided information on metastability of sulfate minerals formed from sea water. Gypsum laid down in natural salt pans is also believed to form under nonequilibrium conditions.

## Acknowledgments

This investigation was done under the direction of Professor John E. Sanders of Yale University. His observations in the field and suggestions on interpretation have added much to the results given in this report. Professors Carl O. Dunbar, M. L. Jensen, John Rodgers, Karl K. Turekian, and Horace Winchell, all of Yale University, have each contributed significantly to the development and presentation of the ideas given here. The contribution of Professor Turekian has been especially large, and the geochemical results were improved by stimulating discussions with him.

The field work in the West Texas Basin was aided by James D. Vine and Roy L. Griggs of the U. S. Geological Survey. I would like to thank them for their help and for the benefit of many discussions. Philip T. Hayes of the Geological Survey collaborated with me on part of the work in Mexico and provided useful information on the Permian rocks of New Mexico.

Chemical analyses of water samples were made in the Albuquerque Laboratory, and of rock samples in the Washington Laboratory, by staff members of the Geological Survey. Development of analytical methods for the rock analyses was supervised by F. S. Grimaldi.

Most of the work was done for the Geological Survey on behalf of the U. S. Atomic Energy Commission. Charles B. Read was supervisor of the project, and the warm personal interest he expressed in the study since its inception has far exceeded that required of his official position. I would like to thank him for this, as well as for his many contributions to the scientific results.

Others who have given advice as experts on specific aspects of the investigation are Charles L. Jones and Steven S. Oriel of the Geological Survey and Charles A. Ross of Yale University.

A grant was received from the Permanent Science Fund of the American Academy of Arts and Sciences to cover the cost of travel and field expenses for part of the work in Mexico.

## PRESENT-DAY SEDIMENTS POTENTIALLY COMPARABLE TO PERMIAN EVAPORITE ROCKS

Graben (1922) has presented a thorough review of salt deposits and has considered the evidence from recent sediments that bears on the origin of fossil salt deposits. It is significant that at the time Graben's monograph was written, and even to the present day, most studies of modern evaporite deposits have been made on the shores of lakes or inland seas rather than of the ocean. Noteworthy exceptions are the recent contributions of Morris and Dickey (1957) on an area in Peru, and Bramkamp and Powers (1955) on a locality on the Persian Gulf.

While much can be learned from studies of the deposits of inland seas such as the classic ones on the Gulf of Kara-Bugaz on the east shore of the Caspian Sea, the deposits there differ in certain important respects from marine evaporite deposits. The water of the Caspian is derived from the Volga River which, in common with other rivers, is rich in sulfate ion. The deposits at Kara-Bugaz, therefore, contain abundant mirabilite (Zenkevich, 1957, p. 894), a sodium sulfate mineral not ordinarily found in marine evaporite deposits.

Other aspects of the chemistry and biota of the two environments also differ to such an extent that sediments formed in lakes and inland seas do not make particularly good models for the interpretation of depositional conditions of ancient marine deposits. Therefore, an area where marine evaporite deposits are forming at the present time was sought for examination.

Marine evaporite deposits are forming at several places in the world today by the dessication of sea water in natural depressions. One

type occurs in shallow lagoons separated from the ocean by sand bars in areas where belts of aridity, resulting from downward moving air in the horse latitudes, cross coastal regions. In Spanish-speaking parts of the Americas, these flat-floored depressions are called salinas. The deposits of salt and gypsum that accumulate in them are the precursors of a type of evaporite rock.

A typical salina, known locally as Pupuri Salina, was selected in Mexico for examination in order to compare its features with possible counterparts in older formations. The origin of the stratigraphic relations, mineralogy, and chemical composition of this deposit can be determined directly because the processes are currently operating. Similar aspects of lithified evaporite deposits therefore might also be ascribed to the same causes.

The area in Mexico was examined during two periods: August 1957 and May 1959. In 1957, during the rainy season, the Salina was mapped by planetable and alidade, and water samples were collected for chemical analysis. The sediments were sampled with a piston-type coring device similar to that described by Ginsburg and Lloyd (1956). Some of the sediments were not adapted to sampling with the coring device and specimens of these were taken from test pits. A preliminary report on the work in 1957 has been given earlier (Moore and Hayes, 1958).

In May 1959, at the end of the winter dry season when salt deposition was proceeding at a maximum rate, the salina was revisted. In the second examination, additional profiles were made of the sediments and further studies were made of the chemical and physical character of water from which the evaporite deposits were being precipitated.

## Setting of Pupuri Salina, Mexico

Pupuri Salina is on the west coast of the mainland of Mexico approximately opposite the south tip of Baja California (fig. 1). It is at lat 25°41' N., long 108°48' W. The salina is on the north shore of Bahia de Chuira and is about 15 kilometers south of Los Mochis in the state of Sinaloa. The area may be reached by road from Los Mochis or by boat from the fishing village of Topolobampo, which is about 15 kilometers to the southwest.

The salina is a kilometer in diameter and is one of many such natural evaporating pans on the shores of the Gulf of California. In places, as at Yavaros 130 kilometers to the north, the salinas have been cultured and are important producers of salt for the region. To the south, however, the rainfall increases until ultimately the desert gives way to rain forest.

The area is on the coast of a fertile plain that extends to the Gulf of California from the mountains composed of volcanic and metamorphic rock on the east. It is underlain by interbedded flood plain and marine sediments of late Cenozoic age. In places hills of andesite of probable Oligocene age project through the sediments of the plain and interrupt the level topography. The village of Topolobampo is built on the slopes of one of these andesite hills.

The plain is traversed by regularly spaced rivers which drain the high mountains to the east and provide water for an extensive irrigation project on the plain. Sediments from Rio Fuerte, 30 kilometers north, and from Rio Sinaloa, 60 kilometers south, are actively but irregularly prograding the coastline so as to leave embayments similar to Bahia de Chuira and Pupuri Salina.

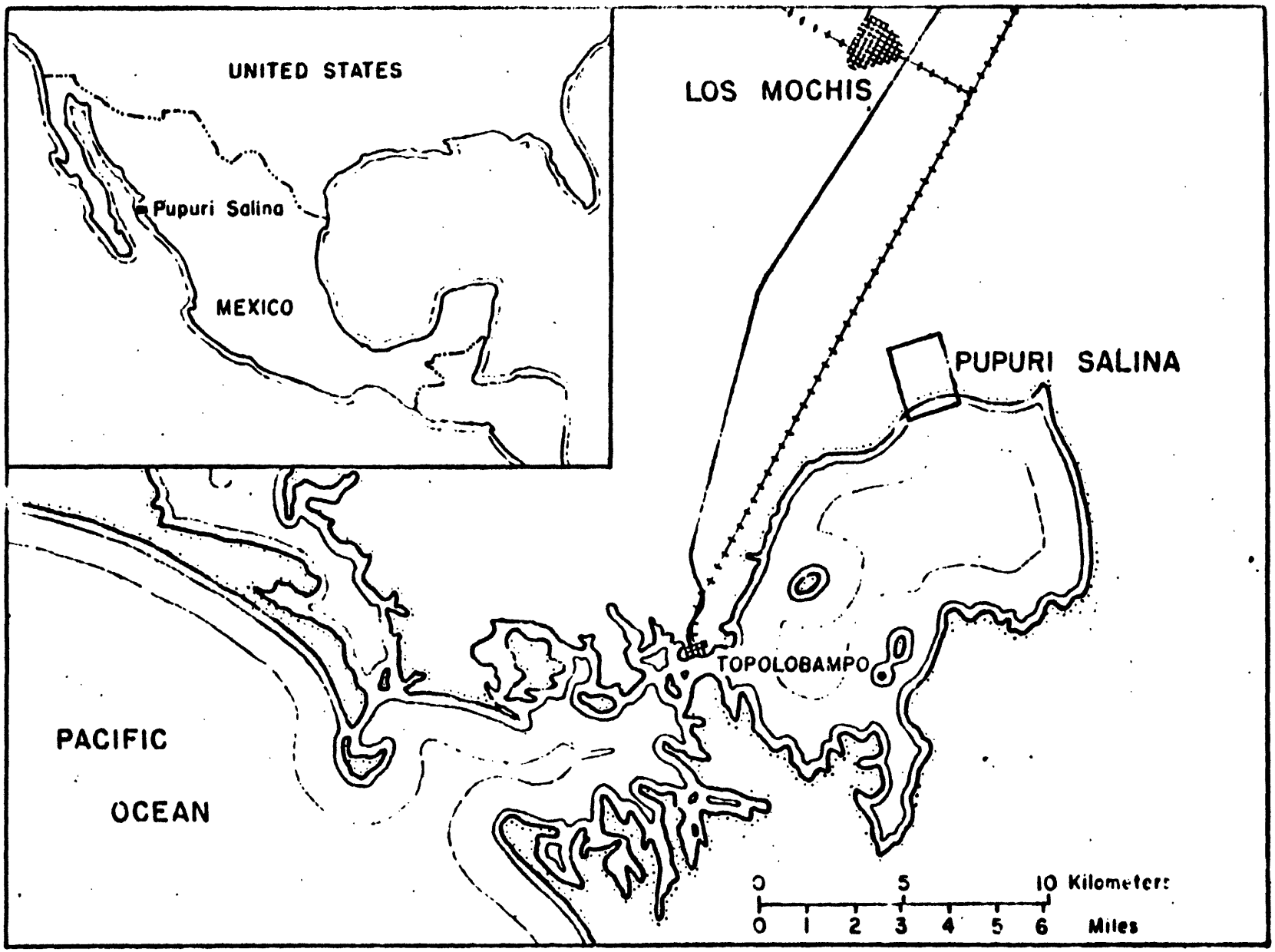


Figure 1.--Index map showing the location of Pupuri Salina, Sinaloa, Mexico.

Bahia de Ohuira is a shallow bay about 10 kilometers in diameter which has an outlet to the sea only a kilometer wide. It contained 4.33 percent salt in August 1957 in contrast with a normal of 3.45 percent for the Pacific Ocean.

The salina is separated from the bay by a barrier beach about 25 meters wide (figs. 2 and 3). On the west side, behind the fronting beach, two older bars or spits remain as records of an earlier stage in the history of the salina. A tidal inlet in the middle that is approximately 600 meters long conducts water from the bay into the salina at high tide and drains the area at low tide (fig. 4). The inlet, which is 10 meters wide at its mouth, is flanked by natural levees about 20 meters wide standing half a meter above the general level of the salina. These levees are interrupted in places by tributary inlets which extend laterally from the main inlet. Most of the salina is a mud flat which is precisely level, to the accuracy of the surveying method used. On the mud flat and on slightly higher ground, evaporite deposits are being laid down, and beyond the limit of the area which is inundated at high tide, a border land stands approximately 5 meters above the level of the salina.

The average temperature of the region is 24°C, ranging from 19°C in January to 30°C in July. The average annual rainfall is 25 centimeters, most of which falls in the summer and autumn so that the driest months are between January and May.

The Gulf of California is characterized by irregular semidiurnal tides. The maximum annual tide range at Pupuri Salina is 1.9 meters.

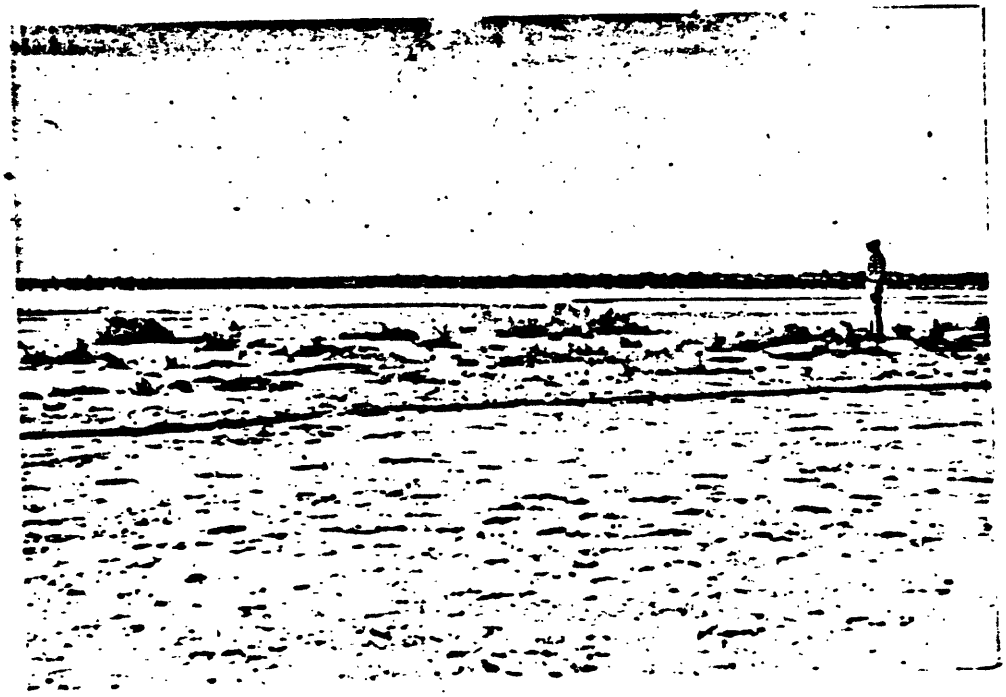

Figure 3.--The barrier beach at Pupuri Salina viewed from the bay. The white band in the distance is the salt deposit.

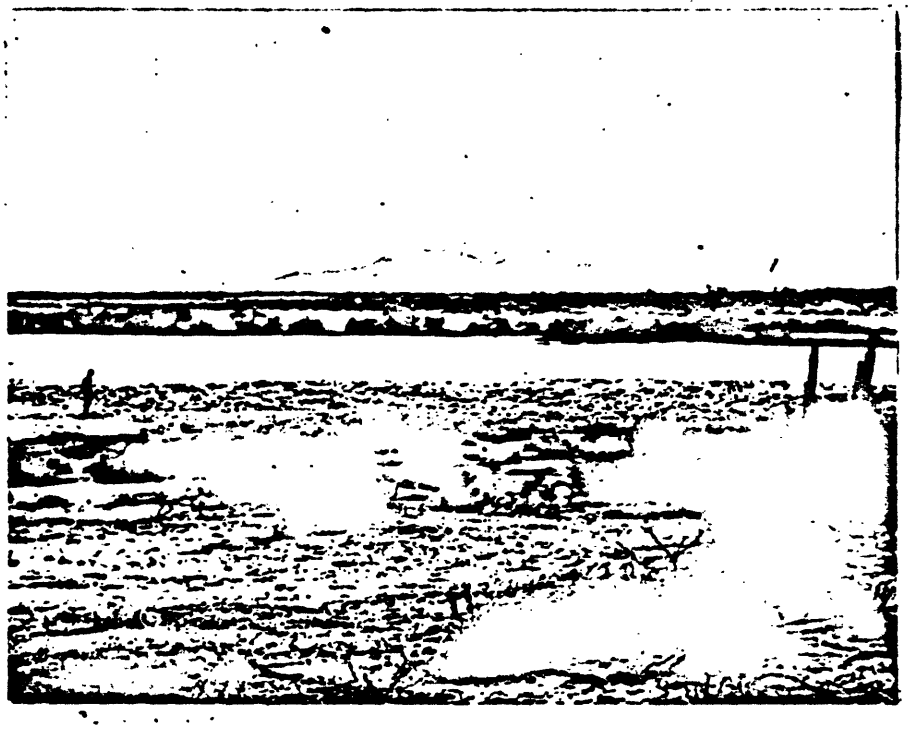

Figure 4.--Margin of Pupuri Salina. The man is standing in the area of thick gypsum at the shore; the line of mangrove in the middle distance marks the tidal inlet; and the hills on the horizon are andesitic volcanic rocks.

The floor of the open bay fronting the salina supports a dense growth of marine grass on which live small turreted snails, Cerithidea mazatlanica Carpenter. A line of mangrove, which is about 30 meters from shore at high tide, fringes the east side of the salina. The trees average 5 meters in height, and the sheltered area between the mangrove and the shore is the habitat of several species of birds, the most beautiful of which is the Roseate Spoonbill. Mangrove also extends along the bank of the tidal inlet, but the trees become progressively smaller until at the upper end of the inlet they are less than a meter high (fig. 5). Salicornia grows on the crest of the natural levee and along the fronting barrier beach. Several species of borrowing crabs live among the pneumatophores of the mangrove along the inlet and on higher ground.

The broad mud flat appears to be without life, but the floors of pools in gypsum near the shore are covered with small spherical colonies of green algae several millimeters in diameter. A typical Lower Sonoran desert flora lives beyond the limit of the relatively barren parts of the salina. It is characterized by cholla, pitaya, and other cacti, as well as by acacia.

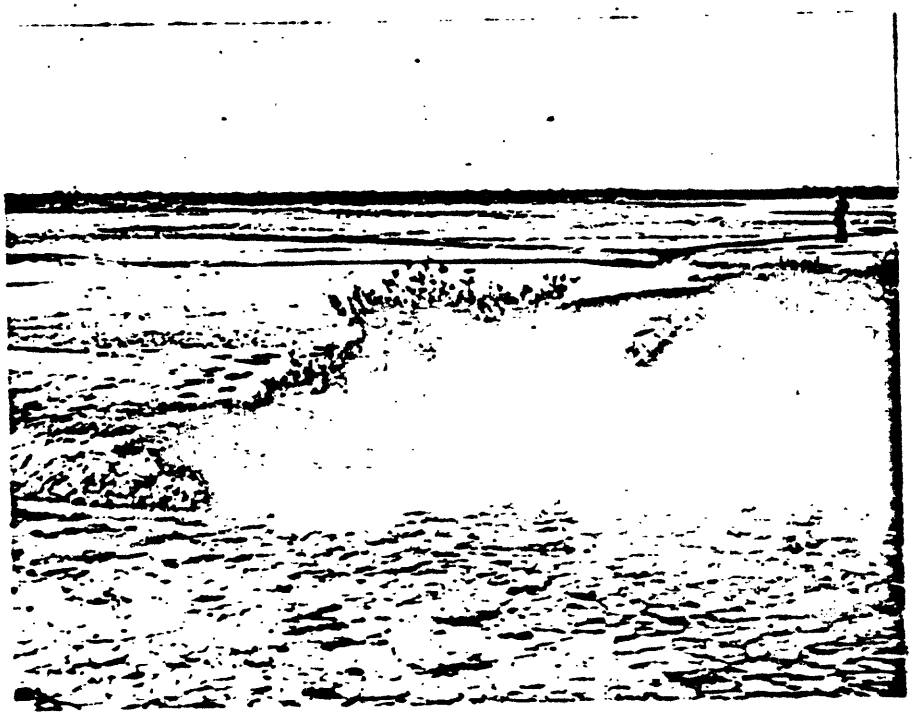

Figure 5.--Upper end of main tidal inlet showing small mangrove and the surface of the mud flat during the wet season.

## Deposits

A major difference existed in the distribution of evaporite deposits at Pupuri Salina during the rainy season in August 1957 and during the dry season in May 1959. During the rainy season, the evaporite deposits were restricted to an area near the shore of the salina and consisted of a permanent layer of gypsum about 10 centimeters thick with which was associated some ephemeral halite crystals (fig. 6). During the dry season, the principal part of the salina, that between the permanent gypsum layer near the shore and the natural levee, was covered by a layer of salt approximately 2 centimeters thick (fig. 7 and 8). A discontinuous layer of gypsum only a millimeter thick coated the mud in the middle of the salina at the heads of tributary inlets. The detailed map and profile (fig. 2 and 9) were prepared in the rainy season so they show the distribution of the permanent deposits.

Dark-gray sandy mud containing some plant remains is being laid down on the floor of Bahia de Obuira. The sediment of the bay passes abruptly into material from the bar which is composed almost wholly of the shells of snails similar to those living on the floor of the bay (fig. 10). It is possible to observe the mechanism by which the bar is being built: The waves bring pieces of grass, to which living snails are clinging, high onto the bar; here the snails die in the heat of the sun; their fleshy parts decay along with the grass; and the shells are added to the growing accumulation.

Several test pits were dug across the bar on the east side of the salina (fig. 11). They show that the bar has occupied its present position

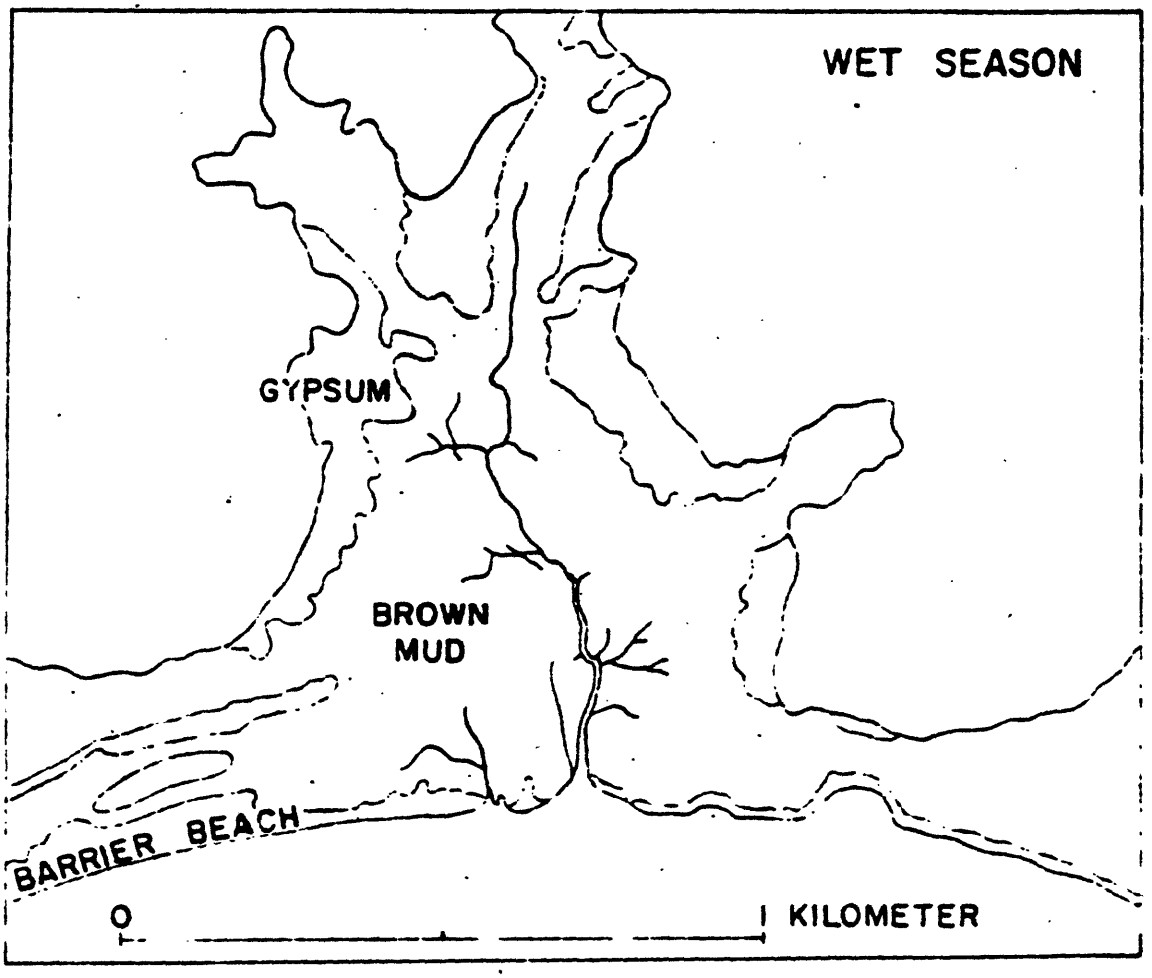


Figure [illegible].--Paper Delta during the wet season in August 1957.

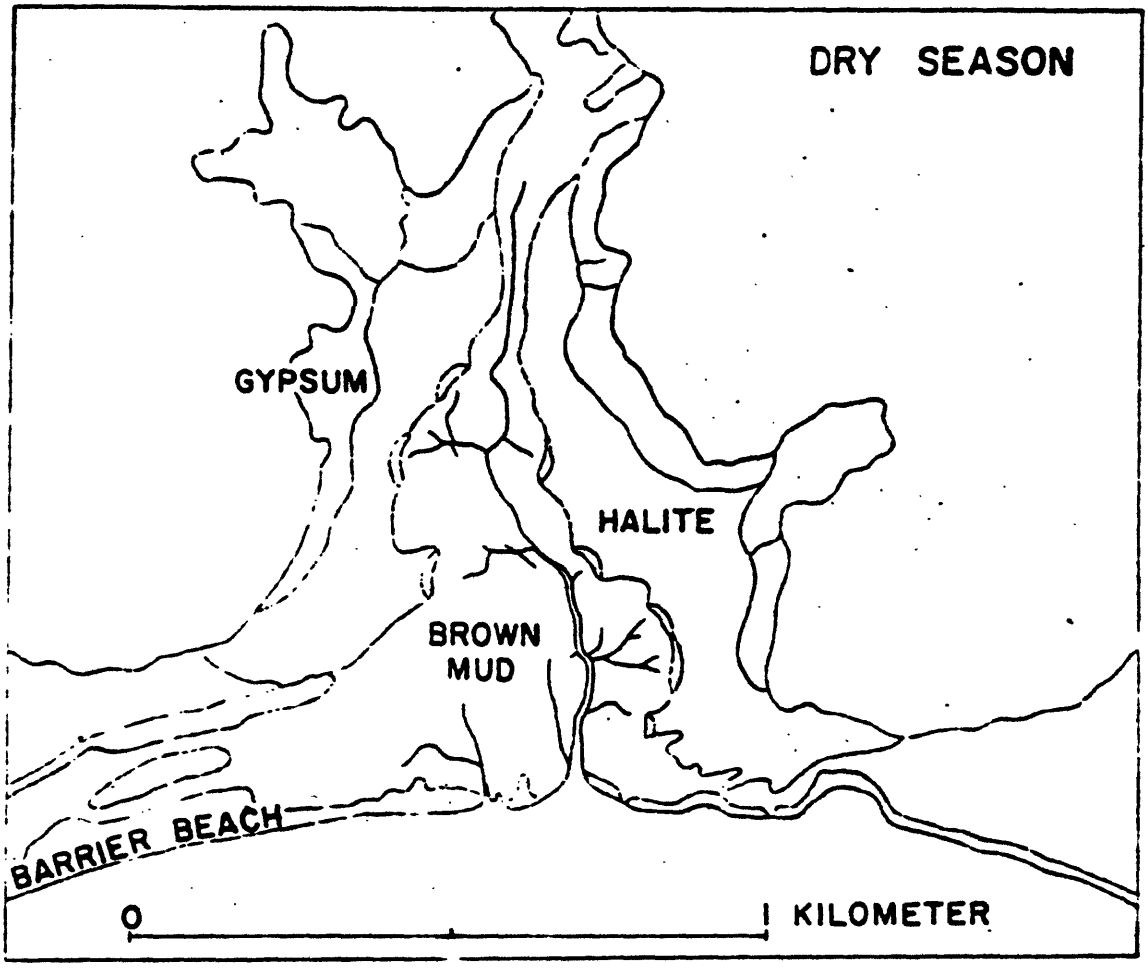


Figure 7.--Pupuri Salina during the dry season in May 1959.

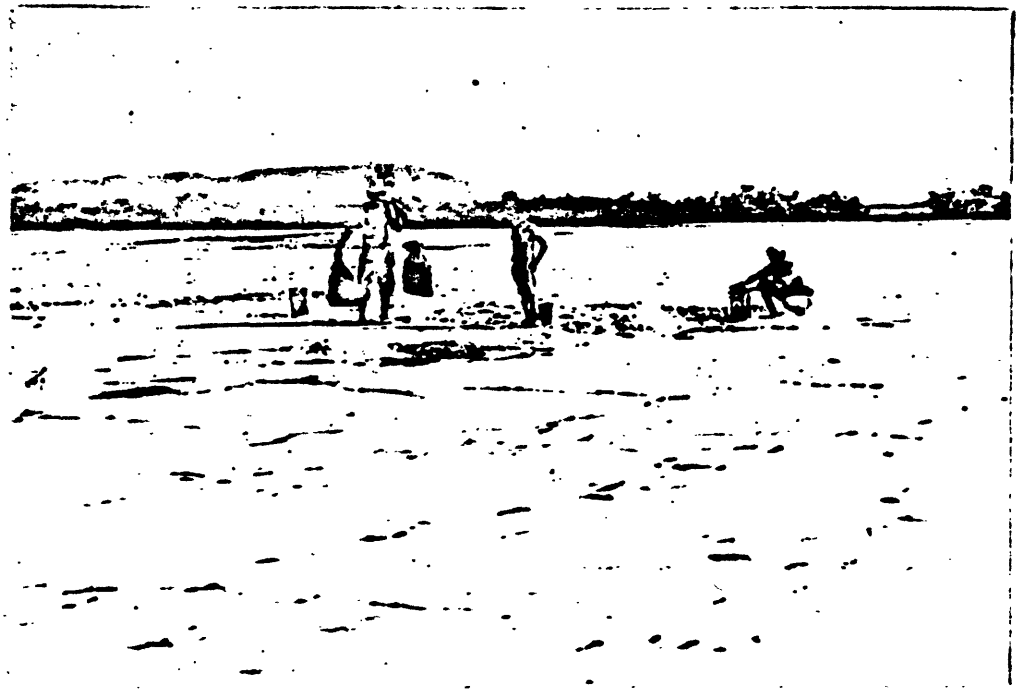

Figure 8. Harvesting salt from Pupuri Salina in May. The mangrove in the background marks the tidal inlet.

Figure 10. Shells of Cerithidea mazatlanica Carpenter which make up the barrier beach at Pupuri Salina.

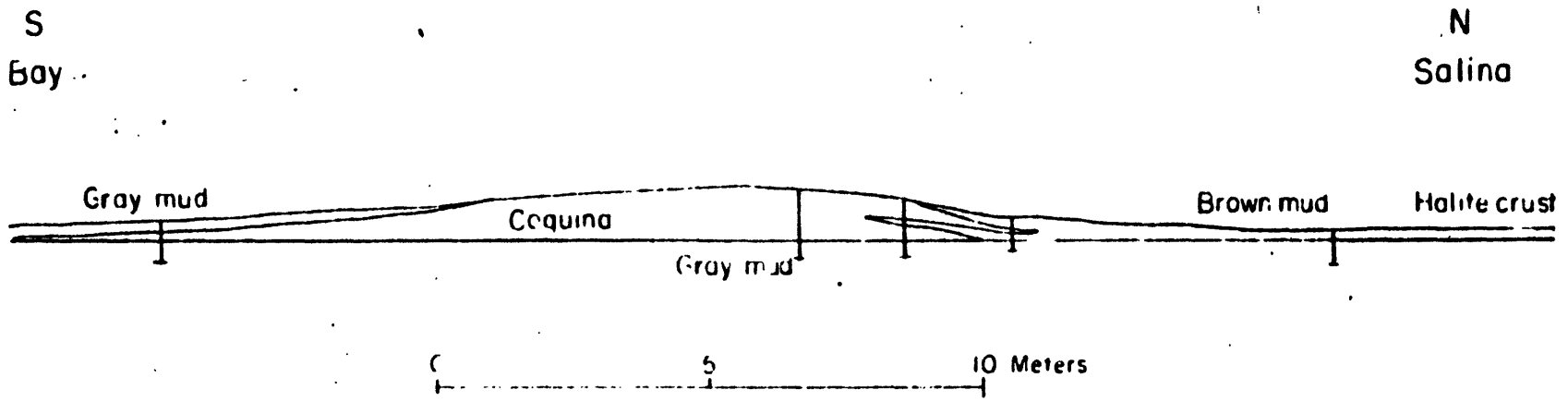


Figure 11.--Section across the barrier beach at the east side of Pupuri Salina. True vertical scale.

since the establishment of the salina, and it has always been a coquina principally composed of snail shells. The bar deposit is 70 centimeters thick and interfingers abruptly with brown mud in the salina and gray mud in the bay. The coquina and brown mud are both underlain by gray mud which evidently antedates establishment of the salina.

The natural levee deposit is composed of dark yellowish brown sandy mud. This mud has a pelletal structure as a result of the activity of burrowing organisms. The pellets average about half a millimeter in diameter.

During the rainy season, the broad flat area between the gypsum deposits near the shore and the tidal inlet is underlain by pale-brown mud (fig. 9). This mud is laminated; individual layers are about half a millimeter thick. In the morning, still moist from the last high tide, the mud flat is very difficult to traverse; by late afternoon, however, the flat has become hard and firm, and mud cracks a centimeter wide separate polygons which are about 10 centimeters in diameter.

The sediment deposited on the mud flat is evidently carried into the area by rain wash from higher ground which borders the salina. Torrential desert rains in August 1957 were seen to deposit thin films of mud on the normally white gypsum deposits at the margin of the salina. After the next high tide had covered the area, however, the layer of mud had disappeared from the gypsum and evidently had moved out onto the flat. This seems to be the process by which the brown laminated mud of the mud flat is laid down.

Around the margin of the salina, gypsum occurs in a discontinous layer about 100 meters wide and as much as 10 centimeters thick. The

gypsum layer is missing in places where arroyos intersect the margin of the salina. In these areas the material balance is probably such that the rate of solution by fresh-water runoff exceeds the rate of deposition.

The surface of the gypsum at the margin of the salina closely resembles cave travertine and is divided into polygonal flat areas about 2 meters in diameter which are separated from each other by ridges 10 centimeters high (fig. 12). These ridges are composed of the buckled upturned edges of the gypsum layer. Similar compression ridges occur in other marine evaporite deposits (Morris and Dickey, 1957, p. 2469), and they also characterize continental deposits such as those at Death Valley, California (Gale, 1914, p. 407).

Clarke and Teichert (1946) have suggested that somewhat smaller wrinkles occurring in a salt lake in Western Australia may have formed by the expansion of growing algae. Algae do not seem abundant enough in the gypsum at Pupuri Salina to be the cause of the compression, though a green algal discoloration approximately a millimeter thick occurs just below the surface of the gypsum layer.

Another possible mechanism that should be considered in explaining the ridges is expansion due to the hydration of anhydrous or partly hydrous minerals. Anhydrite ($CaSO_4$) and bassanite ($2CaSO_4.H_2O$) might be expected to exert a force during their alteration into gypsum ($CaSO_4.2H_2O$), but X-ray and optical studies have not revealed either of these minerals in the deposits.

Expansion and contraction due to heating and cooling are considered by many to be the causes of patterned ground in ice-cemented soil in arctic regions (Washburn, 1956, p. 851), and this explanation also seems

Figure 12. Compression ridges on the surface of gypsum. The notebook case is 15 centimeters wide.

applicable to the present case. The following origin is here suggested for the ridges (fig. 13); (1), when the gypsum layer becomes warm it expands, buckles upward slightly, and cracks under tension at the zones of curvature; (2), crystal growth heals these cracks, especially those opening toward the lower surface which is bathed in brine; (3) subsequent cyclic expansion, healing, and contraction force the ridge higher until its crest ruptures and the lower surfaces of its two isoclinal limbs come into contact.

The coefficient of linear thermal expansion of gypsum is $24 \cdot 10^{-6}$ $^{o}C^{-1}$ (Dane, 1942)[1/]. Assuming a polygon diameter of 2 meters

---

1/ The coefficient $24 \cdot 10^{-6}$ $^{o}C^{-1}$ is derived from Danes's value of 0.58 percent for volumetric expansion when gypsum is raised from 20° to 100°C. The linear thermal expansion of gypsum ranges from $1 \cdot 10^{-6}$ to $43 \cdot 10^{-6}$ $^{o}C^{-1}$ depending on orientation with respect to the crystallographic axes. The crystals in the bed at Pupuri Salina commonly have a preferred orientation in which the c axis is approximately 40° from the vertical. (The longest dimension and therefore the direction of most rapid growth is vertical, evidently because crowding of crystals defeated those not so favorably oriented) The average horizontal coefficient of thermal expansion for crystals in this position is $22 \cdot 10^{-6}$ $^{o}C^{-1}$, approximately that used above.

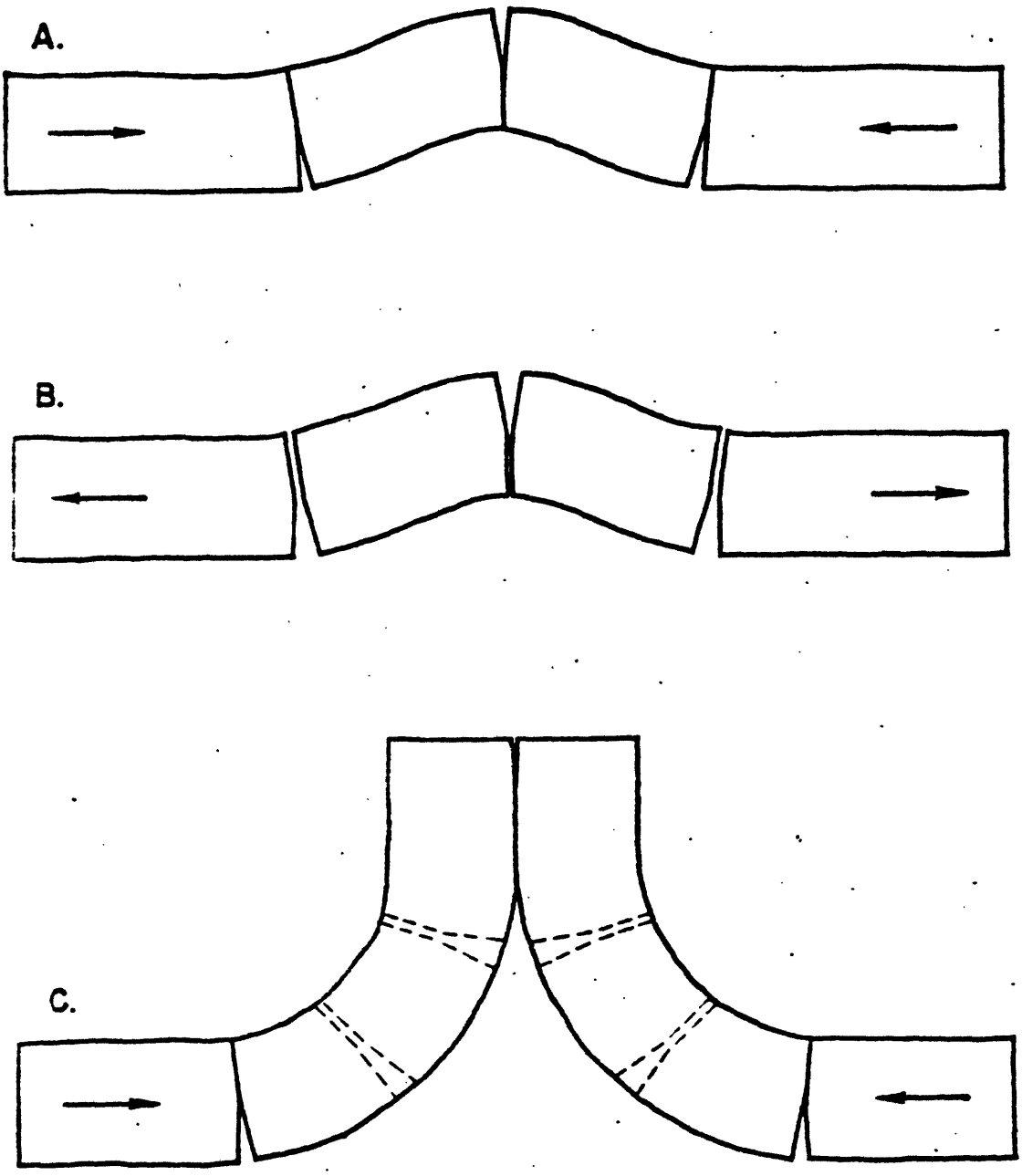


Figure 13.--Growth of compression ridges in gypsum: (A) thermal expansion causes buckling and fracturing; (B) contraction opens cracks which are then healed by crystal growth; and (C) many repetitions of the cycle produce ridges.

and a daily temperature range of 15°C, the expansion affecting each limb of a ridge is 0.36 millimeters. Therefore, the minimum age for a ridge 10 centimeters high is 280 days.

The force of crystal growth has been evoked by Mortensen (1930, p. 487) to explain similar ridges in sodium chloride layers associated with niter deposits in Chile. Morris and Dickey (1957, p. 2469) have also applied it to warped layers of marine gypsum. The force exerted by the growing crystals cannot be separated in the scheme presented above from that caused by thermal expansion, for the formation of gypsum is known to cause rock failure in mines and caves that lack temperature variation; but, if this force is important in the salina, it is considered to be accessory to that caused by the heat of the sun.

The flat areas of gypsum between the ridges are interrupted in places by small pools 10 or 20 centimeters in diameter which commonly extend entirely through the evaporite deposit (fig. 14). These pools are filled with brine, and botryoidal accretions of gypsum occur around the edges and on small islands in the pools.

The flat areas of gypsum are not completely smooth; small mounds or knobs several centimeters in diameter stud their surfaces. In places the weight of a step will cause water to be expelled from the smaller pools and also from small apertures at the summits of these mounds. Evidently during flood tide, water moves under the gypsum layer and issues from these orifices, which are perhaps half a millimeter in diameter, and thereby builds the mounds. Fossilized

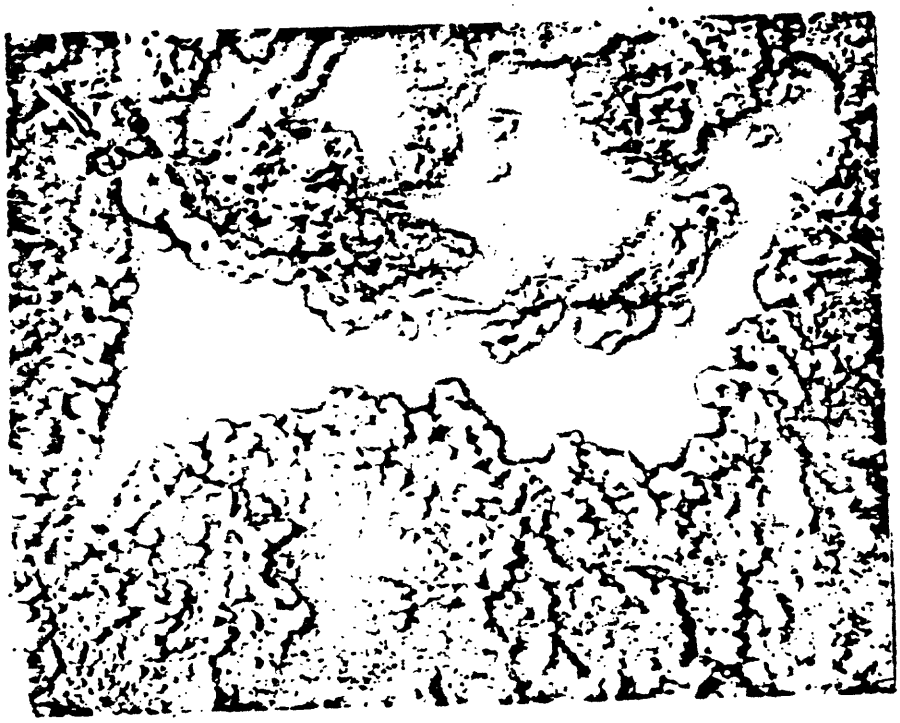

Figure 14. A pool 10 centimeters wide on gypsum. Spherical colonies of green algae live on the floor of the pool.

mounds, also containing the orifices, occur at several horizons in the gypsum.

At its margin toward the tidal inlet, the gypsum layer is underlain by and intertongues with a deposit of black mud which underlies the salt when it is present in the dry season. This black mud is similar to the brown mud except that it contains hydrous iron sulfide (probably hydrotroilite, $FeS \cdot nH_2O$) and fragments of organic material. The sulfide coloring agent is unstable, and specimens taken from the deposit lose their black color and become moderate brown after several months of storage. The black mud also contains minute crystals of pyrite. Volkov and Ostroumov (1957) have described similar deposits of hydrotroilite and pyrite in the sediments of the Black Sea.

The spherical colonies of green algae, when dissected, show the following internal characteristics: an outer layer of living algae, perhaps a millimeter thick, is underlain by a grayish red purple layer which may be colored by bacteria, and this in turn is underlain by black organic material which extends to the center of the sphere.

At the landward edge of the salina, the gypsum layer intertongues with sand which is derived by erosion from older deposits bordering the salina. The surface of the sand is covered by an efflorescent mixture of gypsum and halite.

At the time of the examination in August 1957, no continuous layer of salt existed anywhere in the salina. In late afternoon, however, floating hopper-shaped crystals of halite formed on the pools (fig. 15); by sundown these had grown together and formed a crust over

Figure 15. Hopper-shaped crystals of halite floating on a pool in gypsum X2.

all the exposed areas of brine. With the coming of the next high tide, however, the salt was dissolved again so that only gypsum remained as a permanent deposit.

In May 1959 a crust of halite covered most of the area of brown mud in the salina. The surface of the brine was approximately coincident with the top of the crust. On most days several groups of local inhabitants worked in the salina harvesting the salt for domestic use. Pieces of the crust about 2 centimeters thick were carefully lifted by hand to avoid admixed mud and were piled to drain. Later the salt was carried to shore and sacked. With the coming of the rainy season later in the summer, however, this halite layer is destroyed. The transitory nature of the salt deposits is significant because it indicates that the absence of salt in some gypsum deposits maybe due to its contemporaneous resolution rather than to nondeposition.

The presence of the main layer of gypsum in a position shoreward from the halite deposit raises a question as to the cause of the thick gypsum deposit. A thin crust of gypsum near the tidal inlet in a position that is in harmony with the relative solubility of gypsum and halite implies that the thick deposit at the margin of the salina forms under special conditions. Some of the pools nearest the shore in the gypsum never reach saturation with respect to sodium chloride suggesting that there may be continuous flow of fresh ground water to them from the shore. This water probably contains calcium ion derived from the solution of fossils in older deposits around the salina. In California, gypsum is produced commercially by the mixing

of lime with bittern from artificial salt concentrating ponds (Ver Plank, 1958, p. 115), and the same process may occur naturally at Pupuri Salina to produce the marginal gypsum.

A problem arises as to whether this type of gypsum deposit should be expected as an important constituent of ancient evaporite deposits. Since the calcium ion is thought to be derived from solution of mollusk shells in older deposits around the margin of the salina, the supply will end when the evaporite deposits become thicker. Such gypsum deposits, therefore, probably would not extend far into marine evaporite deposits and would be associated with a redbed shore facies.

Older uplifted deposits of Pleistocene age crop out around the margin of the salina. They are composed predominantly of quartz sandstone and siltstone containing corroded mollusk shells. A 2-meter bed containing abundant clam shells is prominent on the slopes around the salina, and it is separately mapped on figure 2. The eroded surface of these rocks forms the substratum over which the evaporite deposits and associated sediments are being laid down at the margin of the salina.

## Chemical characteristics

On August 13, 1957, water samples were taken for analysis from various environments in and near Pupuri Salina. High tide for the day was 11:39 a.m., and low tide was at 4:56 p.m. All the samples in the salina were taken between 1:45 p.m. and 3:20 p.m., at a time when the tide water was draining away from the salina. A sample was also taken during flood tide at 9:00 a.m. in Bahia de Chuira, 2 kilometers from shore.

The analyses of these water samples are given in table 1. The localities of the samples are: the open bay; the mouth of the tidal inlet; the upper end of the tidal inlet at the limit of the mangrove-covered natural levee; the edge of the thick gypsum deposit where the water was saturated with sodium chloride; and an isolated pool in the gypsum deposit which was not saturated with sodium chloride.

The soluble ions of sodium, potassium, magnesium, boron, and fluorine, tend to increase slowly with chlorine from the open bay to the upper end of the tidal inlet and then to increase abruptly with respect to chlorine at the locality where sodium chloride is being deposited. The minor differences in concentration along the tidal inlet may reflect temporal rather than spatial differences because the samples were collected over a period of several hours; nevertheless, the values for the samples at the edge of the gypsum are the concentrations that exist during salt deposition at this time of the year.

The pH of the samples is compared on figure 16 with the concentrations of calcium, chloride, and bicarbonate in the first four samples in which the salinity progressively increases. Calcium increases uniformly toward the shore while bicarbonate remains nearly constant. Possibly bicarbonate is removed from solution by algae, or carbon dioxide might be driven off by high temperature with the remaining carbonate held in solution by acids of other types, such as humic acids or acid formed from hydrogen sulfide. The lower pH at the edge of the gypsum (7.0) than in the pool in the gypsum (7.8) supports the concept that hydrogen sulfide may play a part

Table 1.--Chemical analyses and related physical measurements of water in or near Laguna Salina, Sinaloa, Mexico

(Analysis in parts per million, except as indicated.)

| Source | Bahia de Chuira 2 km from shore | Mouth of tidal inlet | Upper end of tidal inlet | Edge of gypsum | Pool in gypsum |
|---|---|---|---|---|---|
| Silica ($SiO_2$) | 2.2 | 4.0 | 12 | 1.9 | 3.4 |
| Iron (Fe) | 0.03 | 0.08 | 0.21 | 0.03 | 0.02 |
| Calcium (Ca) | 506 | 679 | 1170 | 1950 | 2290 |
| Magnesium (Mg) | 1510 | 1600 | 1960 | 12900 | 6130 |
| Sodium (Na) | 12500 | 12800 | 13100 | 78900 | 43500 |
| Potassium (K) | 422 | 385 | 255 | 2500 | 1140 |
| Bicarbonate($HCO_3$) | 136 | 156 | 152 | 190 | 121 |
| Sulfate ($SO_4$) | 3130 | 3340 | 2160 | 7110 | 6850 |
| Chloride (Cl) | 22400 | 23300 | 26400 | 162000 | 86500 |
| Fluoride (F) | 2.2 | 2.3 | 2.7 | 12 | 6.9 |
| Boron (B) | 11 | 9.4 | 8.4 | 40 | 20 |
| Dissolved solids | 43300 | 43400 | 48100 | 286000 | 142000 |
| Hardness as $CaCO_3$ | | | | | |
| Total | 7470 | 8270 | 10900 | 57900 | 30900 |
| Noncarbonate | 7360 | 8140 | 10700 | 57800 | 30800 |
| Percent sodium | 77 | 76 | 72 | 74 | 75 |
| Specific conductance (micromhos at 25°C) | 54200 | 56000 | 60900 | 176000 | 142000 |
| pH | 7.1 | 7.7 | 7.5 | 7.0 | 7.8 |
| Temperature (°C) | 31.6 | 33.4 | 34.9 | 39.8 | 37.1 |
| Hour of collection | 9:00 a.m. | 1:45 p.m. | 2:25 p.m. | 2:45 p.m. | 3:20 p.m. |
| Density (g/cc) | 1.028 | 1.029 | 1.032 | 1.209 | 1.110 |
| Tons per acre-foot | 55.2 | 57.4 | 61.3 | 362 | 200 |

H. H. Koester, analyst

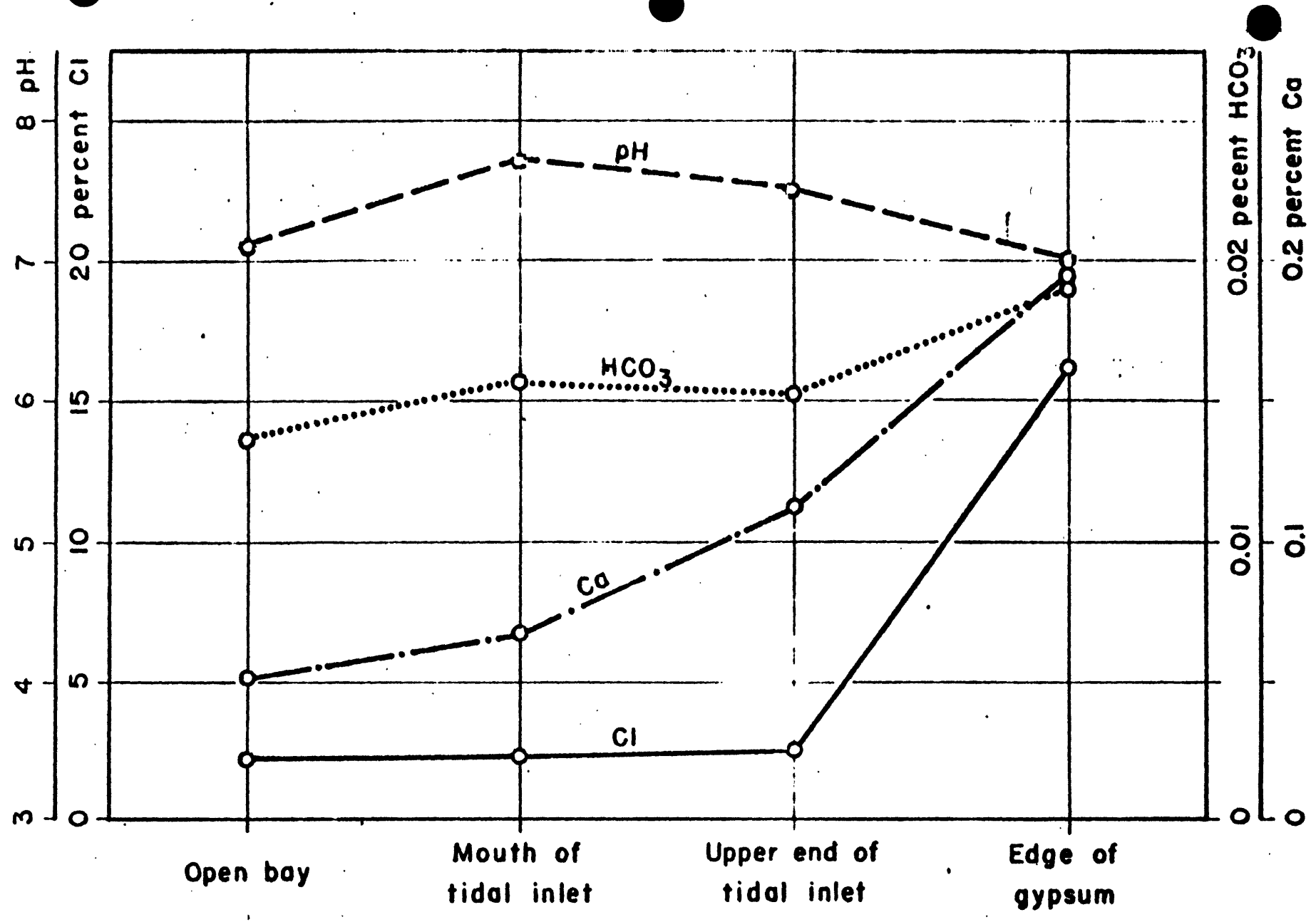


Figure 16.--Change in calcium, chloride, and bicarbonate concentration and change in pH during salt deposition.

because hydrous iron sulfide is abundant at the edge of the gypsum.

In figure 17 the concentrations of iron, silica, and sulfate are compared with chloride in the same four samples considered in figure 15. Iron increases abruptly in the tidal inlet, but this increase may represent particulate iron in clay particles, because the tide was ebbing rapidly when these samples were taken, and silica shows a coordinate increase. Of greater significance is the low concentration of iron at the edge of the gypsum. The iron concentration is as low there as in the open bay, even though the water has been concentrated to a seventh its volume as indicated by the chloride analyses. Active deposition of iron (probably as hydrous sulfide) was evidently taking place at the time of the sampling.

On May 5-6, 1959, temperature measurements and electrometric measurements of pH and redox potential were made of brine from which halite was being deposited. The values were recorded every 3 hours during a 24-hour period (fig. 18). Temperature of the samples ranged from 16.5°C at 5:30 a.m. to 32.5°C at 2:30 p.m. In places where the salt had completely crusted over the surface of the brine so that evaporation was reduced, however, temperature as high as 39.0°C was attained.

The water was continuously acidic, and at night especially low values of pH were recorded. The pH ranged from 6.3 at 2:30 a.m. to 7.0 at 11:30 a.m. If the acidity were caused by carbonic acid, this pH fluctuation would be compatible with the depletion of carbon dioxide during the day by photosynthesis causing higher pH values then than at night. But no organisms were visible in the brine, and

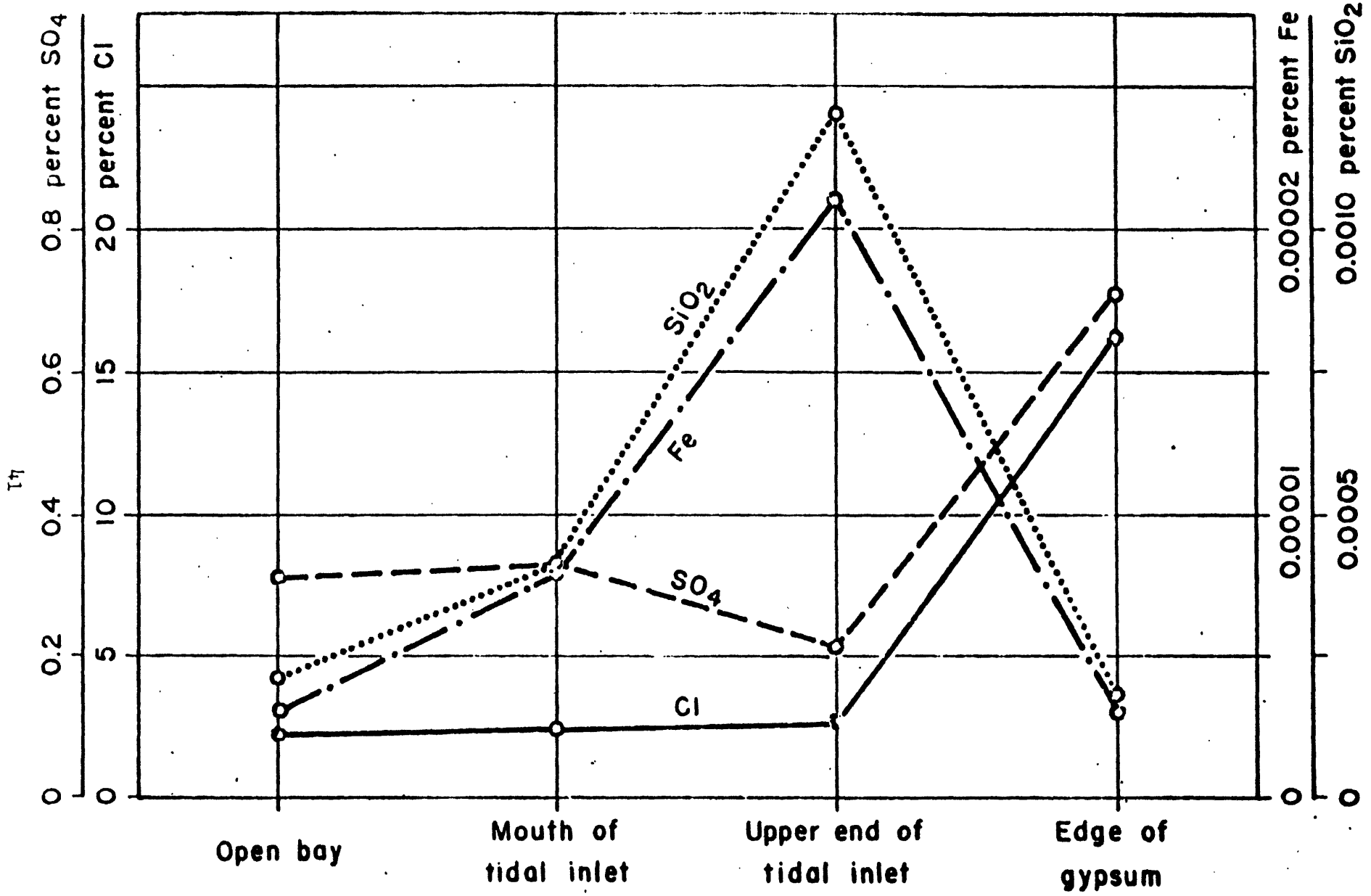


Figure 17.--Change in iron, chloride, sulfate, and silicate concentration during salt deposition.

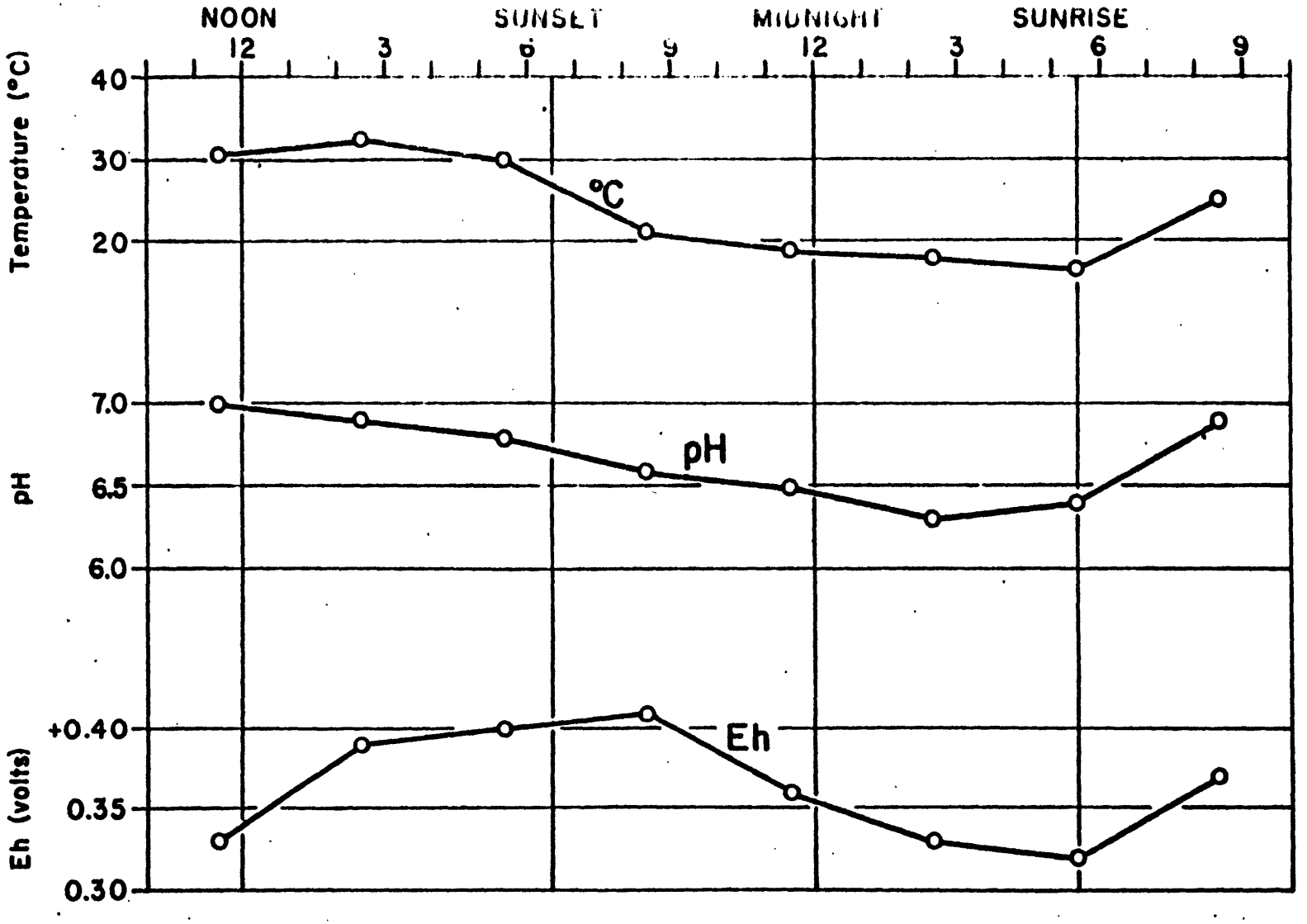


Figure 18.—Temperature, pH, and Eh of water in Pupuri Salina from which halite was being deposited, May 5-6, 1959.

a nearby pool in the gypsum which contained abundant algae was consistently about one pH value more alkaline than the brine from which the salt was being deposited. The salt crust is underlain by black mud containing hydrous iron sulfide which suggests that the acidity might be derived from hydrogen sulfide generated by sulfate-reducing bacteria. The greater alkalinity of the brine during the day than at night may have been caused by the inhibition of bacterial activity by sunlight or by increased evaporation of hydrogen sulfide from the warmer water.

The redox potential[1] follows a curve similar to that of the pH, being more oxidizing during the day and more reducing at night, except that the Eh curve lags the pH curve. Eh ranged from +0.32 volts at 5:30 a.m. to +0.41 volts at 8:30 p.m. Again, the curve is compatible with one to be expected from photosynthetic activity, because more highly oxidizing conditions during the day (larger positive values of Eh) could be correlated with daytime oxygen production by plants. But the water in the control pool containing algae was slightly more reducing than the brine which

---

[1] The Eh values given in this report probably may be compared with each other because the determinations all were made in the same way in the natural environments. It is likely that oxygen contamination occurred, however, and the absolute values of Eh are lower.

lacked discernible plant life; therefore, as in the case of the acidity, changes in concentration of hydrogen sulfide formed by the reduction of sulfate ion by bacteria are believed to be the principal cause of the Eh fluctuations.

Reducing conditions existed in the black mud directly underlying the salt crust. An Eh of -0.09 volts was measured in the mud at 4:10 p.m. and the pH of the mud was 6.9. It has been known for many years that black mud is common in salt lakes (Darwin, 1839, p. 75), and Quaide (1958) has shown that the Eh values of mud in artificial salt concentrating ponds may be as low as -0.42 volts.

The reducing environment underlying areas of evaporite deposition probably results largely from the prevention of water circulation by salt crystals. The high salinity also prevents some of the oxidation normally performed by bacteria. A specialized microscopic biota flourishes in environments of evaporite deposition (Peirce, 1914), but evidently those forms are lacking that might cause complete decay of organic material with possible concomitant establishment of oxidizing conditions. Fossils of bacteria are common in salt deposits (Müller and Schwartz, 1955), but the acidity associated with such areas is sufficient to result in near absence of megafossils, even though floating species probably were trapped and killed when carried by currents into areas of salt deposition.

Facies relations.--The principal evaporite deposit forming during the dry season at Pupuri Salina is a crust of halite which covers most of the area of the salina. The halite interfingers toward the source of sea water with a very thin layer of gypsum around the heads of inlets tributary to the main tidal inlet which supplies water to the salina.

Both of these deposits are ephemeral, however, and thick gypsum around the margin of the salina, thought to have been precipitated by reaction between brine and calcium-bearing ground water from the shore, is the only permanent evaporite deposit.

The profile across Pupuri Salina shown in figure 9 illustrates interfingering relations between the permanent deposits. The sediments record a history of the salina which began with deposition of evaporite deposits and brown mud on gray clay of the open bay, probably at a time when the bar first isolated the salina. An initial period of uniform deposition was succeeded by more rapid submergence which is recorded by transgressive overlap of facies at both sides of the salina. A maximum of 7 centimeters of gypsum has formed since the rapid submergence began. This submergence may be related to a general accelerated rise of sea level during the last 27 years indicated by tide gauges (Marmer, 1949). No absolute information is available to check the rate of gypsum deposition at Pupuri Salina, but it may be instructive to compare it with laminated gypsum rock in the Castile formation of the West Texas Basin in which the laminae average 3 millimeters thick. Seven centimeters of gypsum in 27 years would give an annual increment of 2.6 millimeters. This evidence therefore supports Udden's (1924) suggestion that the laminae of the Castile are annual deposits.

Differential subsidence is occurring in the area of the salina. Gypsum deposits are thicker on the north margin, and desert plants are being engulfed there by the gypsum. The dip of Pleistocene sediments surrounding the salina, though irregular, is gently to the north, as indicated by the outcrop pattern of the shell bed mapped on figure 2.

This north dip may have been responsible for shoaling of the bay to the south which resulted in the origin of the bar and hence of the salina.

The evaporite sediments at Pupuri Salina have many aspects in common with evaporite rocks such as those of Permian age in New Mexico and Texas to be considered in more detail on the following pages. For example, the brown mud may be a counterpart of redbeds that interfinger with the Permian evaporite units. The botryoidal surface of the gypsum in the salina can be compared with similar structures in anhydrite-dolomite rock in the Magenta member; expansion cracks in the gypsum may be analogous to "tepee" structures in the Tansill formation; and fossiliferous dolomite interfingering with halite and anhydrite in the Rustler formation are matched by the coquina barrier beach associated with evaporite deposits at Pupuri Salina.

Important differences also exist between the deposits in Pupuri Salina and those in the Permian formations. In this regard, the fact that halite is not accumulating in permanent deposits at Pupuri Salina should be considered. It is thought that a small change in the balance between salt deposition during the dry season and salt dissolution during the wet season would result in a net accumulation of salt. Even though the balance is now negative, the processes observed at Pupuri Salina are believed to be identical to those that would operate if permanent deposition of salt were occurring. Deposition of salt is analogous to the accumulation of glacial ice: the process of deposition (snowfall) is the same whether, in its

total aspect, the glacier is growing or waning.

A significant difference between the present-day and Permian deposits is the relatively thick shoreward deposit of gypsum and the near absence of gypsum toward the sea where facies relations of the Permian formations suggest the principal gypsum deposition occurred. The Permian counterparts of the shoreward gypsum deposits are believed to lie far to the north of the Permian rocks studied in detail, where the evaporite deposits interfinger with redbeds. The absence of important seaward deposits of gypsum suggests that the thick Permian gypsum beds are not a product of a tide-flat environment such as exists at Pupuri Salina. It will be suggested in a later chapter that the Permian halite rock was formed in shallow water much like that at Pupuri Salina, but that the interfingering beds of gypsum rock toward the sea were formed where the water was somewhat deeper and was characterized by density stratification.

## CHARACTERISTICS OF EVAPORITE FORMATIONS IN WEST TEXAS BASIN

The area of this phase of the investigation is centered approximately around the city of Carlsbad near the southeastern corner of New Mexico (fig. 19). The mapped area extends along the Texas-New Mexico boundary, and is approximately 45 wide and 75 kilometers long. Surface sections were measured along a line 140 kilometers long from Carlsbad to the Apache Mountains, Texas.

The Pecos River flows southward along the east side of the area, and the mountains on the west are drained by its tributaries. After it leaves the area, the Pecos flows southeastward to its junction with the Rio Grande, 600 kilometers from the Gulf of Mexico. The streams to the east of the Pecos are poorly integrated, and that area is largely characterized by interior drainage.

This part of New Mexico and Texas is classified as semi-arid; and, as is characteristic of such regions, the precipitation is variable from year to year. The rainfall at Carlsbad Caverns National Park has ranged from as little as 10 centimeters to as much as 190 centimeters a year. The cause of this wide variation is the lack of regularity in frequency of summer thunderstorms. Most of the precipitation can be ascribed to thundershowers between July and September, and only 20 percent occurs in the six-month period between November and April. The temperature at Carlsbad Caverns ranges between a January mean of 7°C and a July mean of 26°C.

Vegetation on the plains consists of short grass, narrow-leafed yucca, mesquite, greasewood, and several species of acacia. The foothills

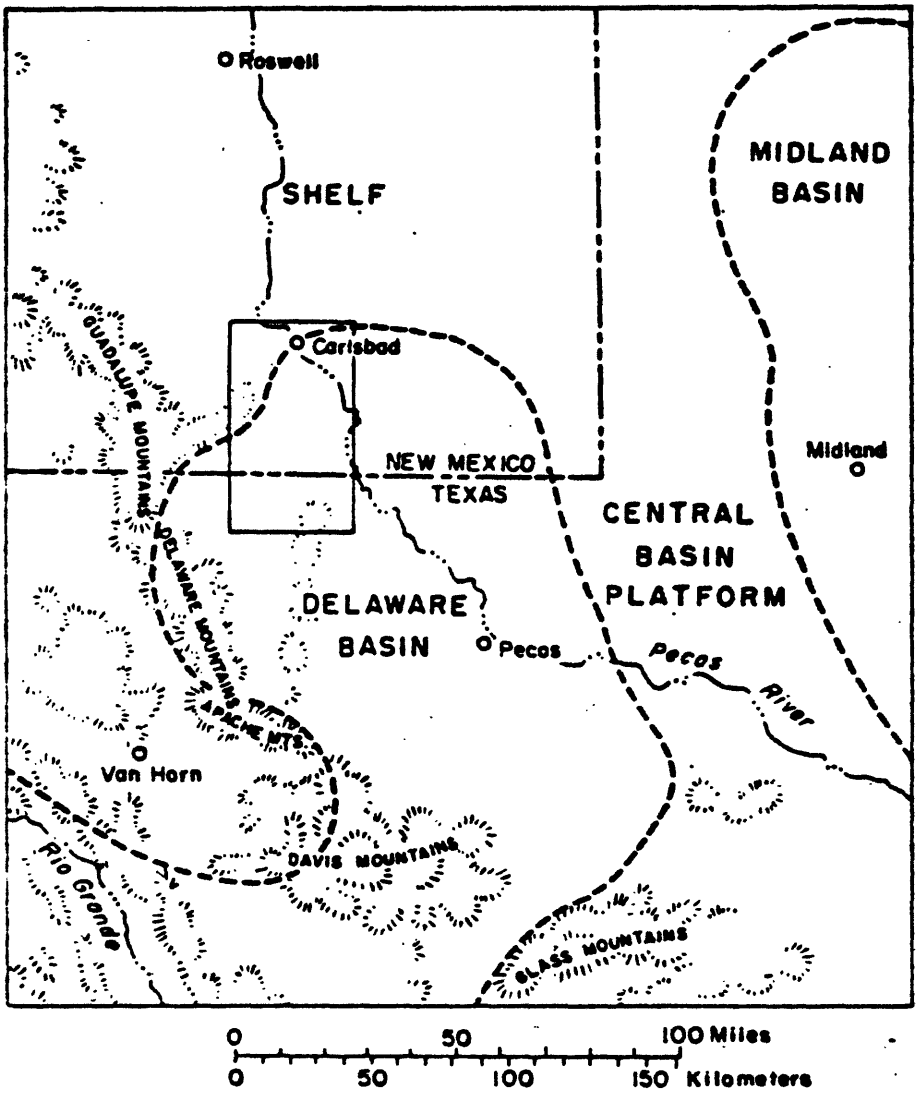


Figure 19.--Index map of southeastern New Mexico and West Texas showing area of this investigation and provinces of Permian time.

have lechiguilla, sotol, broad-leafed yucca, several kinds of cactus, and scattered juniper and madrone trees. Forest trees live on the mountains. Nonindigenous tamarisk, introduced from the Middle East, grows in dense groves along lowland streams.

U. S. highways 62 and 285 pass diagonally through the area trending, respectively, northeast and northwest. They intersect at Carlsbad. A secondary net of paved state highways and graded county roads extends into most of the townships, but some areas are accessible only in a vehicle with four-wheel drive or on horseback.

## Geologic setting

Rocks of Permian age underlie a broad area that extends from North Dakota into Mexico on the west side of the Great Plains. These rocks thicken somewhat irregularly toward the West Texas Basin of New Mexico and Texas, and they attain their maximum thickness of 4300 meters in the Delaware Basin, a part of larger West Texas (Permian) Basin. This area contains one of the most nearly complete sequences of rocks of Permian age in the world, and the rocks are richly fossiliferous except in the uppermost part. In north-central Texas the Permian strata are separated from rocks of Upper Pennsylvanian age by an obscure basal disconformity (Moore, 1949). In West Texas and New Mexico, the Permian rocks grade upward with conformity into rocks of probable Lower Triassic age (see stratigraphy).

The Delaware Basin is about 250 kilometers long and 150 kilometers wide. It is separated from the similar Midland Basin to the northeast by

the Central Basin Platform which is approximately 80 kilometers wide (fig. 19). In the Midland Basin the Permian rocks are about 3000 meters thick. They are only 2100 meters thick on the Central Basin Platform and on the shelf areas outside the margins of the two basins.

In addition to their differences in thickness, the Permian provinces are characterized by differences in lithology. During most of Permian time, sandstone and shale were deposited in the basins, while the Central Basin Platform and the shelf areas chiefly received carbonate sediments with some intercalated evaporite deposits. Toward the end of the Permian period, however, conditions favoring evaporite deposition invaded first the Midland Basin and the Central Basin Platform, and finally occupied all the provinces in an area 400 kilometers in diameter.

This study is especially concerned with these late Permian evaporite deposits and the carbonate and silicate-bearing clastic rocks associated with them.

The area examined in this investigation extends across the northern margin of the Delaware Basin (fig. 20). The Permian rocks thicken here where they cross into the basin from the shelf which lies to the north. After the end of deposition of rocks of Permian age, the region was tilted several times; the dip is now approximately $1\frac{1}{2}^{\circ}$ to the east. The principal tilting probably occurred in Pleistocene time because rocks of late Cenozoic age dip nearly as much as those of Permian age. As a result of this dip, the outcrop pattern of the formations trends north except where departures resulting from faults,

minor folds, and topographic irregularities are present. The oldest rocks at the surface occur on the west side of the area, and the youngest, on the east.

The sedimentary rocks of the region range in age from middle Permian to Pleistocene(?). Those of Permian age locally contain marine evaporite deposits; elsewhere they contain fossils suggesting deposition in a shallow sea of normal salinity. The marine environment of Permian time was succeeded in the Triassic by terrestrial conditions denoted by redbeds containing the remains of land animals. Subsequently, during Cretaceous time, the presence of another marine fauna shows that the sea once again returned to the area. A long gap in the record of sedimentation separates the Cretaceous rocks from those of late Cenozoic age. The Cenozoic formations exhibit cross-stratification that suggests they were formed under fluviatile conditions, and tuffaceous material which they contain records volcanic activity during this latest period of sedimentation.

The sequence of deposition was interrupted by at least three major periods of erosion which are marked by three unconformities: one at the base of rocks of Upper Triassic age, one at the base of rocks of Lower Cretaceous age, and one at the base of rocks of Pleistocene(?) age.

The topical nature of this investigation requires that chief emphasis be placed on late Permian evaporite deposits and rocks laterally equivalent to them. In order to place these formations in their setting, however, some stratigraphic details are included on other rocks cropping out in the area.

## Rocks of Permian age

During Permian time in this region, rocks characteristic of several different environments were being deposited simultaneously. Three provinces can be recognized according to their position with respect to Delaware Basin: the shelf province (including the Central Basin Platform), the basin-margin province, and the basin province. The provinces are named on the basis of the relative thickness of the rocks occupying them, and the names are not intended necessarily to indicate topographic or bathymetric conditions existing during Permian time (Sloss and others, 1949, p. 100). The rates of subsidence and sedimentation were relatively rapid in the basin, relatively slow on the shelf, and intermediate at the basin-margin. As a secondary result of these differences, the formations of each province also have characteristic lithologies.

### Formations of the shelf province

The Permian formations of the shelf consist principally of carbonate rocks and evaporite deposits. The oldest is the San Andres formation, which is overlain by the Grayburg and Queen formations, which in turn are overlain by the formations of the Carlsbad group. Above the Carlsbad group are the Salado and Rustler formations which are not confined to the shelf but extend across each of the provinces. The rocks of the Carlsbad group and Salado and Rustler formations crop out in the map area and will be considered in more detail here.

Carlsbad group.--The Carlsbad group includes, in ascending order: the Seven Rivers formation, the Yates formation, and the Tansill formation. Shelfward each passes laterally first into evaporite deposits and then into redbeds. The formations of the Carlsbad group are not separately mapped on figure 20.

The Seven Rivers formation (Meinzer and others, 1926) is approximately 210 meters thick. Where it grades into the Capitan limestone at the margin of the basin, it consists of thick-bedded yellowish-gray limestone. Shelfward the formation is oolitic and, farther shelfward, pisolitic; likewise, the limestone grades into dolomite rock. A few thin beds of quartz sandstone and siltstone are present in each facies.

Approximately 23 kilometers from the margin of the basin in the subsurface, the dolomite rock of the Seven Rivers formation passes into anhydrite rock which, still farther shelfward, grades into halite rock. Dolomite in other formations on the shelf similarly interfingers with gypsum and halite, and as progressively younger formations were laid down the environment favoring evaporite deposition encroached successively nearer to the margin of the basin (fig. 19a). Below are the formations that are confined to the shelf and the distances at which thecarbonate rocks of each unit pass into evaporite deposits (chiefly after Sheldon, 1954); the youngest formation is at the top:

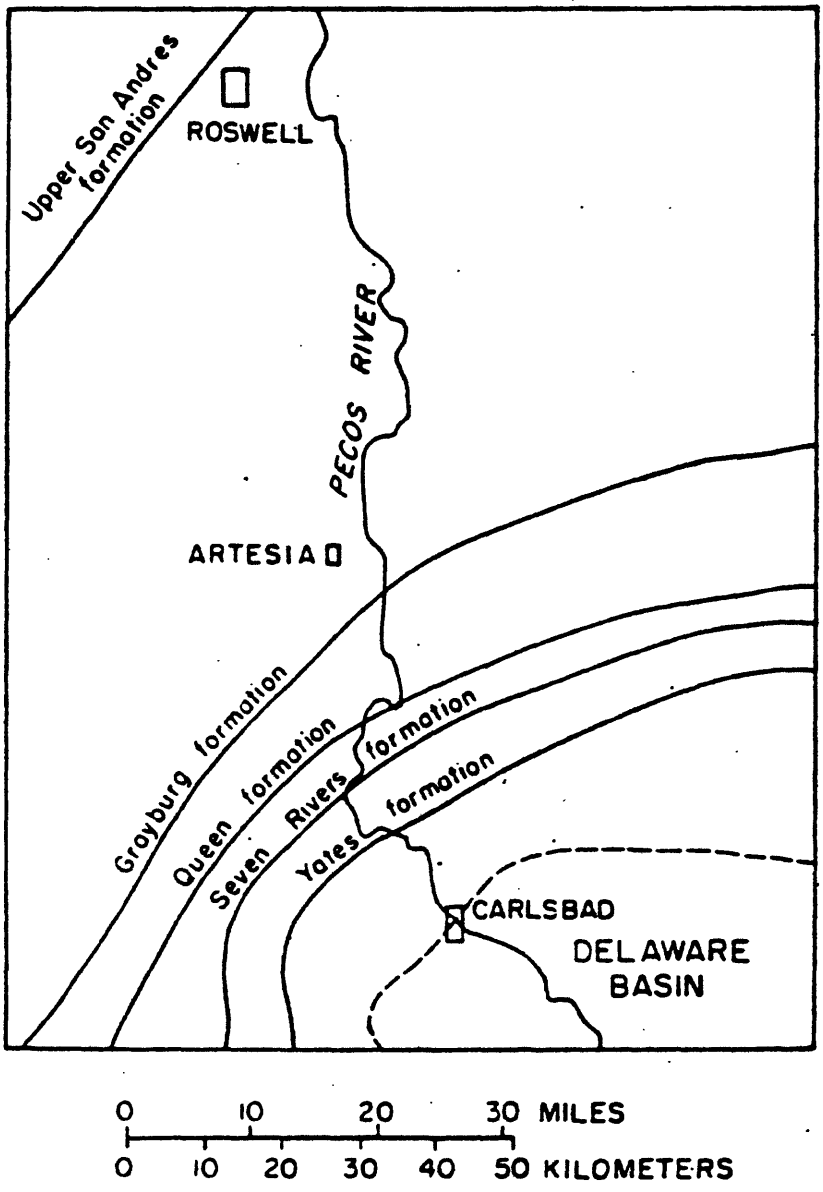


Figure 19a.--Southeastward limit of sulfate rocks in some Permian formations northwest of the Delaware Basin (after Sheldon, 1954).

| Formation | Distance of carbonate-evaporite transition northwest from Carlsbad (kilometers) |
|---|---|
| Tansill | 5 |
| Yates | 15 |
| Seven Rivers | 23 |
| Queen | 29 |
| Grayburg | 35 |
| San Andres | 94 |

Though the belts of dolomite rock in each formation are narrow, they extend for hundreds of kilometers parallel with the margin of the basin. Farther shelfward in each unit, the evaporite deposits grade into redbeds, and a similar relationship exists between the location of this transition in each formation and the stratigraphic position of the formation.

The dolomite rock in the Seven Rivers formation grades into gypsum rock in a relationship which has been described by Bates (1942). The individual beds of dolomite rock thin and become separated by wedge-shaped beds of gypsum, so that, within 2 kilometers, a thick sequence of dolomite rock has passed into a sequence almost wholly composed of gypsum rock; dolomite remains only in widely-spaced layers a few centimeters thick. A wedge of limestone breccia lies at the tip of each tongue of gypsum, and the transition from gypsum rock to limestone is abrupt. The wedges of limestone in the Seven Rivers formation continue a short distance into thin-bedded dolomite rock of the formation where they pinch out.

The Yates formation (Gester and Hayley, 1929) conformably overlies the Seven Rivers formation and is approximately 100 meters thick. In the Guadalupe Mountains it is composed of pisolitic yellowish-gray limestone and dolomite rock and grayish-orange very fine grained quartz sandstone. The quartz sand-bearing beds in this and the other shelf formations commonly pass nearly unchanged from the carbonate to the evaporite facies to the north so correlations may be made between the two facies.

Near where the Yates formation grades into the Capitan limestone to the south, the Yates is characterized by tepee structure (Adams and Frenzel, 1950, p. 308). This structure consists of tent-shaped irregularities of the beds in zones about 2 meters thick. Generally, the structures are about 4 meters wide with a sharp apex, and individual beds in the zone are broken along a vertical fracture. Each tepee affects many 20-centimeter beds of pisolitic dolomite rock, and open spaces created by the warping are filled with travertine-like material. Newell and others (1953, p. 129) have suggested that the structures were formed by the expansion of anhydrite or other salts along joints and bedding planes. Another possibility is that the distortion was caused by daily thermal expansion and contraction of the thin beds during their deposition in shallow water. The cracks that formed during contraction were filled so that later expansion caused buckling.

The Yates formation is not richly fossiliferous, but locally fossils are present in certain beds. The most abundant types are fusulines and calcareous algae, and the fusulines commonly serve as the

nuclei of pisolites. Near the top of the formation, calcite sandstone (calcarenite), containing some layers largely composed of the tests of fusulines, interfingers with massive rock of the Capitan limestone. This part of the Yates formation is believed to represent a Permian sand bar in which the grains were composed of fusuline tests and other particles of carbonate detritus.

The top of the Yates formation is placed, by convention, at the top of the uppermost relatively thick bed of quartz sandstone in the middle part of the Carlsbad group.

The Tansill formation (DeFord, 1939) conformably overlies the Yates formation and is approximately 100 meters thick. In the Guadalupe Mountains the Tansill consists mostly of grayish-orange to yellowish-gray dolomite rock. It contains a few pisolites, but they are much less abundant than in the Yates formation. Fossils are also especially rare in the Tansill, and the only types achieving local importance are those of algae.

As in the case of each of the formations on the shelf, the principal mineral of the carbonate facies of the Tansill formation grades from dolomite to calcite near the transition into the Capitan limestone. In the present investigation, the contact between the Carlsbad group and Capitan has been placed at the point where easily discernible bedding disappears and the rock becomes massive.

The halite and gypsum facies of the Tansill formation are broader at the expense of the carbonate facies than their counterparts

in the older formations. The carbonate belt of the Tansill is only 5 kilometers wide and consists of calcite sandstone near the gradation of the formation into the Capitan limestone. Elsewhere the carbonate belt is composed of dolomite rock believed to have been formed from carbonate minerals that were precipitated by chemical or organic processes. The narrow belt of dolomite rock and the paucity of fossils in the Tansill may have resulted from the fact that the salinity of water supplied to the Tansill lagoon was greater than that of normal sea water.

The contact between the Tansill formation and the overlying Salado formation is poorly exposed in outcrop, but it has been penetrated by many drill holes prospecting for potassium minerals and petroleum. On the basis of detailed studies of closely spaced potassium test holes, Jones (1954, p. 110) has concluded that the Salado rests on the Tansill with conformity. The Salado formation also extends across the basin margin to the Delaware Basin where it overlies the Castile formation.

## Formations of the basin-margin province

The sharp tectonic flexture at the margin of the Delaware Basin created special conditions during Permian time that resulted in the formation of stratigraphic units distinct from those on the shelf or in the basin. The Capitan limestone is the representative of the basin-margin province in the map area.

Capitan limestone.--The Capitan limestone (Richardson, 1904) is the uppermost formation of the Guadalupe series. It consists of massive, light olive-gray limestone approximately 450 meters thick. Much of the

formation is a breccia consisting of a limestone matrix containing blocks of limestone and dolomite rock; the fragments average 10 centimeters in diameter with some up to 10 meters long. A few blocks of very fine-grained quartz sandstone occupy discrete zones in the formation. In places the thicker blocks of dolomite rock and quartz sandstone are arranged along gently dipping planes with crude parallelism to one another. Both the dolomite and sandstone blocks are angular and appear to have been lithified before they were brecciated.

The matrix of the Capitan consists of very fine-grained limestone with irregular areas of somewhat larger calcite crystals. The fine-grained areas incorporate many very small dark particles which are lacking in the coarser crystals. Many specimens contain fragments that include pisolites, fossils, or quartz-sand grains, and very fine-grained quartz sand commonly fills irregular cavities in the rock.

At intervals the formation includes beds of fossiliferous limestone containing brachiopods, fusulines, nautiloids, crinoids, and bryozoa. The fossiliferous limestone beds are composed of calcite sandstone, and they generally lack the brecciation exhibited by the remainder of the formation.

The relative age of the Capitan limestone and Castile formation in the basin was a subject of some controversy from the time the formations were first described by Richardson in 1904. Richardson (1904, p. 43) was not able to satisfy himself completely on the relations between the two units, but he tended to favor the concept that the Castile had been laid down on the truncated edge of an older Capitan limestone. The opinion of most geologists at present is that the Capitan limestone is a

former barrier reef (Lloyd, 1929; King, 1948; Newell and others, 1953), and that the Castile formation is slightly younger and was laid down adjacent to it. In order to explain the fact that the Salado formation directly overlies both the Castile and the Tansill formation which was known to be time-equivalent with the Capitan, Newell and others (1953, p. 15) postulated a hiatus to exist between the Salado and Tansill to account for the time required for deposition of the Castile formation.

The Capitan limestone is equivalent in the basin to the uppermost formation of the Delaware Mountain group, the Bell Canyon formation (King, 1948). On the shelf it is equivalent to the formations of the Carlsbad group. The Capitan is also overlain by the Carlsbad group because the younger formations of the group occupy positions progressively nearer to the basin so as to overlap the Capitan.

## Formations of the basin provinces

The basin province is predominantly characterized by very fine-grained quartz-bearing clastic rock, dark-colored clastic limestone, and evaporite deposits. In the map area these lithologies are found in the Delaware Mountain group and the overlying Castile formation. The evaporite deposits of the Castile formation foreshadow the time during deposition of the overlying Salado formation when virtually no lithologic nor tectonic distinction existed between the basin, basin-margin, and shelf provinces.

Delaware Mountain group.--The Delaware Mountain group (Richardson, 1904) occupies the Delaware Basin and is composed of a thick sequence of fine-grained quartz sandstone and siltstone which contains several thin but persistent beds of dark-gray limestone. The silicate-bearing clastic rocks in the group range in color from greenish gray to yellowish brown. The group is approximately 1200 meters thick (Ahling and others, 1958) and has been divided into three formations which are, in ascending order: Brushy Canyon formation, Cherry Canyon formation, and Bell Canyon formation. (These formations are not separately mapped on figure 20).

Cross-stratification and ripple marks are common throughout the basin in very fine-grained sandstone of the Delaware Mountain group. Lenticular sets of cross-strata averaging 10 meters wide and 50 centimeters thick occur within 15 meters of the top of the group. The wave lengths of ripple marks near the top of the group are approximately 15 centimers; and the amplitudes are approximately one centimeter.

The widespread Lamar limestone member, which is approximately 1 mater thick in the basin, lies about 10 meters below the top of the

Bell Canyon formation. The Lamar is medium dark-gray; it contains uniform beds 5 centimeters thick, and commonly contains discontinuous layers of medium light-gray chert. In the basin it is composed of calcite mudstone (calcilutite), but at the basin margin it consists of calcite sandstone and is lighter colored.

The Lamar member is underlain and overlain by very fine-grained quartz sandstone in beds 1 centimeter thick. A laminated grayish-brown limestone bed 1 meter thick marks the top of the Delaware Mountain group (figs. 21 and 22). The laminae of this limestone are 1/2-1 millimeter thick. When broken, the limestone emits a strong petroliferous odor. It is underlain by platy quartz sandstone and is conformably, but abruptly, overlain by rhythmically layered gypsum rock of the Castile formation containing limestone laminae.

At the basin margin, the rocks between the Lamar limestone member and the top of the Delaware Mountain group grade into calcite sandstone, and the quartz sandstone underlying the Lamar similarly grades into limestone so that the Lamar limestone member attains a thickness of 90 meters at the expense of associated quartz sandstone beds where it passes laterally into the Capitan limestone. Lower limestone beds in the Delaware Mountain group also are much thicker at the margin of the basin.

The Delaware Mountain group is laterally equivalent at the basin margin to the Capitan limestone and underlying rocks. It is equivalent on the shelf to the San Andres formation, the Grayburg formation, the Queen formation, and the Carlsbad group.

Castile formation.--The Castile formation, which directly overlies the Delaware Mountain group, was originally described by Richardson (1904)

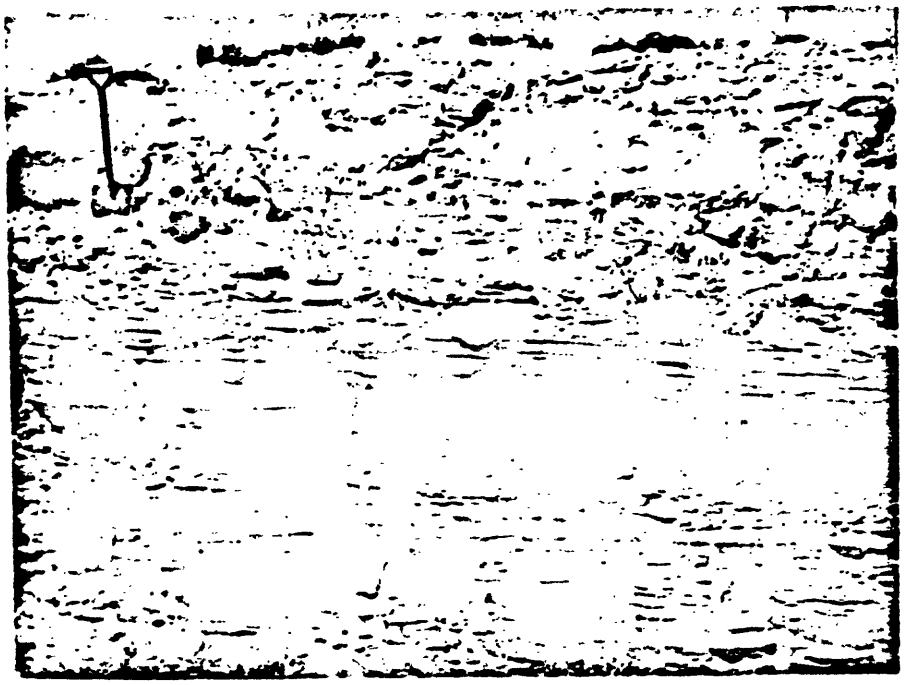

Figure 22.--Contact between gypsum rock of the Castile formation and the upper grayish-brown limestone bed of the Delaware Mountain group near the Pasotex Pipeline road, Texas. Below the limestone bed, which is 1 meter thick, is very fine grained sandstone.

and included both the Castile and Salado formations of this report. In 1935, Lang restricted the Castile in the subsurface to the lower predominately anhydrite-bearing part of the sequence and called the upper predominately halite-bearing part, the Salado. This usage is here applied to the outcrop area of the formations.

In the subsurface the Castile formation is about 600 meters thick in the northern part of the basin and contains several thick beds of halite rock (fig. 23). Toward the southern end of the basin, the lower halite beds pinch out, and the Castile formation becomes thicker at the expense of the overlying Salado formation. In the vicinity of the Apache Mountains, the Castile comprises 700 meters of anhydrite rock.

In outcrop in the vicinity of the Texas-New Mexico state line, the formation consists of a basal member of laminated gypsum rock about 300 meters thick and an upper member of massive gypsum rock about 100 meters thick. In the southern part of the basin near the Apache Mountains, the laminated member is about the same thickness but the massive member has thickened to 300 meters. At various places, gypsum breccia marks the positions of leached salt beds.

The limestone laminae which characterize the lower part of the Castile formation in the Delaware Basin are nearly absent adjacent to the Capitan limestone belt (Hayes, 1957, and personal communication). Closely spaced wells show that several kilometers from the Capitan they are confined to the basal part of the lowest anhydrite bed and to the next higher bed. Nearer to the Capitan limestone, the Castile is entirely composed of massive anhydrite rock.

The basal member in outcrop normally consists of alternating layers of white gypsum and olive-gray limestone, with an average of three alternations per centimeter (figs. 24 and 25). The thickness of the limestone laminae is approximately half that of the gypsum laminae and decreases upward; nevertheless, the basal contact of the formation with limestone of the Delaware Mountain group is abrupt. Udden (1924) has suggested that each couplet in the Anhydrite rock is the deposit of a single year, a supposition that seems reasonable.

The rock contains small "ripples" with wave lengths of a centimeter or two superimposed on larger folds with wave lengths of about a meter (fig. 26). Both are a result of expansion during the alteration of anhydrite to gypsum in the zone of weathering.

The rock emits a petroliferous odor when broken. Especially petroliferous zones several meters in diameter are common in places in the member. These are characterized by gypsum crystals 5 centimeters long which formed by recrystallization. Locally, gypsum crystals more than 2 meters long occur in similar recrystallized zones along faults.

The brecciated members of the Castile formation which mark salt beds consist of blocks of white gypsum rock in a matrix of dusky-yellow silt with gypsum cement. This material is very easily eroded and good exposures are rare.

The upper nonlaminated member of the Castile is composed of massive white alabastrine gypsum whose composition is so uniform that bedding is invisible. It commonly contains expansion cracks making polygons 5 centimeters in diameter; in places, medium dark-gray stains extend dendritically outward from these cracks.

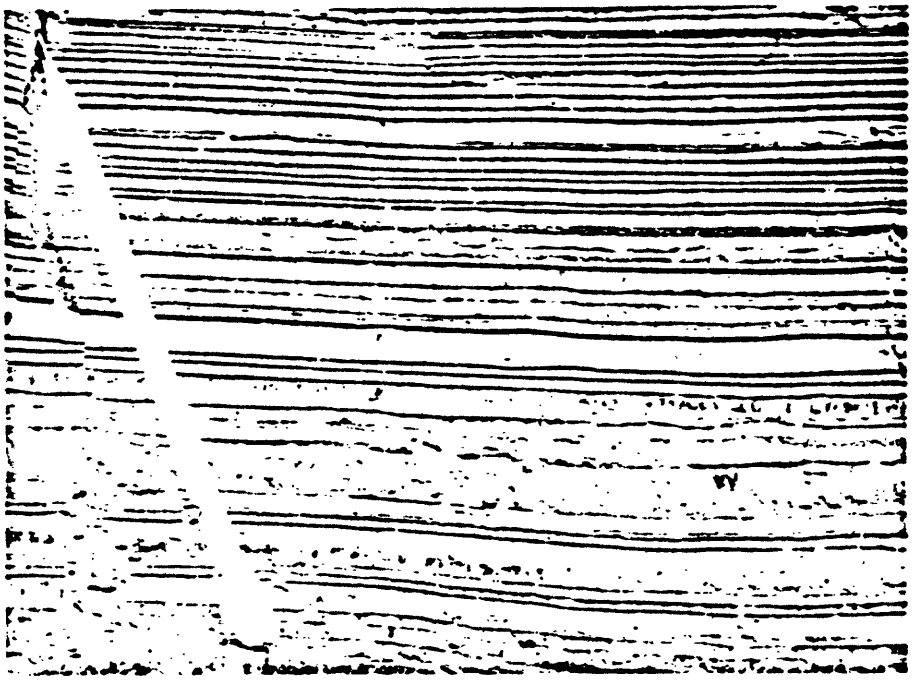

Figure 24.--Laminated gypsum rock and limestone near the base of the Castile formation, near the Pasotex Pipeline road, Texas.

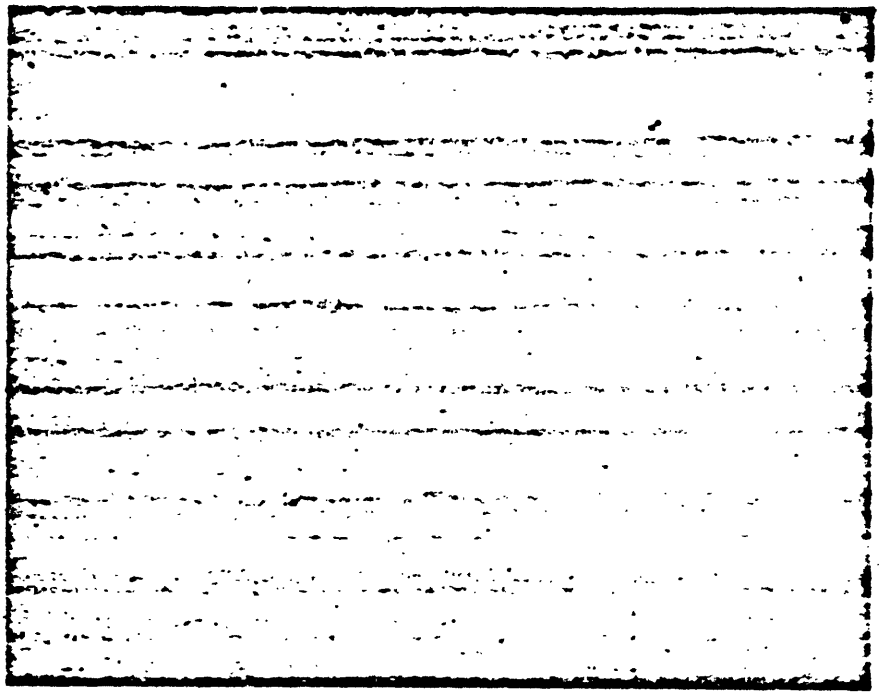

Figure 25.--Thin section of laminated anhydrite rock and dark bituminous limestone of the Castile formation, from a drill hole in sec. 15, T. 26 S., R. 24 E., New Mexico. Polarizers parallel X24.

Figure 26.--Laminated gypsum rock of the Castile formation on U. S. Highway 62, 4 kilometers northeast of state line. A bed of laminated limestone crops out near the top of the roadcut.

The sulfate minerals of the Castile formation have been altered to calcite in isolated areas that are as large as a square kilometer (fig. 27). These limestone masses are much more resistant to erosion than the surrounding unreplaced gypsum. They stand as buttes which have been called "castiles" by Adams (1944, p. 1606) in reference both to the name of the host formation and to their supposed resemblance to castles.

The limestone bodies occur along faults that cut the Castile formation and the underlying Delaware Mountain group; most are located on northeast-trending faults. One "Castile" (fig. 28) 52 kilometers west of Orla, Texas, though near an important fault that trends northeast, is specifically localized by a minor north-trending fault that displaces the underlying Lamar limestone member only 30 centimeters. Also, 15 kilometers south of Pine Spring, Texas, alteration is related to faults at the margin of the Basin and Range Province which trend northwest.

The mechanism of the alteration is best studied in places where the lower laminated member of the Castile formation is affected because in these places the primary olive-gray limestone laminae reveal a record of the course of alteration (fig. 29). Near the margin of an altered zone, the rock is slightly brecciated and the limestone laminae are somewhat more closely spaced than in normal gypsum rock (fig. 30); inward from this zone, the white gypsum laminae are more obscure; and, farther inward, the rock becomes a light olive-gray limestone that lacks lamination and is massive.

The degree of replacement of rock in the "castiles" is strongly controlled by joints. Limestone which still faintly exhibits the

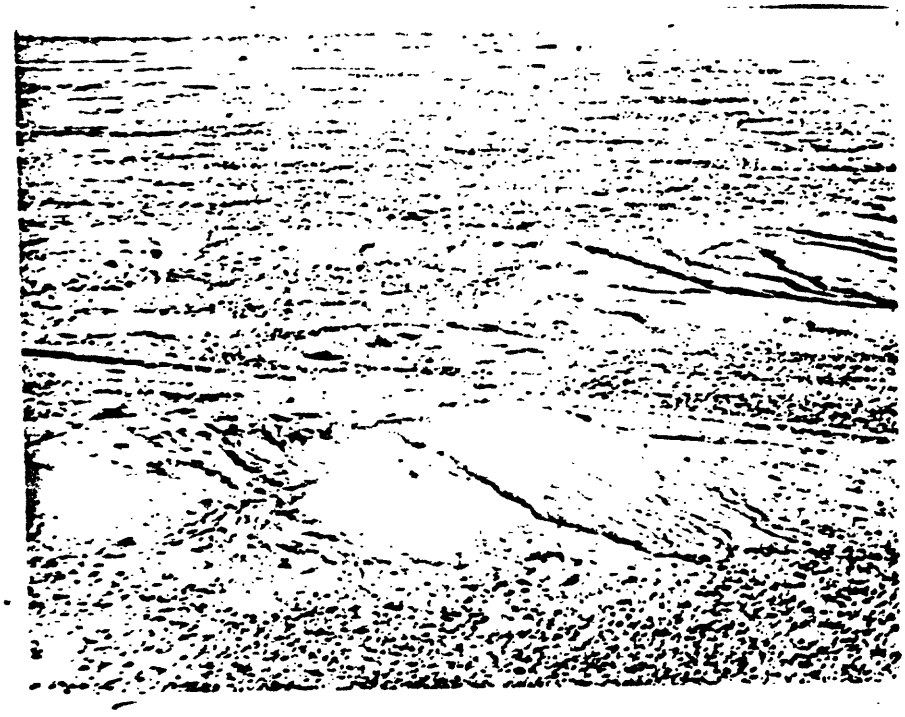

Figure 27.--Aerial view of a limestone hill in the Castile formation 47 kilometers west of Orla, Texas, which was formed by replacement of anhydrite rock. The hill is 50 meters high and is separated from a similar hill on the skyline by typical exposures of unreplaced gypsum rock.

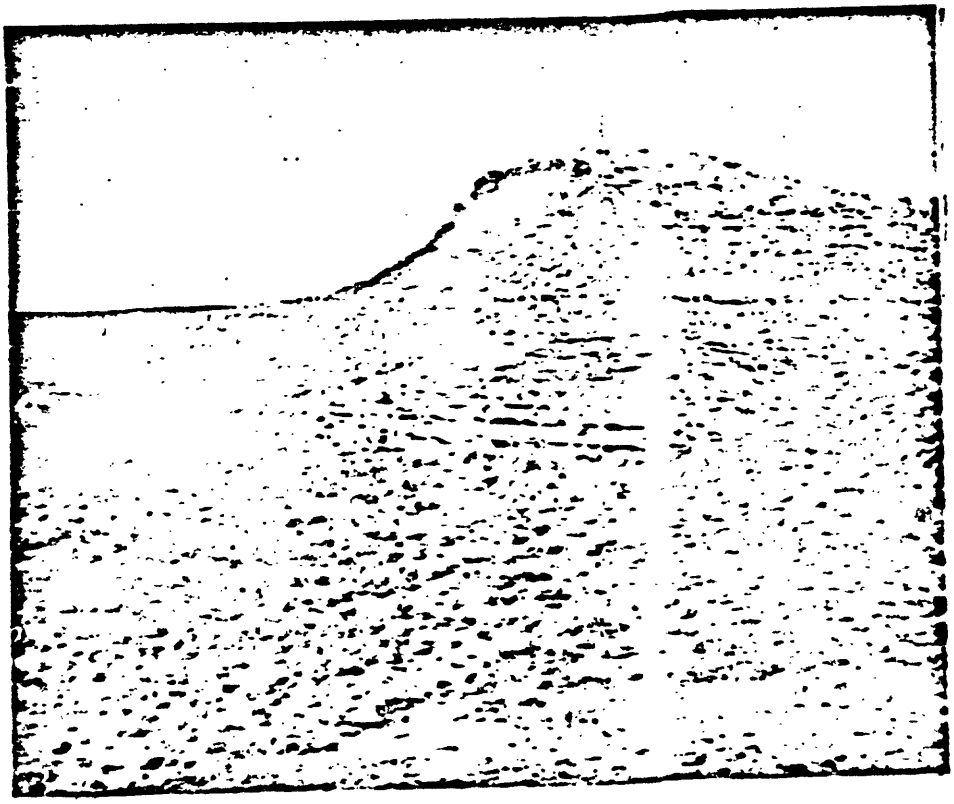

Figure 28.--Massive limestone at the base of the Castile formation overlying quartz sandstone of the Bell Canyon formation 52 kilometers west of Orla, Texas. The limestone, which was formed by replacement of anhydrite rock along a fault, is 12 meters thick and lies 8 meters above the Lamar limestone member, here 1 meter thick. The Lamar forms a small bench whose profile appears in the upper left part of the photograph at the same level with the ridge which forms the distant skyline.

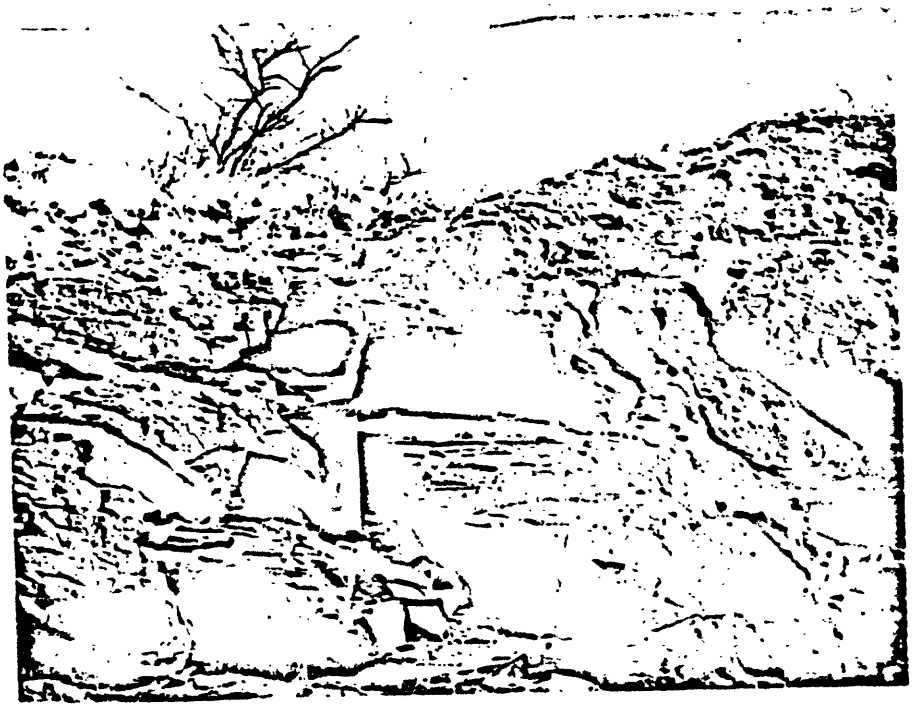

Figure 29.--Limestone in a "castile" 52 kilometers west of Orla, Texas. Rock to left retains laminae and has expansion cracks; rock at right top is massive.

Figure 30.--Thin section of partly replaced anhydrite rock of the lower member of the Castile formation from a "castile" 52 kilometers west of Orla, Texas. Most of the crystals between the brecciated dark limestone laminae are calcite. Polarizers parallel, X4.

original lamination of the Castile commonly occurs on one side of a joint and massive limestone lies on the other. Many "castiles" are near the base of the Castile formation, but some occur at other stratigraphic positions. An accessible example in the upper nonlaminated member of the Castile (fig. 31) is on U. S. Highway 62 on the north side of a fault in sec. 12, T. 26 S., R. 24 E. No fossils have been found in the "castiles."

Where only partly replaced, the secondary limestone in the Castile formation has prominent expansion cracks in outcrop. This suggests that the replacement took place below the zone of weathering and that anhydrite rock, rather than gypsum rock, was altered to limestone. Minor amounts of unreplaced anhydrite were subsequently hydrated to gypsum to produce the cracks during the present cycle of erosion.

Sulfur is associated with the limestone in these buttes and during World War II some was mined in the area. In sec. 11, T. 26 S., R. 24 E., sulfur is being deposited at the present time from a cold spring coming to the surface along a fault that nearby has localized a large area of secondary limestone in the Castile. Sulfur has also been found in drill holes in the shelf sediments of the Carlsbad group. One such occurrence is in the National Farmers Union drill hole no. 1-A in the NE¼NE¼ sec. 13, T. 20 S., R. 26 E.

## Formations present in all three provinces

By the end of deposition of the Castile formation, localized downwarping in the Delaware Basin had virtually ceased. The subsequent formations cross the margin of the basin and are present in the shelf, basin-margin, and basin provinces.

Figure 31.--Thin section of limestone formed by replacement of anhydrite rock of the upper member of the Castile formation from center west side sec. 12, T. 26 S., R. 25 E., New Mexico. Crossed polarizers, X300.

Salado formation.--The Salado formation (Lang, 1935) rests on the Tansill formation on the shelf and interfingers with the Castile formation in the Delaware Basin. It is not in direct contact with the Capitan limestone at the margin of the basin because the top of the Capitan is adjacent to the Castile shelfward of the line along which carbonate rock of the Tansill thins to a featheredge above.

The Salado formation is 500 meters thick in the subsurface near the margin of the Delaware Basin. It is about 84 percent chloride rocks, 12 percent sulfate rocks, and 4 percent silicate-bearing clastic rocks. The formation contains virtually no limestone nor dolomite rock.

Lang (1944) suggested that the Fletcher anhydrite member, 21 meters thick, be the basal member of the Salado formation. The Fletcher at its type well rests directly on dolomite rock of the Tansill formation. Unfortunately, the dolomite facies at the top of the Tansill is less than 5 kilometers wide, and the Fletcher is not easily separated from anhydrite rock of the Tansill formation farther shelfward. Similarly, toward the basin, the Fletcher shortly joins the main mass of the Castile anhydrite. It is proposed, therefore, that the Fletcher anhydrite be a member of the Tansill formation on the shelf and a member of the Castile formation in the basin. The top of the Fletcher member would then mark the base of the Salado formation in both provinces.

A criterion is needed to separate the Salado formation from the Castile formation in the basin where the two formations interfinger. Beds of anhydrite rock more than 10 meters thick, separated by halite rock, generally do not brecciate when they crop out, and thinner beds do. The mapped formation boundary is the contact between outcropping

coherent beds of gypsum rock and zones of gypsum breccia. By the use of the above thickness criterion, the approximate correlation between the map formation boundary (fig. 20) and the subsurface Salado and Castile tongues (fig. 23) can be estimated.

The halite rock of the Salado formation ranges from greenish gray to grayish orange, and only rarely is it white, even though commonly nearly pure. The transparency of the halite causes minor impurities to impart their color to the rock.

Anhydrite is the principal sulfate mineral in the formation in the subsurface. The beds of anhydrite rock are ordinarily light olive-gray and average 30 centimeters thick. Approximately a quarter of the anhydrite rock has been secondarily altered to a rock composed of the mineral polyhalite, $2CaSO_4 \cdot MgSO_4 \cdot K_2SO_4 \cdot 2H_2O$. The polyhalite rock is moderate reddish orange and is widespread in the formation. In outcrop it transforms to moderate-red gypsum rock.

Beds of quartz sandstone and siltstone in the subsurface are chiefly greenish gray which suggests conditions of chemical reduction; nevertheless, some are moderate brown and the local environment is evidently oxidizing. The silicate-bearing clastic rocks commonly directly underlie beds composed of sulfate minerals. The areal extent of some beds only a few centimeters or a few tens of centimeters thick is more than 10,000 square kilometers. The thin layers of the Salado are perhaps as persistent laterally as those of any formation in the world.

Potassium minerals are mined extensively from discontinuous layers in the Salado in an area directly over the margin of the Delaware Basin

about 15 miles east of Carlsbad (Jones, 1954). The principal ore mineral is sylvite, and some langbeinite is also mined. The potassium deposits occur in veins as well as in layers, and they extend through a large stratigraphic range from the Tansill formation to the Rustler formation overlying the Salado. The restricted areal extent of the potassium deposits at the margin of the basin in light of the persistence of very thin beds of sulfate and clastic rocks over great distances in the basin and on the shelf suggests that the ore deposits are epigenetic (Jones, 1959).

In outcrop the Salado formation consists of a breccia of light-gray and moderate-red gypsum rock with a matrix of pale reddish-brown silt (fig. 32). The fragments of moderate-red gypsum in the Salado are useful for separating it from the underlying Castile formation especially in flat terrain where the units are poorly exposed.

Because the moderate-red gypsum rock is a surface expression of secondary polyhalite rock at depth, its distribution in the formation is not an exact reflection of the original stratigraphy. Progressively lower beds of anhydrite rock were replaced by polyhalite to the north in the basin (Jones, 1954). Along the Delaware River, for example, the basal 12 meters of the formation lacks red gypsum and consists of a breccia of light-gray gypsum with a matrix of dusky-yellow silt.

The breccia of the Salado formation typically contains boulders 20 centimeters in diameter that have been rounded by solution. This rounding is characteristic of outcropping gypsum breccia in both the Salado and Castile formations where thick sequences of salt have been removed, and intercalated beds of anhydrite rock have collapsed and

Figure 32.--Typical outcrop of silty gypsum breccia of the Salado formation in sec. 8, T. 24 S., R. 26 E., New Mexico.

brecciated. Superficially they resemble stream-eroded boulders, but their universal presence in the upper 100 meters of drill holes, regardless of stratigraphic position in the evaporite formations, shows that the soluble fragments were rounded at depth by slowly percolating water.

The contact between the Salado and the overlying Rustler formation is placed below a very fine grained dolomitic quartz-sandstone sequence which underlies the Culebra dolomite member of the Rustler (fig. 21; appendix). This is the horizon selected by Richardson (1904) for the base of the Rustler formation at its type locality in Horsehoe Draw in the Rustler Hills of Texas.

Rustler formation.--The Rustler formation conformably overlies the Salado formation and is composed of approximately 50 percent halite rock where unleached. The remainder is quartz sandstone and siltstone, carbonate rock, and anhydrite rock similar to that in the Salado. The formation thickens rather uniformly from the shelf into the basin and is approximately 100 meters thick at the basin margin.

The basal yellowish-gray sandstone member of the Rustler (fig. 33), which grades into carbonate rock and is much thicker to the south, is overlain by several thin beds of white gypsum rock and grayish-red siltstone. These in turn are overlain by the Culebra dolomite member, a cliff-forming unit composed of massive yellowish-gray dolomite rock with distinctive pock-like cavities on weathered surfaces. The Culebra is approximately 10 meters thick at the margin of the basin and is overlain by a poorly exposed sequence of grayish-red siltstone and white gypsum rock which in the subsurface, contains most of the

Figure 33.--Cross-bedded quartz sandstone near the base of the Rustler formation at Red Bluff, New Mexico.

halite rock of the formation. This sequence is overlain by the Magenta member (Adams, 1944) which consists of thin-bedded dolomite and gypsum rock. Beds of pale yellowish-green gypsum 5 centimeters thick, with flat lower surfaces and botyroidal upper surfaces are intercalated with beds of grayish red purple dolomite. The gypsum layers also contain dolomite laminae which conform to the botyroidal structure.

At the top of the formation, two thick beds of white gypsum rock with pale yellowish-green streaks are separated by a 3-meter bed of moderate reddish-brown sandy siltstone that is similar to the siltstone of the overlying Pierce Canyon formation.

The geologic age of the Rustler is important because the formation was laid down at or near the close of Permian time and, therefore, also of Paleozoic time. Fossils are rare in the formations above the Capitan limestone and its equivalents, but a brachiopod and molluscan fauna has been described by Walter (1953) from the Culebra member and units underlying it, at the base of the Rustler formation. Walter's statement on the age indicated by this fauna is as follows:

> The brachiopod fauna is diagnostic of neither time nor facies. With the exception of Euphemites circumcostatus Walter n. sp., which may be significant of a young age, the gastropods are not particularly diagnostic. . . .Of the known Guadalupian faunas, those of the Whitehorse more closely resemble the Rustler molluscan fauna.

Oriel (in press) has reviewed the stratigraphic and paleontologic evidence bearing on the position of the top of the Permian system. It is significant that in parts of Arizona, Utah, and Montana (Spieker, 1956, p. 1808; Moritz, 1951, p. 1785) rocks of Permian age are overlain with apparent conformity by rocks of Early Triassic

age. In New Mexico and Texas the rocks above the Capitan limestone are probably of sufficient thickness to account for fossiliferous rocks in other parts of the world (Schenck and others, 1941, p. 2199) that are younger than the Guadalupe series and older than Lower Triassic.

Evidence available at the present time suggests that the boundary between the Permian and Triassic systems in this area lies near the contact between the Rustler and overlying Pierce Canyon formations. When the boundary can be placed more precisely in this conformable sequence, it is anticipated that it will not be marked by an important lithologic discontinuity unless one is specifically assigned to it by convention.

## Rocks of Permian or Triassic age

Pierce Canyon redbeds.--The Pierce Canyon redbeds were named by Lang in 1935 from exposures and drill hole samples in the Delaware Basin. In the subsurface of the Midland Basin, the name Dewey Lake redbeds was applied to this stratigraphic unit by Page and Adams in 1938. The formation is continuous across the Central Basin Platform between the two basins, and its continuity is established by correlation of well logs. (Most geologists dealing with the subsurface have preferred the name Dewey Lake for the unit, even in the Delaware Basin; see Ahlen and others, 1958.

Miller (1957 and unpublished) has shown that the microscopic petrology of the Pierce Canyon redbeds is closely akin to that of the underlying Rustler formation but differs sharply from that of overlying rocks of Late Triassic age. The Pierce Canyon rests with

conformity on a 12-meter bed of gypsum rock at the top of the Rustler. In outcrop this contact is irregular and superficially resembles an unconformity because the gypsum was distorted during its hydration from anhydrite.

The Pierce Canyon is a uniform sequence of moderate reddish-brown sandy siltstone containing distinctive light greenish-gray reduction spots 3 millimeters in diameter. Its thickness is approximately 60 meters in the area just east of this report (see appendix), but in places where more strata are preserved below the erosion surface at the base of Upper Triassic rocks, it is more than 120 meters thick.

## Rocks of Cretaceous age

In the NE1/2 sec. 31, T. 25 S., R. 25 E., about 100 meters southeast of U. S. Highway 62, an elliptical area about 100 meters long contains abundant marine fossils of early Washita age. The area is bounded by gypsum rock and contains a breccia composed of quartz sandstone and limestone blocks that contain the fossils. Lang (1947) has interpreted the breccia as material that collapsed into a sinkhole. The locality is significant because it shows that rocks of Cretaceous age once extended across the area, but it is too small for inclusion on the geologic map (fig. 20). Fifteen kilometers south of the southern border of the map area, rocks of Cretaceous age occur in their normal stratigraphic positions.

## Rocks of Tertiary or Quaternary age

The Gatuna formation of Pleistocene(?) age (Lang, 1938) occupies a broad belt on the east side of the Pecos River, and a few outliers

on the west side have survived erosion. It contains grayish orange pink to moderate reddish brown quartz sandstone, siltstone, and conglomerate. Much of this material was derived from underlying redbeds of Permian and Triassic age, but the Gatuna also contains a large percent of volcanic ash. Cross stratification is ubiquitous in the formation, and some individual sandstone channels are as much as 10 meters thick and 30 meters wide.

Detailed studies were not made of the Gatuna formation in this investigation and it is not mapped on figure 20. Although it is easily differentiated by its lithology from rocks of Paleozoic and Mesozoic age, the internal relations of the Gatuna are complicated by collapse resulting from solution of underlying evaporite deposits. No fossils were found in the formation and therefore its age designation could not be verified. In the field work, the Gatuna formation was never seen to overlie the Ogallala formation (Darton, 1899) of Miocene(?) and Pliocene age which crops out to the east of the map area; and the Gatuna may, in fact, be a basal member of the Ogallala rather than being younger as accepted at present by most geologists familiar with the rocks. The physiographic criteria commonly employed in this region for distinguishing between Cenozoic stratigraphic units should be abandoned in the light of the extensive modification of topography by solution that has occurred and is still occurring.

An erosion surface at the base of the Gatuna formation truncates progressively older rocks to the west. East of the map area, the rocks of the Gatuna formation are poorly exposed and are largely covered by surficial material.

## Deposits of Quaternary age

Alluvium is locally present along the streams, and in places stream gravel has been cemented by gypsum and calcite into well-indurated conglomerate. Caliche, possibly of several ages, is widespread, especially on the east side of the area, and it is locally as much as 10 meters thick. In order better to depict the older geologic units central to this report, these surficial deposits have not been included on the geologic map (fig. 20).

## Structure

In the area of the northwest margin of the Delaware Basin, structure includes both tectonic types and types resulting from solution at depth. It is difficult in the field to separate the two; and they, in turn, are further complicated by differential compaction over the abrupt facies changes at the margin of the basin.

### Folds and faults

The principal structure of the northwest margin of the Delaware Basin is a homocline with uniform eastward dip of $1\frac{1}{2}^{\circ}$ which affects the deposits of Permian age and to a slightly lesser extent, those of late Cenozoic age. Superimposed on this regional dip are minor anticlines and synclines that trend northeast in the vicinity of the Capitan limestone belt. These may in part be related to differential compaction or to solution.

Many northwest-trending normal faults which mark the margin between the Great Plains and Basin and Range Provinces of the United

States occur just beyond the southwest corner of the area. The rocks were downfaulted to the west in late Cenozoic time during the uplift of the Guadalupe Mountains. A few northeast-trending normal faults also cut the rocks in the Delaware Basin and along Guadalupe Ridge. Those that affect the Capitan limestone commonly occur in pairs so as to form grabens in which keystone blocks have been downdropped. These are thought to have resulted from tension developed during warping at the margin of the basin, either because of differential compaction, solution, or tectonic causes.

## Collapse features

The east dip of rocks of the area combined with subsequent erosion has brought formations that contain salt at depth to the surface. The salt itself does not crop out, however, and its removal has resulted in many structural complications of the outcropping formations.

Nevertheless, the leaching of the salt ordinarily is more uniform than might perhaps be expected, and the upper surface of the unleached rock is nearly a plane, normally at a depth of somewhat more than 100 meters. Overlying formations are not too greatly disturbed, and their outcrop patterns on small-scale maps are fairly normal. In detail, the formations are somewhat broken and warped, and in places beds are displaced slightly from their proper stratigraphic positions.

Locally, however, salt has been differentially dissolved and overlying rocks are brecciated and far below their normal positions. An example involving Cretaceous rocks has been outlined above. Another sinkhole more than 2 kilometers in diameter, at the northwest shore of

Red Bluff Lake, Texas, contains rocks belonging to the Pierce Canyon formation and younger rocks that are nearly 300 meters below their normal stratigraphic positions. Similar less extreme cases are common in the area.

Some salt solution probably is related to erosion surfaces older than the present one. The area was truncated at least three times, and some of the leaching probably occurred during these periods.

Also significant is salt solution not closely related to erosion surfaces. In a narrow belt directly over the Capitan limestone around the margin of the Delaware Basin, the Salado formation has been greatly thinned by solution, and for long distances the salt in the formation has been entirely removed. Maley and Huffington (1953) suggest that this solution was accomplished by surficial water which entered the salt from above along fractures opened by differential compaction at the margin of the basin. As the top of the Salado formation is more than 600 meters below the surface, however, in places where it has been completely leached, this explanation is believed to be untenable, and it is proposed here that the solution was accomplished by upward-moving water from the west which was driven by artesian pressure.

This water is thought to have moved across the basin from the eroded edge of the underlying Delaware Mountain group in the Delaware Mountains. When it reached the facies change at the edge of the sandstone group it rose to the surface and leached the salt along its course.

The geologic formations that are thickened along a line overlying this belt of leached salt can be employed to interpret the structural

and hydrodynamic history of the Delaware Basin. Rocks of Triassic age are abnormally thick in this belt across the north margins of both the Delaware and Midland Basins, implying that in Triassic time the rocks dipped to the north, and the sandstone units of both basins cropped out in mountains to the south.

On the east side of the Delaware Basin, deposits of late Cenozoic age thicken above the leached salt. This reflects the present structure and topography of the basin in which water is moving 100 kilometers eastward through permeable rocks from a catchment area in the Delaware Mountains.

## Facies relations of evaporite formations

The interfingering relationship between the predominately halite-bearing Salado formation and the other evaporite and clastic rocks with which it is associated may provide a clue to the origin of the evaporite deposits of the West Texas Basin and similar evaporite sequences in other parts of the world.

At the north edge of the West Texas Basin, north of the area considered in detail in this report, halite rock of the Salado formation interfingers with redbeds of terrigenous origin. At the south edge of the basin, the formations above and below the Salado formation each thicken at the expense of the Salado. Anhydrite rock of the underlying Castile formation occupies a progressively larger part of the sequence toward the south edge of the basin (fig. 23). Similarly, the clastic and carbonate rocks of the overlying Rustler formation replace the Salado at the south (fig. 21).

The sequence from south to north of gypsum, halite, and redbeds in the Castile and Salado formations suggests that the Permian sea lay to the south beyond the present outcrops in the Apache Mountains. This supposition is supported by the observation that dolomite rock interfingers with anhydrite of the Castile formation farther southeast in the Glass Mountains (Adams, 1944).

The overlying clastic rocks of the Rustler formation may represent a barrier beach north of which contemporaneous halite rock of the Salado formation was formed. The environment favoring quartz and carbonate sand deposition in the Rustler formation transgressed northward through the

basin. At the conclusion of Salado and Rustler deposition, the sea retreated again to the south, and in its wake the tidal-flat deposits of the Pierce Canyon redbeds were laid down. The deposition of the Pierce Canyon in latest Permian or earliest Triassic time marked the end of evaporite deposition in West Texas Basin.

Marine evaporite deposits derive most of their components from sea water so their composition reflects in a general way the composition of the oceans. The behavior of certain ions during evaporation, however, causes them to be present in quantities quite different from their relative concentration in the sea. In addition, the operation of other processes besides evaporation may introduce organic, detrital, volcanic, and cosmic material into the sediments; and later changes related to pressure, ground-water movement, and tectonic activity may further alter the chemistry.

## Laboratory investigation of salt deposition

In a classic series of experiments in 1849, Usiglio evaporated sea water to dryness to determine the sequence of compounds that is obtained. Some of Usiglio's determinations have been questioned, and a check of his results for sulfate and carbonate minerals using the methods of mineralogical analysis that have become available in the last 100 years seemed desirable.

Fifty liters of sea water were obtained from Gordon A. Riley of the Bingham Oceanographic Laboratory, Yale University, for use in this work. The water was taken in glass from the surface of the middle of Long Island Sound and is less saline than water from the open sea water. Its salinity is 2.74 percent, in contrast with 3.45 percent for normal sea water. The water was clear when first obtained, but after standing for several weeks in a warm room a brown gelatinous deposit, probably composed of dead plankton, accumulated on the bottom of the bottle. The water was decanted for use in the experiments.

The sample of sea water was evaporated to dryness in the laboratory at three different temperatures: 10°, 69°, and 105°C. Successive salts were collected at periodic intervals as they were deposited during each evaporation experiment.

## Method

The data given by Usiglio (1849, p. 185) suggest that the major components of sea water (carbonate, sulfate, sodium chloride, and potassium and magnesium salts) can be fairly well separated by evaporation provided suitable limits are chosen. The salts laid down during concentration of sea water from the Mediterranean Sea are listed in table 2. The ranges of concentration for Usiglio's Mediterranean sample in which each of the four components was dominantly concentrated are given in table 3 and are compared with the calculated corresponding concentrations of Long Island Sound water of lesser salinity used in these studies.

(Text continued on page 94)

Table 2.—Salts laid down during concentration of sea water (grams)

(After Usiglio, 1849)

| Volume (liter) | $Fe_2O_3$ | $CaCO_3$ | $CaSO_4 \cdot 2H_2O$ | NaCl | $MgSO_4$ | $MgCl_2$ | NaBr | KCl |
|---|---|---|---|---|---|---|---|---|
| 1.000 | -- | -- | -- | -- | -- | -- | -- | -- |
| 0.5333 | 0.0030 | 0.0642 | -- | -- | -- | -- | -- | -- |
| 0.316 | -- | trace | -- | -- | -- | -- | -- | -- |
| 0.245 | -- | trace | -- | -- | -- | -- | -- | -- |
| 0.190 | -- | 0.0530 | 0.5600 | -- | -- | -- | -- | -- |
| 0.1445 | -- | -- | 0.5620 | -- | -- | -- | -- | -- |
| 0.131 | -- | -- | 0.1840 | -- | -- | -- | -- | -- |
| 0.112 | -- | -- | 0.1600 | -- | -- | -- | -- | -- |
| 0.095 | -- | -- | 0.0508 | 3.2614 | 0.0040 | 0.0078 | -- | -- |
| 0.064 | -- | -- | 0.1476 | 9.6500 | 0.0130 | 0.0356 | -- | -- |
| 0.039 | -- | -- | 0.0700 | 7.8960 | 0.0262 | 0.0434 | 0.0728 | -- |
| 0.0302 | -- | -- | 0.0144 | 2.6240 | 0.0174 | 0.0150 | 0.0358 | -- |
| 0.023 | -- | -- | -- | 2.2720 | 0.0254 | 0.0240 | 0.0518 | -- |
| 0.0162 | -- | -- | -- | 1.4040 | 0.5382 | 0.0274 | 0.0620 | -- |
| 0.0000 | -- | -- | -- | 2.5885 | 1.8545 | 3.1640 | 0.3300 | 0.5339 |
| Sum | 0.0030 | 0.1172 | 1.7488 | 29.6959 | 2.4787 | 3.3172 | 0.5524 | 0.5339 |

Table 3.--Concentrations of sea water in which marine salts are approximately separated into four major components (Data in middle column from Usiglio, 1849)

| Fraction | Mediterranean Sea Salinity 3.766 percent (liters) | Long Island Sound Salinity 2.74 percent (liters) |
|---|---|---|
| Carbonate | 1.0 -0.21 | 1.0 -0.15 |
| Sulfate | 0.21-0.11 | 0.15-0.08 |
| Sodium chloride | 0.11-0.03 | 0.08-0.02 |
| K and Mg salt | 0.03-0.00 | 0.02-0.00 |

In the first run, 3,333 milliliters of water were evaporated by boiling in a covered beaker. The boiling began with 1,000 milliliters of water and as the water was boiled down more was added until 3,333 milliliters had been evaporated to 500 milliliters. Fresh sea water was heated to boiling before it was added to the brine so that the temperature of the solution remained constant.

When the volume reached 500 milliliters, some salts had been deposited, and the brine was transferred to another beaker in which the boiling was continued. The first salt sample was composed of material precipitated in the first beaker and subsequent samples were obtained at intervals in the same way. The samples obtained in this run which evaporated at a temperature averaging 105°C are given in table 4.

(Text continued on page 95)

Table 4.--Samples obtained from Long Island Sound water evaporated at 105°C

| Sample number | Volume (milliliters) | Quantity (grams) |
|---|---|---|
| 1-1 | 3333-500 | 5.2 |
| 1-2 | 500-267 | 9.9 |
| 1-3 | 267- 67 | 166.5 |
| 1-4 | 67- 0 | 7.1 |

The second run, at approximately 69°C, was similar to the first except that the sample was evaporated in a sealed vessel under vacuum. The rate of evaporation and temperature of the solution were controlled by a boiling water bath around the sample and a water aspirator which provided a mild vacuum over the sample. The relations between the flask holding the sample and the other pieces of apparatus are shown in figure 34.

During most of the crystallization, the temperature of the sample remained at 60° ± 1°C, but the temperature was cooler when the sample was removed from the bath for collection of the salt. At the end of each sample period the salts were collected on filter paper and the volume of remaining liquid was determined. As some salt adhered to the walls of the flask, the weight of salt given below is the sum of the weight of that collected plus the excess weight of the dry flask. As in the first run, the filtered liquor was returned to a clean container after the removal of each sample. A sea water sample of 3,333 milliliters was used in this run and the evaporation took about 15 hours; the results are given in table 5.

(Text continued on page 97)

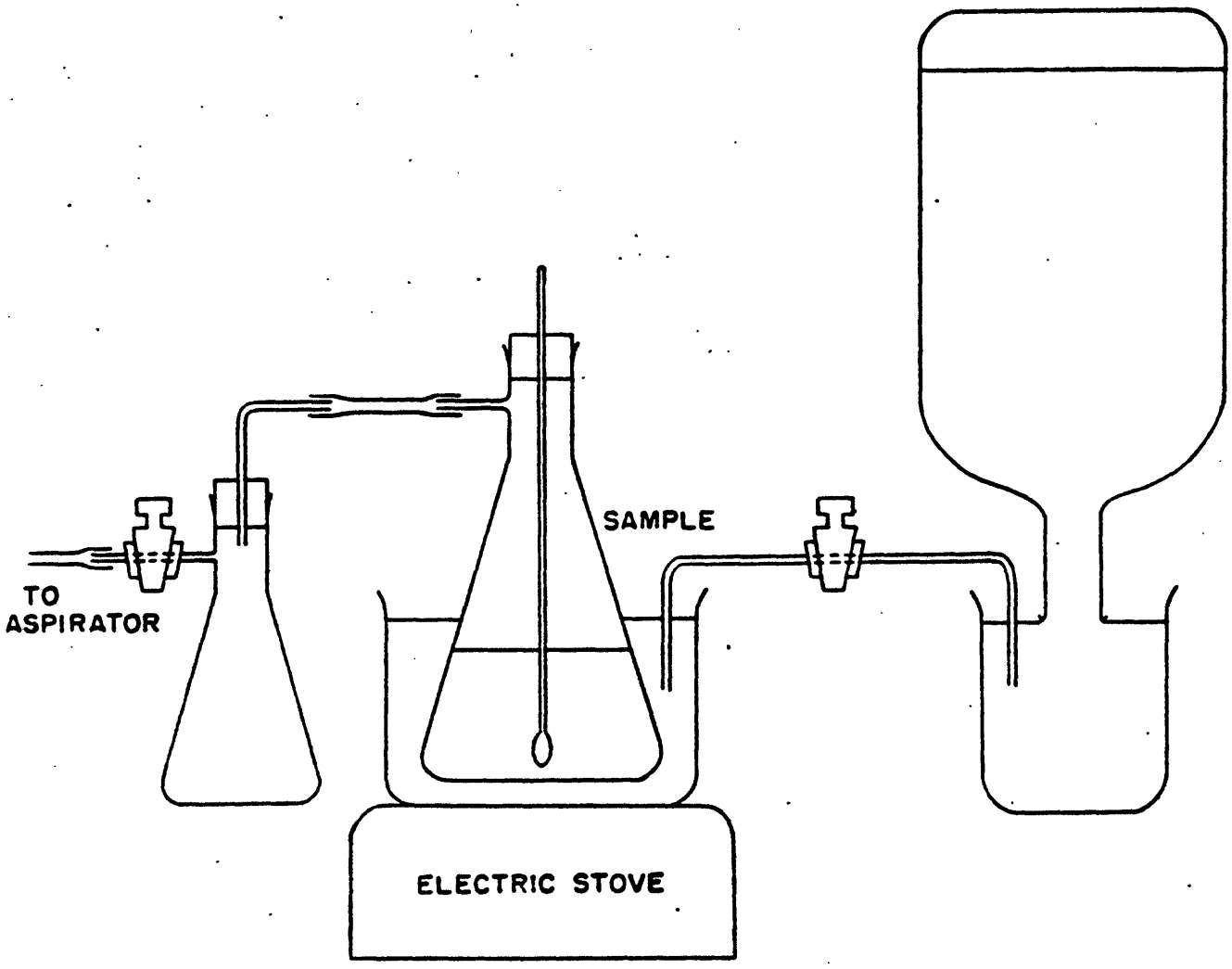


Figure 34.--Arrangement of apparatus for the evaporation of sea water at approximately 69°C.

Table 5.--Samples obtained from Long Island Sound water evaporated at 69°C

| Sample number | Volume (milliliters) | Quantity (grams) |
|---|---|---|
| 2-1 | 3333-228 | 18.4 |
| 2-2 | 228-105 | 44.1 |
| 2-3 | 105- 48 | 20.1 |
| 2-4 | 48- 23 | 8.9 |
| 2-5 | 23- 0 | 10.5 |

The third run was similar to the others except that an oil pump was used for the evaporation so that a lower temperature could be achieved. The sample was placed in a sealed flask exposed to room temperature and the water evaporated from it was collected in traps as shown in figure 35. During most of the crystallization the temperature stood at $10° \pm 1°C$, but during times when the salt samples were being collected the temperature was somewhat higher. A sea water sample of 3,333 milliliters was used in this run, as in the others, and about 270 hours were required for the evaporation. The salts were removed periodically and at these times the volume of remaining liquid was measured. The crystallization began when the volume reached about 350 milliliters. The approximate weights of the salt samples are given in table 6 along with the volume of water from which they were derived.

(Text continued on page 99)

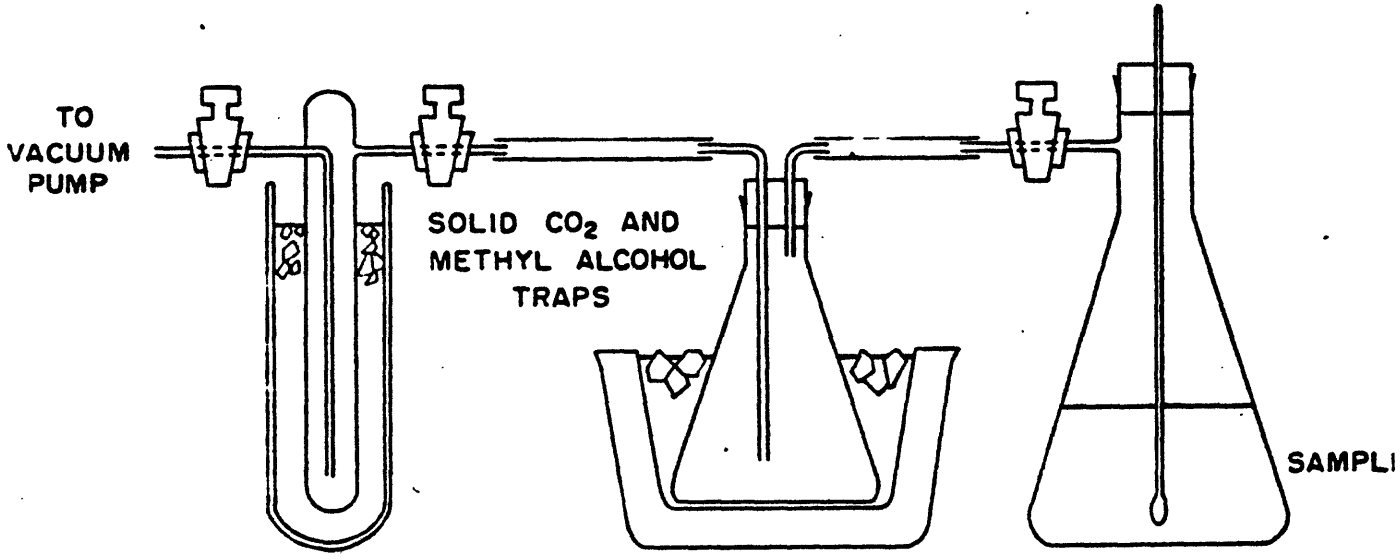


Figure 35.--Arrangement of apparatus for the evaporation of sea water at approximately 10°C.

Table 6.--Samples obtained from Long Island Sound water evaporated at 10°C

| Sample number | Volume (Milliliters) | Quantity (grams) |
|---|---|---|
| 3-1 | 3333-276 | 3.9 |
| 3-2 | 276-230 | 3.1 |
| 3-3 | 230-160 | 17.5 |
| 3-4 | 160-117 | 7.6 |
| 3-5 | 117- 70 | 9.4 |
| 3-6 | 70- 28 | 7.9 |
| 3-7 | 28- 0 | 15.4 |

The principal difficulty with these experiments was the inability to control the size of individual salt samples by the methods used. Deposition was so rapid, especially in the high-temperature runs, that it was possible to allow only a brief period of stabilization of the temperature of the solution before it was necessary to remove the next sample. Hence no control could be obtained between the several runs so that the samples would be of the same weight or from the same part of the evaporation sequence. This is not believed to be a disadvantage to the mineralogical results given here, however, because chief concern is with the first one or two samples in each run.

Mineral determinations were made by X-ray methods employing a North American-Phillips machine. These identifications were supplemented by determinations of refractive index.

## Results

The salts separated into fractions much as was expected. Only in the run at 105°C, however, was there sufficient carbonate in the first fraction

for analysis. It is calcite. The first fraction in the run at 10 C was smaller than that in the run at 105°C (3.9 as compared with 5.2 grams), so it is curious that no carbonate mineral was found in the run at 10°C as it should have been less diluted with sulfate. The sample actually consisted of euhedral crystals of gypsum. Perhaps the high vacuum employed in this run removed carbon dioxide from solution and caused hydroxyl ion to form at the expense of carbonate. Under some conditions, loss of carbon dioxide from solutions containing bicarbonate ion results in the precipitation of calcium carbonate according to the following reaction

$$Ca^{++} + 2HCO_3^- = CO_2 + CaCO_3 + H_2O$$

Under conditions where rates of reaction are low, however, and strong supersaturation with respect to bicarbonate ion can be expected, removal of carbon dioxide causes bicarbonate to break down into hydroxyl ion as follows

$$HCO_3^- = OH^- + CO_2$$

This proposed mechanism is the reverse of the first part of the familiar lime-water experiment where carbon dioxide from the breath is added to a solution of calcium hydroxide to form a precipitate of calcium carbonate.

The sulfate compound formed in each sample of the run at 10°C is gypsum; that formed in the runs at 69 and 105°C is the hemihydrate of calcium sulfate, bassanite ($2CaSO_4 \cdot H_2O$).

Studies by D'Ans and others (1955) indicate that under equilibrium conditions, in a solution saturated with respect to sodium chloride, gypsum forms at a temperature less than 18°C, anhydrite at temperatures

between 18 and 76°C, and the hemihydrate at temperatures greater than 76°C. As anhydrite did not form at 69°C in samples that also contained halite and hence were saturated with respect to sodium chloride, conditions of thermodynamic equilibrium evidently did not obtain. It is thought that bassanite formed in the run at 69°C because evaporation took place under vacuum at a rapid rate allowing supersaturation of the solution to the point where the solubility of the hemihydrate as well as that of anhydrite was exceeded. The rate of reaction for the metastable hemihydrate is faster than that of anhydrite, so bassanite was deposited.

These experiments open the possibility that, under natural conditions, sulfate minerals might form outside their normal range of stability by supersaturation accompanying very rapid precipitation. Under such conditions the more soluble minerals bassanite and gypsum would be favored over anhydrite. Bassanite is so unstable under conditions at the surface, however, that the process, in effect, would operate simply to favor gypsum over anhydrite.

## Chemical composition of evaporite rocks

The chemical composition of sea water is perhaps better known than that of any other natural substance. Water of the oceans contains about 3.45 percent solid material in solution, and the approximate concentration of more than 50 elements has been established.

The physical and chemical factors controlling the formation of marine evaporite deposits are such that the ratios between components in

the deposits are not the same as those of sea water. In contrast with our knowledge of sea water, the chemical composition of these deposits has been less well known in the past than that of most other important groups of rocks.

The purpose of this section is to present an estimate of the average chemical composition of evaporite deposits. Many new chemical analyses of rock salt and associated sediments are given, and earlier published analyses are summarized.

## Relation to lithology

Several areas in the United States, in addition to the area of this investigation, are underlain by thick sequences of salt. For example, bedded salt of Silurian age occurs in New York and nearby states; of Devonian age in North Dakota and Montana; of Pennsylvanian age in Utah and Colorado; and of Permian age in Kansas.

Halite rock is nearly always associated in evaporite deposits with anhydrite rock as is the case in the West Texas Basin. Other common associates are claystone and carbonate rocks, including dolomite rock and limestone. Black shale, sandstone, and siltstone are less common in evaporite deposits but each is important in some regions.

As salt is a relatively light material with a specific gravity of 2.17 and in many places is overlain by heavier rocks whose specific gravities are 2.5 or more, evaporite deposits are commonly unstable with respect to gravity. In regions of marked tectonic activity, elongate masses of salt tend to rise through the overlying rocks because of the density difference. These bodies, the well-known salt anticlines, may

breach younger rocks and reach the surface of the earth. Several such anticlines occur in the Paradox Basin of Utah and Colorado.

In regions of less pronounced tectonic activity, the rising salt masses tend toward more equidimensional shapes in the form of salt plugs. Salt plugs composed of salt of Permian(?) age are common in the Gulf Coast region from Texas to Alabama. Salt anticlines and salt plugs also occur in other places in the world.

Although chemical precipitation as a result of evaporation is the process that is dominant in the formation of evaporite deposits, other processes play a part in their deposition and resulting chemical composition. Two such processes are the action of organisms which produce biogenic limestone and organic black shale, and the transportation of water-borne detrital material with the resultant formation of beds of sandstone and claystone. Of lesser importance is transportation through the air which may lead to the incorporation of small quantities of volcanic ash, windblown silt, and cosmic dust into the sediments. Highly soluble components may be introduced before their normal position in the evaporation sequence in minute inclusions of brine trapped within the crystals of certain minerals.

In places evaporite deposits are modified after deposition by secondary processes which may change their chemical composition. Solutions either of remobilized brine, water from the dehydration of hydrous minerals, or meteoric ground water may alter the composition of the deposits. More important, such waters may cause recrystallization and secondary segregations of some minerals. In a few local areas volcanic rocks have intruded salt deposits, and dikes, sills, and volcanic solutions have been

introduced into the formations. Finally, in areas where the salt itself has begun to flow upward into plugs or anticlines through overlying sediments, rocks of various types may be plucked from the walls and included in the salt. These extraneous rocks usually do not bulk large in the salt bodies but may slightly change their gross chemical compositions.

## Major elements

The chemical composition of 53 dissolved constituents of sea water expressed as percent of total solutes is given in table 7. Disregarding the oxygen and hydrogen, the elements of sea water may be divided into three groups with respect to their abundance. Chlorine and sodium, which together make up 85 percent of the salt in the ocean, may be considered as one group. Magnesium, sulfur, calcium, and potassium range between 1 and 4 percent and comprise a second group. None of the rest of the elements makes up more than 0.2 percent of the total solids, and they may be considered together as a third group. The elements of the first two groups are generally present in salt deposits in concentrations sufficiently great so that they may be detected by routine analytical methods.

The first detailed laboratory studies on the salts deposited during the evaporation of sea water were made by Usiglio (1849) on water from the Mediterranean Sea. The character of the salts laid down at successive stages of concentration were as follows: ferric oxide and calcium carbonate, gypsum (hydrous calcium sulfate), sodium chloride, and, finally, the highly soluble potassium and magnesium compounds some of which remained in the final liquor.

Table 7.--Dissolved constituents of sea water.

(After Harvey, 1953; Richards, 1957)

| Element | Percent | Element | Percent |
|---|---|---|---|
| A | $8.10^{-4}$ | Mg | 3.7 |
| Ag | $9.10^{-7}$ | Mn | $9.10^{-6}$ |
| Al | $4.10^{-4}$ | Mo | $3.10^{-5}$ |
| As | $9.10^{-6}$ | N | 0.02 |
| Au | $3.10^{-7}$ | Na | 30 |
| B | 0.01 | Ne | $7.10^{-7}$ |
| Ba | $2.10^{-4}$ | Ni | $1.10^{-6}$ |
| Bi | $6.10^{-7}$ | P | $2.10^{-4}$ |
| Br | 0.19 | Pb | $9.10^{-6}$ |
| C | 0.08 | Ra | $3.10^{-13}$ |
| Ca | 1.2 | Rb | $6.10^{-4}$ |
| Cd | $2.10^{-7}$ | Rn | $3.10^{-17}$ |
| Ce | $1.10^{-6}$ | S | 2.7 |
| Cl | 55 | Sb | $6.10^{-7}$ |
| Co | $1.10^{-6}$ | Se | $1.10^{-7}$ |
| Cr | $3.10^{-7}$ | Se | $1.10^{-5}$ |
| Cs | $6.10^{-6}$ | Si | $8.10^{-3}$ |
| Cu | $9.10^{-6}$ | Sn | $9.10^{-6}$ |
| F | $4.10^{-3}$ | Sr | 0.03 |
| Fe | $1.10^{-5}$ | Th | $1.10^{-7}$ |
| Ga | $1.10^{-6}$ | Ti | $3.10^{-6}$ |
| He | $9.10^{-8}$ | U | $6.10^{-6}$ |
| Hg | $9.10^{-8}$ | V | $6.10^{-6}$ |
| I | $1.10^{-4}$ | W | $3.10^{-7}$ |
| K | 1.1 | Y | $9.10^{-7}$ |
| La | $9.10^{-7}$ | Zn | $2.10^{-5}$ |
| Li | $1.10^{-4}$ | | |

The general picture which Usiglio obtained in his laboratory studies is commonly reflected in the sequence of evaporite deposits in nature. Beds of limestone or dolomite rock are usually overlain by rocks composed of calcium sulfate, then sodium chloride, and finally the more soluble minerals of potassium and magnesium. Table 8 lists some of the minerals commonly found in marine evaporite deposits.

More detailed studies have been made by Van't Hoff and his co-workers (1912), particularly of the part of the system in which magnesium and potassium minerals are deposited. Van't Hoff also applied the principles of physical chemistry and the phase rule to the separation of salts from solution. Instead of beginning with complex sea water, he prepared artificial solutions of various compositions and studied the relations at different temperatures. The final results of his work and that of later workers, of which the data of D'Ans (1933) are perhaps the most complete, were a series of phase diagrams by which the minerals probably deposited from sea water at certain temperatures may be predicted. For example, at a temperature of 25°C in a solution saturated with respect to sodium chloride the following minerals will be deposited in this order: bloedite, epsomite, kainite-epsomite, hexahydrite-kainite, kieserite-kainite, kieserite-carnallite, and, finally, the three salts kieserite-carnallite-bischofite precipitating together until the evaporation is complete (Phillips, 1947).

Van't Hoff applied his results to the salt deposits of Stassfurt, Germany, and found that the Stassfurt deposits contain many minerals which can form only at temperatures close to that of boiling water. He therefore first interpreted the evidence as suggesting that the Stassfurt Sea was very warm. It is now recognized that these deposits were deeply

(Text continued on page 108).

Table 8.--Some minerals of evaporite deposits.

| | |
|---|---|
| Anhydrite | $CaSO_4$ |
| Aragonite | $CaCO_3$ |
| Bischofite | $MgCl_2.6H_2O$ |
| Bloedite | $Na_2Mg(SO_4)_2.4H_2O$ |
| Calcite | $CaCO_3$ |
| Carnallite | $KMgCl_3.6H_2O$ |
| Dolomite | $CaMg(CO_3)_2$ |
| Epsomite | $MgSO_4.7H_2O$ |
| Gypsum | $CaSO_4.2H_2O$ |
| Halite | $NaCl$ |
| Hexahydrite | $MgSO_4.6H_2O$ |
| Kainite | $KMgSO_4Cl.3H_2O$ |
| Kieserite | $MgSO_4.H_2O$ |
| Langbeinite | $K_2Mg_2(SO_4)_3$ |
| Leonite | $K_2Mg(SO_4)_2.4H_2O$ |
| Picromerite (schönite) | $K_2Mg(SO_4)_2.6H_2O$ |
| Polyhalite | $K_2Ca_2Mg(SO_4)_4.2H_2O$ |
| Sylvite | $KCl$ |

buried after their formation, and the present mineralogy reflects an increased temperature and pressure to which the rocks were subjected at depth.

Abundant evidence exists in salt deposits throughout the world that few of the potassium and magnesium minerals that now occur in the deposits were laid down in their present form from sea water. Both post-depositional temperature changes and migrating solutions have altered their character. Polyhalite, one of the most common minerals of American potash deposits, was probably not deposited from an original brine but came about by replacement of anhydrite or gypsum.

Anhydrite is the most common sulfate mineral of salt deposits, but probably it made up little of the original sulfate content of the deposits. The physiochemical studies discussed earlier, and the exclusive presence of gypsum in solar evaporation basins in California and Mexico, suggest that most calcium sulfate in evaporite deposits probably originally was deposited as gypsum, even though it is now anhydrite. The heat and pressure of burial are thought to cause the transformation. Water made available by the process contributes to other changes in the chemistry of salt deposits.

## Minor elements

Many salt plugs possess a near-surface cap rock composed predominantly of gypsum and anhydrite. This cap rock is believed to have been formed by the solution of salt by ground water as the plug moved upward resulting in the concentration of impurities as a residual deposit.

Salt dome cap rocks in places contain concentrations of unusual minerals suggesting that the chemical composition of the salt may not be simple (Goldman, 1952). Microscopic studies of water-insoluble residues from the salt itself in domes has also shown that rare minerals are present (Taylor, 1937). Table 9 is a list of minerals which have been found in water insoluble residues of salt.

When the present investigation was started, it was found that the average concentration of minor elements in salt deposits was poorly known. Therefore, samples of halite rock and associated sediments were collected for analysis.

The samples used in this work came from deep core holes drilled with brine to prevent solution of soluble minerals. Samples were analyzed from salt beds of Cambrian age from the Siberian Platform, U.S.S.R.; from the Paradox member of the Hermosa formation of Pennsylvanian age near Moab, Utah; from the Salado formation of Permian age near Carlsbad, New Mexico; from three salt domes containing salt of Permian(?) age from the Gulf Coast region of Texas and Louisiana; and from an artificial salt pan in San Francisco Bay, California.

Analyses were made for 33 elements. The chemical composition of samples of halite rock are given in table 10; anhydrite rock and polyhalite rock in table 11; and limestone, claystone, and siltstone in table 12.

In addition to the analyses reported here, a review of published data on the chemical composition of halite rock has been made. This information is integrated with the new data in table 13 which is an estimate of the average concentration of 41 elements in halite rock.

Table 9.--Minerals from water-insoluble residues of salt deposits.
(After Taylor, 1937)

| Mineral | Composition |
|---|---|
| Anhydrite | $CaSO_4$ |
| Aragonite | $CaCO_3$ |
| Barite | $BaSO_4$ |
| Boracite | $Mg_3B_7O_{13}Cl$ |
| Brookite | $TiO_2$ |
| Calcite | $CaCO_3$ |
| Celestite | $SrSO_4$ |
| Chalcocite | $Cu_2S$ |
| Chlorite | $H_4Fe_3Si_2O_9$ |
| Dolomite | $CaMg(CO_3)_2$ |
| Fluorite | $CaF_2$ |
| Gibbsite | $Al(OH)_3$ |
| Goethite | $HFeO_2$ |
| Gypsum | $CaSO_4.2H_2O$ |
| Hauerite | $MnS_2$ |
| Hematite | $Fe_2O_3$ |
| Kaolinite | $H_4Al_2Si_2O_9$ |
| Kaliborite | $KMg_2B_{11}O_{19}.9H_2O$ |
| Limonite | $HFeO_2.\underline{n}H_2O$ |
| Magnesite | $MgCO_3$ |
| Magnetite | $Fe_3O_4$ |
| Malachite | $CuCO_3$ |
| Opal | $SiO_2.\underline{n}H_2O$ |
| Pyrite | $FeS_2$ |
| Pyrrhotite | $Fe_{1-\underline{x}}S$ |
| Quartz | $SiO_2$ |
| Rutile | $TiO_2$ |
| Strontianite | $SrCO_3$ |
| Sulfoborite | $Mg_6H_4(BO_3)_4(SO_4)_2.7H_2O$ |
| Sulfur | S |
| Tourmaline | $H_8Na_2Fe_6B_6Al_{12}Si_{12}O_{62}$ |
| Zircon | $ZrSiO_4$ |

Table 10.--Analyses of halite rock in percent.

(Methods development and analyses supervised by F. S. Grimaldi.)

| | 1 | 2 | 3 | 4 | 5 |
|---|---|---|---|---|---|
| Ag | ---- | ---- | ---- | ---- | ---- |
| Al | 0.00032 | 0.0023 | 0.0035 | 0.0035 | 0.0011 |
| B | 0.000071 | 0.000053 | 0.00016 | 0.000065 | 0.00013 |
| Ba | 0.00002 | 0.00027 | 0.00018 | 0.00018 | 0.00009 |
| Br. | 0.032 | 0.002 | 0.02 | 0.003 | 0.004 |
| C | 0.008 | 0.006 | 0.01 | 0.006 | 0.01 |
| Ca | 0.24 | 0.47 | 1.16 | 0.13 | 1.09 |
| Cl | 59.78 | 59.57 | 57.94 | 60.13 | 58.43 |
| Cr | 0.0001 | ---- | ---- | ---- | ---- |
| Cu | 0.000088 | 0.00065 | 0.00023 | 0.00022 | 0.00055 |
| F | <0.0005 | 0.013 | 0.005 | <0.001 | <0.001 |
| Fe | 0.00077 | 0.00077 | 0.0015 | 0.0022 | 0.00091 |
| H | 0.002 | 0.001 | 0.017 | 0.003 | 0.001 |
| I | <0.0002 | <0.0002 | <0.0002 | <0.0002 | <0.0002 |
| K | 0.34 | 0.032 | 0.16 | 0.17 | 0.017 |
| Li | <0.0001 | ---- | ---- | ---- | ---- |
| Mg | 0.0042 | 0.025 | 0.13 | 0.066 | 0.0024 |
| Mn | <0.00002 | <0.00002 | <0.00002 | <0.00002 | <0.00043 |
| Mo | <0.00001 | <0.00003 | <0.00003 | <0.00003 | <0.00003 |
| Na | 38.59 | 38.61 | 37.40 | 38.82 | 37.92 |
| Ni | 0.00021 | 0.00016 | 0.00024 | 0.00020 | 0.00022 |
| O* | 0.77 | 0.87 | 2.11 | 0.45 | 1.63 |
| Pb | 0.00023 | 0.00012 | 0.00011 | 0.000074 | 0.00054 |
| S | 0.22 | 0.38 | 1.00 | 0.19 | 0.88 |
| Se | <0.00005 | <0.00005 | <0.00005 | <0.00005 | <0.00005 |
| Si | 0.012 | 0.0065 | 0.024 | 0.016 | 0.0022 |
| Sr | 0.00093 | 0.0085 | 0.018 | 0.0056 | 0.0062 |
| Th | <0.00002 | <0.00002 | <0.00002 | <0.00002 | <0.00002 |
| Ti | 0.00011 | 0.000060 | 0.00016 | 0.00013 | 0.000060 |
| U | 0.0000011 | 0.0000025 | 0.0000015 | 0.0000015 | 0.0000010 |
| V | <0.00003 | <0.00003 | <0.00003 | <0.00003 | <0.0003 |
| Zn | 0.00014 | 0.000056 | 0.000012 | 0.00011 | 0.00012 |
| Zr | <0.00004 | <0.00004 | <0.00004 | <0.00004 | <0.00004 |

*Difference from 100 percent, calculated.

(Continued on next page.)

Table 10.--Analyses of halite rock in percent--Continued.

| | 6 | 7 | 8 | 9 |
|---|---|---|---|---|
| Ag | ---- | ---- | ---- | 0.00001 |
| Al | 0.0013 | 0.0015 | 0.0011 | 0.00069 |
| B | 0.00001 | 0.00034 | 0.00037 | 0.00037 |
| Ba | 0.00009 | 0.00027 | 0.00027 | 0.00002 |
| Br | 0.003 | 0.005 | 0.01 | 0.10 |
| C | 0.006 | 0.006 | 0.006 | 0.01 |
| Ca | 1.54 | 1.72 | 0.46 | 0.16 |
| Cl | 57.71 | 56.97 | 59.74 | 59.47 |
| Cr | ---- | ---- | ---- | 0.0001 |
| Cu | 0.00023 | 0.00021 | 0.00010 | 0.000080 |
| F | <0.001 | <0.001 | 0.001 | <0.0005 |
| Fe | 0.00070 | 0.0013 | 0.00063 | 0.00052 |
| H | 0.001 | 0.001 | 0.002 | 0.073 |
| I | <0.0002 | <0.0002 | <0.0002 | <0.0002 |
| K | 0.0083 | 0.0027 | 0.0042 | 0.035 |
| Li | ---- | ---- | ---- | <0.0001 |
| Mg | 0.0097 | 0.010 | 0.011 | 0.13 |
| Mn | 0.0011 | 0.0020 | 0.00009 | 0.00020 |
| Mo | <0.00003 | <0.00003 | <0.00003 | <0.00001 |
| Na | 37.21 | 37.01 | 38.64 | 38.45 |
| Ni | 0.00035 | 0.00023 | 0.00035 | 0.00005 |
| $O^*$ | 2.28 | 2.87 | 0.75 | 1.41 |
| Pb | 0.00015 | 0.00012 | 0.000065 | 0.00034 |
| S | 1.22 | 1.39 | 0.36 | 0.24 |
| Se | <0.00005 | <0.00005 | <0.00005 | <0.00005 |
| Si | 0.0037 | 0.0065 | 0.0032 | 0.0061 |
| Sr | 0.0081 | 0.0052 | 0.0047 | 0.0074 |
| Th | <0.00002 | <0.00002 | <0.00002 | <0.00002 |
| Ti | 0.000096 | 0.000034 | 0.000060 | 0.00012 |
| U | 0.0000010 | 0.0000010 | 0.0000010 | 0.0000010 |
| V | <0.00003 | <0.00003 | <0.00003 | <0.00003 |
| Zn | 0.00030 | 0.00012 | 0.000008 | 0.00026 |
| Zr | <0.00004 | <0.00004 | <0.00004 | <0.00004 |

*Difference from 100 percent, calculated.

(Explanation on next page.)

Table 10.--Analyses of halite rock in percent--Continued

1. Massive halite rock; upper part of Lower Cambrian salt beds; from a test well in the southern part of the Siberian Platform, U.S.S.R.

2. Massive halite rock; Paradox member of the Hermosa formation of Pennsylvanian age; 2,394 ft.; Delhi-Taylor No. 8, sec. 1, T. 25 S., R. 20 E., Grand County, Utah.

3. Thin-bedded halite rock; Paradox member of the Hermosa formation of Pennsylvanian age; 2,902 ft.; Delhi-Taylor No. 8, sec. 1, T. 25 S., R. 20 E., Grand County, Utah.

4. Halite with polyhalite blebs; Salado formation of Permian age; 1,872 and 1,956 ft.; U. S. Potash Corp. No. 125 (S), sec. 25, T. 23 S., R. 34 E., Lea County, N. Mex.

5. Halite rock; Orchard salt dome; 1,258 to 1,275 ft.; Duval Sulphur and Potash Co., Moore Estate, well no. 554, Fort Bend County, Tex.

6. Halite rock; Venice salt dome; 2,893 to 2,896 ft.; Tidewater Oil Co., Buras Levee District, no. 5, Paquemines Parish, La.

7. Halite rock; Venice salt dome; 3,785 to 3,805 ft.; Tidewater Oil Co., Buras Levee District, no. 5, Paquemines Parish, La.

8. Halite rock, Block 16 salt dome; 2,351 to 2,361 ft.; Humble Oil Corp.; lease 800, core test no. 3, Jefferson Parish, La.

9. Halite; artificial salt pans of Leslie Salt Co., Newark, Calif.

Table 11.--Analyses of anhydrite rock and polyhalite rock in percent.

(Methods development and analyses supervised by F. S. Grimaldi.)

| | | 1 | 2 | 3 | 4 |
|---|---|---|---|---|---|
| Al | | 0.017 | 0.0042 | 0.0095 | 0.0095 |
| B | | 0.0021 | 0.00062 | 0.0013 | 0.00013 |
| Ba | | <0.0009 | 0.0023 | 0.0013 | 0.0015 |
| Br | | <0.002 | <0.002 | <0.002 | <0.002 |
| C | Carbonate | 1.76 | 0.18 | 2.82 | 0.041 |
| | Organic | 0.10 | 0.01 | 0.07 | 0.01 |
| | Total | 1.86 | 0.19 | 2.89 | 0.052 |
| Ca | | 27.17 | 25.44 | 22.43 | 11.81 |
| Cl | | 0.15 | 6.94 | 2.05 | 4.71 |
| Cu | | 0.0014 | 0.00046 | 0.00014 | 0.0013 |
| F | | <0.001 | <0.001 | 0.035 | 0.005 |
| Fe | | 1.03 | 0.0020 | 0.0084 | 0.0070 |
| H | | 0.060 | 0.028 | 0.007 | 0.61 |
| I | | <0.0002 | <0.0002 | <0.0002 | <0.0002 |
| K | | 0.17 | 0.025 | 0.075 | 11.83 |
| Mg | | 1.83 | 0.43 | 5.91 | 3.90 |
| Mn | | 0.015 | 0.00014 | 0.00093 | 0.00046 |
| Mo | | 0.00043 | <0.00003 | <0.00003 | <0.00003 |
| Na | | 0.067 | 4.67 | 1.31 | 3.06 |
| Ni | | 0.00012 | <0.00008 | 0.00008 | <0.00008 |
| O* | | 46.62 | 41.74 | 47.13 | 44.44 |
| Pb | | 0.00052 | 0.000084 | 0.000074 | 0.000046 |
| S | | 20.04 | 20.42 | 17.97 | 19.48 |
| Se | | <0.00005 | <0.00005 | <0.00005 | <0.00005 |
| Si | | 0.90 | 0.030 | 0.089 | 0.043 |
| Sr | | 0.054 | 0.071 | 0.074 | 0.040 |
| Th | | <0.00002 | <0.00002 | <0.00002 | <0.00002 |
| Ti | | 0.010 | 0.000078 | 0.0010 | 0.00050 |
| U | | 0.000042 | 0.000043 | 0.000025 | 0.0000015 |
| V | | 0.00025 | 0.00003 | 0.00012 | <0.00003 |
| Zn | | 0.000038 | 0.000034 | 0.00016 | 0.00025 |
| Zr | | 0.0036 | 0.0013 | 0.0038 | 0.0022 |

*Difference from 100 percent, calculated.

1. Anhydrite rock; Paradox member of the Hermosa formation of Pennsylvanian age; 3,616 ft.; Delhi-Taylor No. 8, sec. 1, T. 25 S., R. 20 E., Grand County, Utah.

Table 11.--Analyses of anhydrite rock and polyhalite rock in percent--Continued.

2. Massive anhydrite rock with minor halite inclusions; Salado formation of Permian age; 2,452 ft.; U. S. Potash Corp. No. 125(S), sec. 25, T. 23 S., R. 34 E., Lea County, N. Mex.

3. Laminated anhydrite rock (Cowden); Salado formation of Permian age; 2,841 ft.; U. S. Potash Corp. No. 125(S), sec. 25, T. 23 S., R. 34 E., Lea County, N. Mex.

4. Polyhalite rock with halite inclusions; Salado formation of Permian age; 2,125 ft.; U. S. Potash Corp. No. 125(S), sec. 25, T. 23 S., R. 34 E., Lea County, N. Mex.

Table 12.--Analyses of limestone, claystone, and siltstone in percent.

(Methods development and analyses supervised by F. S. Grimaldi.)

| | 1 | 2 | 3 | 4 | 5 |
|---|---|---|---|---|---|
| Al | 1.15 | 6.12 | 3.21 | 1.42 | 0.95 |
| B | 0.0071 | 0.0040 | 0.015 | 0.024 | 0.0040 |
| Ba | 0.015 | 0.028 | 0.034 | 0.081 | 0.013 |
| Br | 0.006 | 0.01 | 0.006 | <0.002 | <0.002 |
| C (Carbonate | 9.47 | 2.34 | 3.38 | 1.66 | 0.15 |
| C (Organic | 0.15 | 8.23 | 0.01 | 0.04 | ---- |
| C (Total | 9.62 | 10.57 | 3.39 | 1.70 | 0.16 |
| Ca | 28.82 | 8.58 | 3.63 | 12.60 | 0.19 |
| Cl | 0.47 | 2.03 | 2.48 | 1.69 | 47.92 |
| Cu | 0.00013 | 0.0046 | 0.0096 | 0.000056 | 0.0013 |
| F | 0.035 | 0.31 | 0.76 | 0.12 | 0.012 |
| Fe | 0.68 | 3.18 | 1.06 | 0.52 | 0.33 |
| H | 0.14 | 1.06 | 0.38 | 0.56 | 0.16 |
| I | <0.0002 | <0.0002 | <0.0002 | <0.0002 | <0.0002 |
| K | 0.83 | 3.78 | 1.91 | 4.08 | 0.78 |
| Mg | 2.71 | 2.75 | 3.00 | 7.41 | 1.56 |
| Mn | 0.036 | 0.050 | 0.021 | 0.010 | 0.0039 |
| Mo | 0.0022 | 0.00050 | <0.00003 | 0.00010 | <0.00003 |
| Na | 0.082 | 0.082 | 0.71 | 0.82 | 30.80 |
| Ni | 0.00079 | 0.0094 | 0.0020 | 0.0012 | 0.00044 |
| O* | 47.87 | 42.40 | 48.51 | 48.69 | 10.69 |
| Pb | <0.000009 | 0.00037 | 0.00093 | 0.0011 | 0.00040 |
| S | 0.87 | 2.70 | 0.62 | 13.12 | 0.40 |
| Se | 0.00006 | <0.00005 | <0.00005 | <0.00005 | <0.00005 |
| Si | 6.54 | 16.59 | 24.96 | 6.98 | 5.92 |
| Sr | 0.028 | 0.27 | 0.011 | 0.025 | 0.0093 |
| Th | 0.00017 | 0.00097 | 0.00045 | 0.00023 | 0.00015 |
| Ti | 0.066 | 0.36 | 0.23 | 0.12 | 0.078 |
| U | 0.00065 | 0.0025 | 0.00021 | 0.00017 | 0.000048 |
| V | 0.00073 | 0.014 | 0.0020 | 0.0012 | 0.00039 |
| Zn | 0.00021 | 0.0021 | 0.00080 | 0.00028 | 0.00061 |
| Zr | 0.025 | 0.043 | 0.047 | 0.016 | 0.017 |

*Difference from 100 percent, calculated.

1. Limestone; Paradox member of the Hermosa formation of Pennsylvanian age; 3,699 ft.; Delhi-Taylor No. 8, sec. 1, T. 25 S., R. 20 E., Grand County, Utah.

Table 12.--Analyses of limestone, claystone, and siltstone in percent--Continued.

2. Black shale; Paradox member of the Hermosa formation of Pennsylvanian age; 3,788 ft.; Delhi-Taylor No. 8, sec. 1, T. 25 S., R. 20 E., Grand County, Utah.

3. Siltstone; Paradox member of the Hermosa formation of Pennsylvanian age; 3,951 ft.; Delhi-Taylor No. 8, sec. 1, T. 25 S., R. 20 E., Grand County, Utah.

4. Claystone; Salado formation of Permian age; 1,860, 1,954, 2,290, 2,333, and 2,361 ft.; U. S. Potash Corp. No. 125(8), sec. 25, T. 23 S., R. 34 E., Lea County, N. Mex.

Table 13.--Average concentrations of elements in halite rock.

| Element | Range (percent) | Average (percent) | Sources of data |
|---|---|---|---|
| Ag | 0.00001 | 0.00001 | Table 10 |
| Al | 0.0011-0.0035 | 0.002 | Table 10 |
| As | 0.0001-0.001 | 0.0006 | Thomson and Wardle, 1954 |
| B | 0.000011-0.00037 | 0.0003 | Table 10 |
| Ba | 0.00009-0.0009 | 0.0003 | Goldschmidt, 1954; table 10 |
| Br | 0.002-0.04 | 0.01 | D'Ans and Kühn, 1940; Haslam and others, 1950; Aleksandrov and Levchenko, 1953; table 10 |
| C | 0.006-0.01 | 0.01 | Table 10 |
| Ca | 0.038-1.72 | 1 | Clarke, 1924; Yasui and Suzuki, 1955; table 10 |
| Cl | 56.97-60.13 | 58 | Clarke, 1924; table 10 |
| Cr | 0.0001-0.007 | 0.0004 | Goldschmidt and others, 1948; table 10 |
| Cs | 0.0002(carnallite) | 0.0002? | Jander and Busch, 1930 |
| Cu | 0.000002-0.02 | 0.0001 | Lietz, 1951; Thomson and Wardle, 1954; Yasui and Suzuki, 1955; Herrmann, 1958; table 10 |
| F | 0.0002-0.013 | 0.001 | Koritnig, 1951; table 10 |
| Fe | 0.00063-0.077 | 0.001 | Clarke, 1924; Yasui and Suzuki, 1955; table 10 |
| H | 0.001-0.017 | 0.01 | Clarke, 1924; table 10 |
| He | 0.000000002 | 0.000000002 | Thomson and Wardle, 1954 |
| I | 0-0.0001 | 0.00001 | Anonymous, 1956; table 10 |
| K | 0.0027-0.17 | 0.06 | Table 10 |
| Li | < 0.0001-0.01 | 0.001 | Santos and others, 1952 table 10 |
| Mg | 0.0024-0.13 | 0.04 | Clarke, 1924; table 10 |
| Mn | 0.000002-0.0020 | 0.00001 | Thomson and Wardle, 1954; Yasui and Suzuki, 1955; Herrmann, 1958; table 10 |
| Mo | < 0.00003 | < 0.00003 | Table 10 |
| N | 0.0042 | 0.004? | Miller and Heymal, 1956 |
| Na | 37.01-38.82 | 38 | Clarke, 1924; table 10 |
| Ni | 0.0001-0.00035 | 0.0002 | Thomson and Wardle, 1954; table 10 |
| O | 0.45-2.87 | 2 | Clarke, 1924; table 10 |
| P | 0.0047 | 0.005? | Haslam and others, 1950 |
| Pb | 0.000002-0.00054 | 0.0001 | Born, 1934; Lietz, 1951; Thomson and Wardle, 1954; Herrmann, 1958; table 10 |

Table 13.--Average concentrations of elements in halite rock--Continued

| Element | Range (percent) | Average (percent) | Sources of data |
|---|---|---|---|
| Ra | 0.000000000004-0.000000000021 | 0.000000000001 | Kemeny, 1941 |
| Rb | 0.0005-0.037 | 0.01 | Berg, 1929; Thomson and Wardle, 1954 |
| S | 0.19-1.39 | 0.8 | Clarke, 1924; table 10 |
| Se | < 0.00005 | < 0.00005 | Table 10 |
| Si | 0.0022-0.24 | 0.01 | Clarke, 1924; Yasui and Suzuki, 1955; table 10 |
| Sn | 0.000003-0.000005 | 0.000004 | Herrmann, 1958 |
| Sr | 0.0047-0.41 | 0.01 | Runnels and others, 1952; Thomson and Wardle, 1954; table 10 |
| Th | 0.0000002 | 0.0000002 | Thomson and Wardle, 1954; table 10 |
| Ti | 0.000060-0.00016 | 0.0001 | Table 10 |
| Tl | < 0.000005 | < 0.000005 | Shaw, 1952 |
| U | 0.000000013-0.0000025 | 0.000001 | Kemeny, 1941; Thomson and Wardle, 1954; table 10 |
| V | < 0.00003 | < 0.00003 | Goldschmidt and others, table 10 |
| Zn | 0.000008-0.00030 | 0.00003 | Lietz, 1951 Herrmann, 1958; table 10 |
| Zr | < 0.00004 | < 0.00004 | Table 10 |

## Source of elements

Many of the minor elements in evaporite sequences are much more abundant in clastic rocks than in halite-rich rocks; so that even though clastic rocks make up a relatively small part of a formation, they may contain the major concentration of an element in the unit. It seems worthwhile, therefore, to consider in which of the several lithologic types certain elements tend to be concentrated. Table 14 compares the chemical composition of salt with that of some other rocks which are common in evaporite deposits and for which data are available.

The elements concentrated in limestone and dolomite are oxygen, calcium, carbon, magnesium, phosphorous, and strontium. Those concentrated in anhydrite are oxygen, calcium, sulfur, strontium, and barium.

Few elements tend to be concentrated in the salt with chlorine and sodium; but, owing to the fact that anhydrite is rich in strontium, halite rock which holds considerable anhydrite generally contains a relatively large amount of strontium. The elements that accumulate in the final liquors during salt deposition are potassium, magnesium, hydrogen, lithium, bromine, and possibly iodine, though very likely most iodine evaporates and is not retained.

Hence a relatively small suite of elements is concentrated in limestone, anhydrite rock, and salt, and most of the minor elements, particularly the metals, are present in fine-grained clastic rocks. Elements that are primary constituents of clastic rocks are oxygen, silicon, aluminum, iron, potassium, calcium, hydrogen, titanium, manganese, zircon, chromium, fluorine, barium, rubidium, bromine, the rare earths, lithium, and beryllium. Elements extracted from sea water and deposited with

Table 14.--Chemical composition of some rock types in percent.

Data from Green (1959) and this report.

| Element | Sandstone | Shale | Carbonate rock | Halite rock |
|---|---|---|---|---|
| Ag | 0.00004? | 0.0009 | 0.00002? | 0.00001 |
| Al | 4 | 8 | 1 | 0.002 |
| As | 0.0001 | 0.009 | 0.0002 | 0.0006 |
| B | 0.02 | 0.01 | 0.002 | 0.0003 |
| Ba | 0.02 | 0.02 | 0.03 | 0.0003 |
| Br | 0.0001 | 0.0008 | 0.001 | 0.01 |
| C | 1 | 2 | 10 | 0.01 |
| Ca | 4 | 5 | 30 | 1 |
| Cl | 0.002 | 0.01 | 0.04 | 58 |
| Cr | 0.006? | 0.01 | 0.001 | 0.0004 |
| Cs | 0.0002 | 0.0005 | 0.0001 | < 0.0002? |
| Cu | 0.003 | 0.005 | 0.001 | 0.0001 |
| F | 0.03 | 0.05 | 0.05 | 0.001 |
| Fe | 3 | 4 | 1 | 0.001 |
| H | 0.2 | 0.6 | 0.09 | 0.01 |
| I | 0.0006 | 0.0007 | 0.00004 | 0.00001 |
| K | 1 | 2 | 0.00002 | 0.06 |
| Li | 0.002 | 0.007 | 0.001? | 0.001 |
| Mg | 1 | 2 | 4 | 0.04 |
| Mn | 0.04 | 0.1 | 0.1 | 0.00001 |
| N | -- | 0.1 | 0.03 | 0.004? |
| Na | 0.5 | 0.5 | 0.06 | 38 |
| Ni | 0.0006? | 0.007 | 0.002 | 0.0002 |
| O | 51 | 52 | 49 | 2 |
| P | 0.04 | 0.08 | 0.1 | 0.005? |
| Pb | 0.0009 | 0.008 | 0.002 | 0.0001 |
| Ra | 0.00000-000007 | 0.00000-00001 | 0.00000-000004 | 0.000000000001 |
| Rb | 0.005 | 0.02 | < 0.0005 | 0.01 |
| S | 0.2 | 0.1 | 0.8 | 0.8 |
| Si | 32 | 24 | 4 | 0.01 |
| Sr | 0.003? | 0.03 | 0.04 | 0.01 |
| Th | 0.0002 | 0.001 | 0.0002 | 0.0000002 |
| Ti | 0.3 | 0.5 | 0.04 | 0.0001 |
| U | 0.00005 | 0.0004 | 0.0002 | 0.000001 |
| Zn | 0.002 | 0.01 | 0.001 | 0.00003 |

organic material in black shale are vanadium, zinc, copper, molybdenum, nickel, lead, tin arsenic, uranium, silver, cobalt, germanium, and gold. A relatively thin bed of black shale can be a major host for many of the rare elements in an evaporite sequence.

Table 15 gives the proportion of rock types in the Salado formation. Table 16 gives estimates of the total chemical composition of the Salado calculated from data in tables 10, 14, and 15.

When considered in their setting in a formation composed predominantly of rocks formed by evaporation of water, the so-called chemical sediments (chloride, sulfate, and carbonate rocks) have the major part of the content of a relatively small suite of elements. These elements are chlorine, sodium, oxygen, calcium, sulfur, magnesium, strontium, bromine, and phosphorous. A small percent of clastic rocks in the section, particularly if it includes black shale, will have most of the rare metals of the formation.

If the case for halite rock alone is examined, however, a somewhat different picture evolves. The elements that are highly concentrated in salt are some of those that are also major constituents of sea water. But some elements which are present in the ocean in extremely minor amounts are greatly concentrated in halite rock with respect to sea water, though their absolute amounts in the salt may be small.

These relations can best be seen when the relative amounts of elements in halite rock are compared with their amounts in the ocean. Figure 36 presents these ratios plotted graphically on the periodic table to emphasize the grouping of the elements. The elements are divided by symbols into those present in high, normal, or low concentrations in rock salt with respect to sea water.

Table 15.--Proportion of lithologic types in the Salado formation.

| | Percent |
|---|---|
| Chloride rocks (halite rock, sylvite rock, etc.) | 84 |
| Sulfate rocks (anhydrite rock, gypsum rock, and polyhalite rock | 12 |
| Carbonate rocks (limestone and dolomite rock) | 0 |
| Clastic rocks (quartz sandstone, siltstone, and claystone) | 4 |

Table 16.--Estimate of the chemical composition of the Salado formation.

| Element | Percent |
|---|---|
| Ag | 0.00001 |
| Al | 0.2 |
| As | 0.0006 |
| B | 0.001 |
| Ba | 0.001 |
| Br | 0.009 |
| C | 0.07 |
| Ca | 4 |
| Cl | 50 |
| Cr | 0.0006 |
| Cs | 0.0002 |
| Cu | 0.0003 |
| F | 0.01 |
| Fe | 0.1 |
| H | 0.02 |
| I | 0.00001 |
| K | 0.1 |
| Li | 0.001 |
| Mg | 0.1 |
| Mn | 0.002 |
| Na | 32 |
| Ni | 0.0002 |
| O | 9 |
| P | 0.006 |
| Pb | 0.0001 |
| Rb | 0.01 |
| S | 3 |
| Si | 1 |
| Sr | 0.02 |
| Th | 0.000008 |
| Tl | 0.01 |
| U | 0.000008 |
| Zn | 0.0001 |

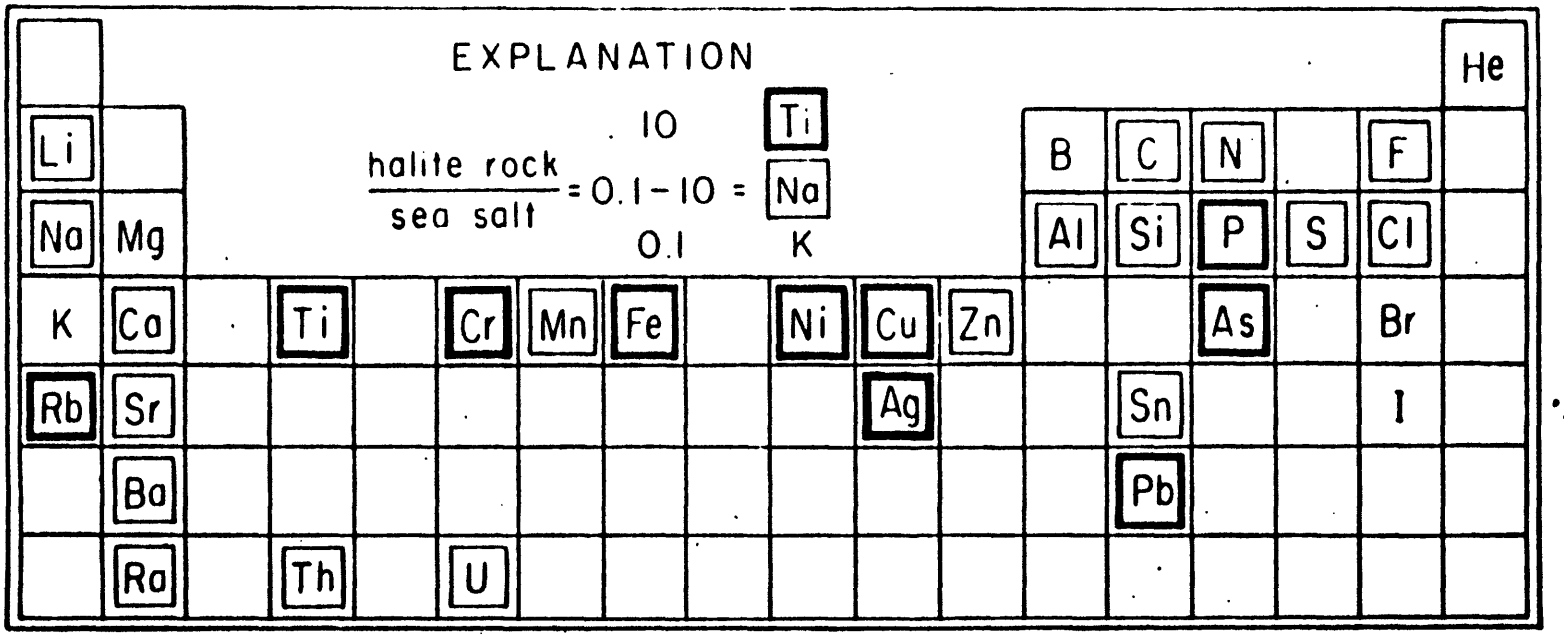


**Figure 36.--Ratio between the relative concentrations of some elements in halite rock and their concentration in the ocean.**

The ratio between sodium and a fairly large number of elements is about the same in halite rock as in the ocean and evidently these elements are neither enriched nor depleted during the evaporation of sea water. Perhaps more interesting, however, are those that are present in either much smaller or much greater amounts. Normal rock salt contains relatively less potassium, magnesium, and boron than the ocean because these ions are extremely soluble and tend to remain in solution in the brine rather than being deposited. Bromine and iodine also are present in low concentrations probably because they are lost to the atmosphere by evaporation.

The elements that are more abundant in halite rock than in the ocean are less easily explained. It is interesting to note that many of the metals are enriched, in some cases many times more than their concentration in sea water. Phosphorous is also enriched; and, as phosphorous is a common element in organic material, its abundance suggests that the presence of the metals may be related to organic activity. Perhaps these elements are derived from the remains of marine life that was killed when it came in contact with the highly saline water of the evaporation basin.

Megafossils are rare in salt deposits but Miller and Schwartz (1955) have shown that fossils of microorganisms are abundant. Concentration of metals might be effected by the adsorption of certain elements on decaying organic material or by the fossilization of specialized microorganisms, known from present-day brines, that accumulate metals as part of their life processes.

The existence of reducing conditions a few centimeters below the surface in shallow sites of evaporite deposition such as that at Pupuri Salina may be of special importance in considering the genesis of some accumulations of petroleum. Carpelan (1953) has shown that the organic productivity of artificial salt ponds is 20 to 30 times that of coastal sea water. The equating of environments of salt precipitation with strongly oxidizing conditions (Krumbein and Garrels, 1952) has perhaps been overly emphasized in the past. I believe that halite rock and gypsum rock are potential source beds for petroleum. Organic material trapped in salt could be freed by solution of the salt for migration in brine to structural and stratigraphic traps. Likewise, the dehydration of gypsum at depth during its conversion to anhydrite must release large quantities of water which could contain organic raw materials of petroleum. The well known spatial association between evaporite deposits and oil pools may in many cases be a direct genetic relationship.

## ORIGIN OF HALITE ROCK AND GYPSUM ROCK

In order to explain thick sequences of halite rock and gypsum rock, Ochsenius (1877) advanced a bar theory for the origin of evaporite deposits. This theory, which was based on an earlier suggestion by Bischof (1864), proposed that salt and gypsum deposits form in areas separated from the sea by a sand bar behind which sea water that flows over the bar or seeps through it is desiccated. The bar theory has formed the basis for most subsequent thinking on the origin of evaporite deposits.

According to the unmodified bar theory a succession of deposits would follow the sequence of compounds precipitated from sea water during its evaporation. Superimposed on this vertical succession would be a similar horizontal progression imposed by the inflow of normal sea water over the bar. The horizontal facies would range from carbonate minerals near the source of sea water, through sulfate minerals, to halite at the opposite edge of the basin.

Earlier suggestions that thick layers of rock salt have been formed by the desiccation of seas cut off completely from the ocean may be rejected because of the great initial depth of water required to explain the known thicknesses of salt. King (1947, p. 475) has calculated that, to account for the gypsum of the Castile formation, water with a depth of a million meters would have to be evaporated. Even if the brine were concentrated into a small part of the isolated sea, the depth of water required would be too great to account for many known deposits of salt.

Briggs (1948) has recently adapted the bar theory to explain evaporite deposits in the Salina Basin of Michigan which interfinger with carbonate rocks that he feels were formed on the opposite side of the basin from the point of ingress of sea water. Briggs proposed that halite and gypsum are formed during periods of strong evaporation when only the central part of the basin is filled with water; at other times, when the basin is completely filled, limestone forms around the margins of the basin. Probably an alternative paleogeographic interpretation could be invoked in the Salina Basin to place the carbonate rocks in a more reasonable position near the source of sea water.

## The reflux concept

If inflow of normal sea water were followed by evaporation to dryness, approximately 30 times more halite than gypsum would be present in evaporite deposits. But in an evaporite sequence such as that of the Castile and Salado formations, the abundance of gypsum and halite is about the same. This fact led King (1947) to propose a modification of Ochsenius' bar concept which he named the reflux theory. The reflux theory suggests that sea water with normal density enters an evaporation basin through a channel in a bar. As it moves across the basin and is evaporated, its density increases, and the denser brine tends to seek lower levels in the basin. In a basin where dynamic equilibrium has been established, a density discontinuity develops between the inflowing surface water and brine occupying the deep parts of the basin.

Throughout most of the basin the inward-flowing upper layer floats on the lower and essentially no mixing takes place below wave base. Brine can be added to the lower layer only at the distal edge of the basin where the density of the upper layer has reached that of the lower. An outward flow from the basin, the reflux, occurs along the floor of the channel through the bar. This countercurrent maintains constant density and chemical composition in the lower layer and makes it possible for gypsum to continue to be deposited for a long period of time without deposition of halite.

Scruton (1953) has shown that modern lagoons where evaporation exceeds precipitation and runoff are indeed characterized by inflow of sea water at the surface and reflux below. Bramkamp and Powers (1955) have studied a lagoon on the shore of the Persian Gulf which in November had an upper layer a meter thick that contained 9 percent salt and a thin lower layer that contained 20 percent salt. A thermal inversion existed in the lagoon, the lower layer having a temperature of 34°C and the upper layer, 27°C. Gypsum was forming at the shore of the lagoon and sulfide-rich lime mud on the floor.

## A multiple-inlet hypothesis

The observationsin this report provide some information that may be significant in interpreting the origin of the Salado formation and other evaporite deposits. Most recent writers on the origin of evaporite deposits have assumed that sea water entered the evaporation basin through a single, relatively narrow channel, although this was not

inherent in Ochsenius' original theory. The barrier beach that separates Pupuri Salina from the bay is approximately a kilometer long, the length of a diameter of the salina. In this length the salina is drained by two inlets, and it receives water from the bay through an additional two inlets.

The arcuate east shore of the bay in Mexico shown on figure 1 is the barrier beach of a salina 50 times larger than Pupuri Salina and of which Pupuri Salina might be considered a scale model. This barrier beach is about seven kilometers long and is about the length of a diameter of the larger salina.

It is proposed that long barrier beaches or barrier islands associated with numerous and fairly regularly-spaced inlets are the usual bars of evaporite basins regardless of size. These barrier beaches are maintained by alongshore beach transport of sand and shell material on their seaward sides. The spacing of the inlets is determined by the tidal interchange with the evaporation basin and other factors. Alongshore transport causes migration of the inlets so that individual inlets do not leave prominent records in the stratigraphy. The present gulf coast of Texas might be cited as an example that has about the same scale as the Salado evaporation basin. For example, a change in climate could transform Laguna Madre on the gulf into a saline basin for which Padre Island is the barrier island.

During deposition of the Salado formation, a series of barrier islands is believed to have extended along the southern margin of West Texas Basin. The quartz and carbonate clastic rocks of the Rustler

formation are interpreted as remains of these old barrier islands. Inflow to the basin occurred at various places along the southern margin of the basin and was not confined to a specific narrow channel. Associated with the sediments of the barrier islands were a few thin beds of botryoidal carbonate minerals such as are preserved in the Magenta member. Halite and gypsum were deposited in the main part of the basin, and at the north margin, terrigenous redbeds were laid down.

In the southern part of the basin, near the postulated source of sea water, the Salado formation interfingers with gypsum rock of the Castile formation (fig. 23). The Castile lies in the Delaware Basin, the deepest part of West Texas Basin, and the regional facies pattern suggests that the Castile formation was formed in deeper water than the Salado.

A comparison between evaporite deposition in density-stratified lagoons and salt deposition in shallow Pupuri Salina which lacks density stratification suggests that the Castile formation was formed in relatively deep water characterized by density stratification as suggested by King (1947) and the Salado formation was formed in shallow water mixed by wind action (fig. 37). Both environments are thought to have existed simultaneously in the basin, and the salt deposition occurred in a shallow tide-flat environment far from the source of sea water while gypsum was deposited in the area of more rapid downwarping near the source of sea water to the south.

The water from which the salt of the Salado formation was deposited may have been less than a meter deep. Where a density discontinuity established itself in the deeper water, dilution by mixing from the upper

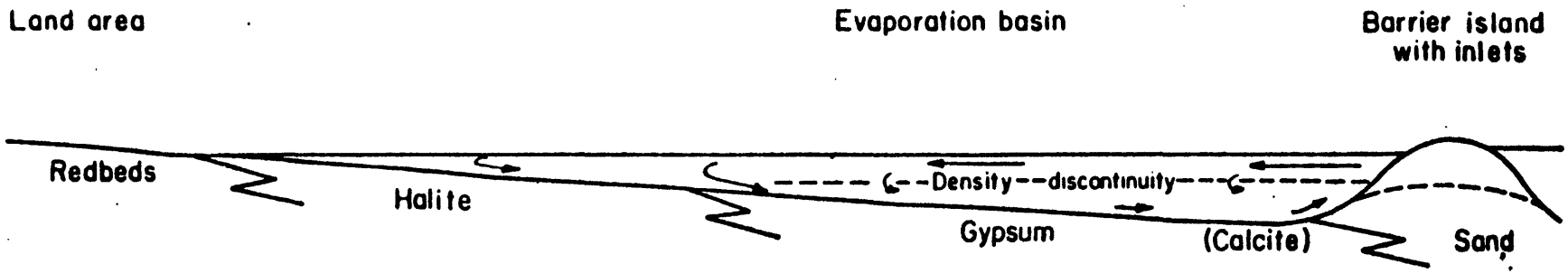


Figure 37.--Postulated depositional conditions for evaporite and related formations in West Texas Basin. Sea water entering the evaporation basin floats on dense brine to the point where depth of water equals depth of wind mixing. Halite is deposited farther shoreward in water probably largely less than a meter deep. At the point where the upper layer is desiccated to the same density as the lower layer, brine is added to the lower layer, and an equal amount is recharged to the sea through inlets. Mixing of the two stratified water layers at their interface results in deposition of gypsum and, in places, calcite.

layer inhibited precipitation of sodium chloride, but at the same time it caused the deposition of gypsum because the solubility of calcium sulfate was depressed in the more highly saline mixture.

In the deeper water with a density discontinuity, the upper less saline water layer evidently supported a rich biota of microorganisms whose former presence is reflected in the bituminous character of the laminated gypsum rock in the Castile formation. No doubt the rain of organic material from the upper layer was partly protected from decay by semisterile conditions existing in the more highly concentrated brine of the lower layer.

During parts of the year, clouds of finely divided calcium carbonate settled from the upper layer to the bottom and formed the limestone laminae of the Castile formation. Because the limestone of these laminae is now recrystallized, it has not been possible to determine whether the original precipitation was inorganic or was fostered by algae and bacteria. The association of the limestone laminae with bituminous material lends support to the idea that organisms played a role in the precipitation.

## SEA WATER CHEMISTRY THROUGH GEOLOGIC TIME AS REFLECTED IN SALT DEPOSITS

In the chapter on evaporite chemistry I have tacitly assumed that the chemical composition of halite rock is independent of its geologic age. The chemical analyses made for this study and those recorded in the literature have been averaged to prepare table 13 which is an estimate of the average composition of halite rock. An attempt will now be made to evaluate the validity of this assumption and to compare the chemical composition of rock salt of different ages. Such an evaluation offers a possibility of shedding new light on the geologic history of sea water.

Rubey (1951) has thoroughly reviewed the lines of evidence that have been employed in the past to gain an insight into the evolution of sea water, so only a brief summary of them will be given here. A method that was once thought to give virtually a true measurement of the chemical composition of ancient sea water was the analysis of connate water trapped in sedimentary rocks (Lane, 1908; 1945). Unfortunately, more recent investigations have shown that many processes are at work to change the chemical composition of connate water (Chave, 1960), so its present composition bears little relation to that at the time of deposition.

Spiro (1958) has employed analyses of ions adsorbed on clay minerals as a measure of the past composition of sea water. The compaction of the grains during burial is thought to fix the ions and prevent diagenetic and later changes. This supposition is unproved, however, and the method probably suffers from the same defects as the connate-water method.

The relative concentrations of minor elements in fossils offer another approach to the problem, but again the values might be changed by migrating solutions in such a way that the concentrations are systematically related to the length of time the enclosing rocks have been buried so as to show a false correlation with geologic age. Lowenstam (1959) has recently removed some of this uncertainty by selecting for consideration only those samples that give concordant isotopic and trace-element values of paleotemperature, and therefore presumably have not been altered. Lowenstam's results suggest that the composition of sea water has not changed significantly at least since Mississippian time.

Another approach to the problem is the theory that the ionic concentration in the body fluids of organisms is related to the chemical composition of the ocean at the time the organisms evolved (Macallum, 1904). A close similarity exists between the ions in vertebrate blood and dilute sea water, the only important difference being the greater content of magnesium in present sea water.

The most successful method that has been used in the past to study the evolution of sea water is the method of geochemical balance in which the chemical composition of the ocean is compared with the contribution of rivers, the weathering of rocks, and the quantity of sediment deposited. This method has shown especially that carbon dioxide of volcanic origin has been continuously added to the oceans to replace the carbonate removed as limestone (Rubey, 1951).

The present procedure of employing marine salt deposits to measure the characteristics of ancient oceans may be a direct approach to the problem, but it, too, has uncertainties. We may first consider the

evidence from salt deposits on the total salinity of the ocean. The most significant fact in this connection is the abrupt appearance of marine salt deposits in Cambrian time and their absence in Precambrian time. Extensive deposits of Cambrian salt occur in Siberia, Pakistan, and Iran, and important deposits also exist in various places in the world in every subsequent period with the possible exception of the Ordovician (Lotze, 1957). The absence of rock salt deposits of Precambrian age may reflect a dilute ocean during Precambrian time or it may record the fact that most Precambrian rocks are metamorphosed and rock salt is a highly reactive material that is destroyed by intense metamorphism. The salt deposits of the Gulf of Kara-Bugaz derive their water from the Caspian Sea whose salinity is only a third that of present sea water. This implies that the formation of evaporite deposits would be inhibited only by an extremely dilute ocean.

The nine samples ranging in age from Cambrian to Recent that were analyzed for this study show no systematic increase or decrease of any element with respect to age, with the possible exception of manganese (table 10). The Cambrian and two Pennsylvanian samples each contain less than 0.00002 percent manganese. One of the Permian samples contains less than 0.00002 percent manganese but the other four Permian samples and the modern sample range from 0.00009 to 0.0020 percent. The scatter is so broad, however, that the apparent relationship may be fortuitous and the variation might be caused by factors other than geologic age. The minor variations of most of the other elements can be explained by obvious special characteristics of the samples such as the presence of clastic material, anhydrite, or secondary potassium minerals.

The results suggest either that the ratio between elements has been constant in the sea since Precambrian time or that the separation of phases during evaporite deposition selects specific quantities of minor elements regardless of their concentration in solution. The deposits of the Gulf of Kara-Bugaz offer support for a concept that the fairly constant chemical composition of marine evaporite deposits indeed reflects true constancy in the relative abundance of the ions in sea water since Precambrian time. The water of the Caspian Sea differs from normal sea water in that it contains three times as much sulfate ion. As noted in a previous section, the deposits at Kara-Bugaz contain abundant quantities of mirabilite ($Na_2SO_4 \cdot 10H_2O$), a mineral not ordinarily found in marine evaporite deposits.

In summary, marine evaporite deposits by themselves provide no unequivocal evidence as to the geologic history of sea water, but they suggest that the oceans may have been relatively dilute prior to Cambrian time and that the ratio between most ions has remained approximately constant.

## CONCLUSIONS

In this investigation into the significance of evaporite deposits, research has been undertaken on three types of material: (1) artificial evaporite minerals formed in the laboratory under controlled conditions; (2) halite and gypsum being deposited from sea water at the present time on the west coast of Mexico; and (3) halite rock and gypsum rock of Permian age in West Texas Basin. The following conclusions resulted from the study:

(1) Salt deposits are normally formed from acidic water, and after burial to shallow depth, the interstitial water characteristically becomes reducing.

(2) Gypsum is the usual original mineral of marine sulfate deposits; it is formed in part metastably owing to rapid precipitation under non-equilibrium conditions.

(3) Gypsum rock and halite rock are postulated to be potential source beds for petroleum. Organic material preserved in them may be transported to structural and stratigraphic traps by water moving out of the rocks. Part of this water is interstitial and part originates from gypsum crystals as a result of transformation to anhydrite.

(4) Examination of present-day evaporite deposits in Mexico in both the rainy and dry seasons has shown that absence of salt in some gypsum deposits may be due to its contemporaneous resolution rather than to original non-deposition.

(5) Paleogeographic reconstructions of sequences that include halite rock must consider the fact that salt may be leached to great depth below the present or earlier erosion surfaces; this was not done in Galley's (1958)

recent lithofacies maps of West Texas Basin.

(6) Thick evaporite deposits usually are formed behind a long series of barrier islands or a barrier beach with numerous inlets rather than in a basin separated from the sea by a single channel; the inlets migrate and their deposits occur throughout the deposits of the barrier.

(7) Salt deposits of Permian age in the Salado and Rustler formations are believed to have been formed within the tide zone; gypsum of the Castile formation was deposited in deeper water with a dense lower layer from which brine was recharged to the sea.

(8) Subject to certain qualifications, the evidence from deposits of halite rock suggests that the Precambrian ocean may have been rather dilute and that the ratio between ions in sea water has remained approximately constant since Precambrian time.

# APPENDIX.--DESCRIPTION OF CORE FROM A.E.C. DRILL HOLE NO. 1, EDDY COUNTY, NEW MEXICO

## Introduction

Drilling at the Project GNOME site in the approximate center of sec. 34, T. 23 S., R. 30 E., NMPM, was undertaken in August and September 1958 by the W-W Drilling Company. Objectives of the project, which is a part of Operation Plowshare of the U. S. Atomic Energy Commission, are to explore the feasibility of the production of thermal energy and useful radioisotopes from a wholly-contained underground nuclear explosion in rock salt. The purpose of drilling this hole, which is at the precise location of the proposed experiment, was to determine (1) the lithologic and water-bearing characteristics of the rocks of Cenozoic, Mesozoic, and Paleozoic age that lie above the salt-bearing sequence of the Salado formation; (2) the depth to the top of the unleached salt and associated evaporite deposits in the Salado formation; and (3) the local details of the salt-bearing sequence in the Salado formation.

Philip Pack of Holmes & Narver, Inc., and G. W. Moore, E. R. Cox, John Havens, and B. R. Alto of the U. S. Geological Survey collaborated in observing the coring operation and in preparing a preliminary log during the period of drilling. Moore is responsible for the log that was prepared from the core after the drilling had terminated.

A selected list of mineral names used in the lithologic description follows:

| Mineral | Chemical composition |
|---|---|
| Anhydrite | $CaSO_4$ |
| Dolomite | $CaMg(CO_3)_2$ |
| Gypsum | $CaSO_4.2H_2O$ |
| Halite | NaCl |
| Langbeinite | $K_2SO_4.2MgSO_4$ |
| Leonite | $MgSO_4.K_2SO_4.4H_2O$ |
| Polyhalite | $2CaSO_4.MgSO_4.K_2SO_4.2H_2O$ |

These minerals combine in various mixtures to form rocks. The major constituent generally gives its name to the rock (as anhydrite rock), but any or all of the above minerals in addition to silt, clay, and sand may be minor constituents.

## Summary

| Feet | Name of formation | Age |
|---|---|---|
| 0.0 - 10.0 | | Recent |
| 10.0 - 80.0 | Gatuna formation | Pleistocene(?) |
| 80.0 - 291.5 | Pierce Canyon redbeds | Permian or Triassic |
| 291.5 - 360.2 | Rustler formation Upper member | Permian |
| 360.2 - 380.3 | Rustler formation Magenta member of Adams (1944) | Permian |

| Feet | Name of formation | Age |
|---|---|---|
| 380.3 - 497.4 | Rustler formation<br>Middle member | Permian |
| 497.4 - 529.0 | Rustler formation<br>Culebra dolomite member | Permian |
| 529.0 - 429.9 | Rustler formation<br>Lower member | Permian |
| 649.9 - 709.7 | Salado formation<br>Upper leached member | Permian |
| 709.7 - 1026.5 | Salado formation<br>Undifferentiated | Permian |
| 1026.5 - 1030.4 | Salado formation<br>Vaca Triste sandstone member of Adams (1944) | Permian |
| 1030.4 - 1178.6 | Salado formation<br>Undifferentiated | Permian |
| 1178.6 - 1179.7 | Salado formation<br>Marker bed 120 | Permian |
| 1179.7 - 1242.5 | Salado formation<br>Undifferentiated | Permian |
| 1242.5 - 1261.3 | Salado formation<br>Union bed of local usage | Permian |
| 1261.3 - 1500.0 | Salado formation<br>Undifferentiated | Permian |

## Lithologic Description

| Feet | |
|---|---|
| 0.0 - 7.0 | Sand, fine-grained, light-brown, well rounded, unconsolidated. (Dune sand.) |
| 7.0 - 10.0 | Limestone, sandy, white, contains fine-grained quartz sand, well indurated. (Caliche.) |
| 10.0 - 43.0 | Sand, fine-grained, light-brown, fairly well rounded, very friable. (Top Gatuna formation of Pleistocene(?) age.) |
| 43.0 - 45.2 | Sandstone, medium-grained, pale reddish-brown, has scattered 3-mm pebbles, calcite cement, carries water. |
| 45.2 - 45.7 | Conglomerate, pebble, pale-red; 5-mm pebbles of limestone, siltstone, quartzite; matrix of coarse-grained sandstone, well indurated, calcite cement. |
| 45.7 - 53.0 | Sandstone, medium- to coarse-grained, pale-red; scattered 3-mm pebbles; friable, carries water. |
| 53.0 - 80.0 | Sandstone, medium- to coarse-grained, moderate-brown, friable. |
| 80.0 - 84.5 | Sandstone, very fine grained, moderate reddish-brown; has 2-mm light greenish-gray reduction spots about 1 cm apart; 0.5-mm calcite veins; poorly indurated except basal 0.5 ft which is fairly well indurated; calcite cement. (Top Pierce Canyon redbeds of Permian or Triassic age.) |
| 84.5 - 120.6 | Siltstone, sandy, moderate reddish-brown; 1-5 mm light greenish-gray reduction spots about 1 cm apart; rare 0.5-mm calcite veins; fairly well indurated, slightly fissile, some calcite cement. |

| Feet | |
|---|---|
| 120.6 - 120.8 | Claystone, silty, moderate reddish-brown; 2-mm light greenish-gray spots; poorly indurated, plastic. |
| 120.8 - 139.0 | Siltstone, sandy, moderate reddish-brown; 1-5 mm light greenish-gray reduction spots about 1 cm apart, several light-greenish layers 0.1 ft thick; rare 0.5-mm calcite veins; fairly well indurated, slightly fissile, some calcite cement. |
| 139.0 - 166.5 | Sandstone, medium-grained, moderate reddish-brown with 5-cm light greenish-gray patches, well rounded, well sorted; a few 0.5-mm calcite veins; induration irregular, fairly well indurated to very friable, carries water. |
| 166.5 - 291.5 | Siltstone, sandy, moderate reddish-brown; 1-10 mm light greenish-gray reduction spots about 5 cm apart; some 1-mm calcite veins; fairly well indurated, slightly fissile, calcite cement; below 217 ft are 0.5-1 mm blebs of gypsum about 5 mm apart. |
| 291.5 - 297.7 | Gypsum rock, olive-gray, 1-cm crystals; 5-cm masses of anhydrite in basal 2 ft; upper contact bears evidence of solution; rock is massive. (Top of Rustler formation of Permian age.) |
| 297.7 - 318.0 | Anhydrite rock, olive-gray, 1-mm crystals; some gypsum crystals throughout, especially near top and bottom contacts which are gradational; massive. |
| 318.0 - 327.5 | Gypsum rock, olive-gray, 1 cm crystals; 5-cm masses of anhydrite in top ft; massive. |
| 327.5 - 327.6 | Siltstone, greenish-gray, friable. |

| Feet | |
|---|---|
| 327.6 - 328.0 | Siltstone, sandy, moderate reddish-brown, brecciated; contains 5-mm breccia fragments of gypsum rock; fairly well indurated. |
| 328.0 - 337.5 | Siltstone, sandy, moderate reddish-brown with 1-mm light greenish-gray reduction spots 5 mm apart; upper 3 ft fairly well indurated, basal part very friable; some calcite cement. |
| 337.5 - 338.4 | Siltstone breccia, moderate reddish-brown with 3-mm irregular light greenish-gray spots; has 10-mm fragments of broken siltstone, some gypsum fragments; fairly well indurated, calcite cement. |
| 338.4 - 339.8 | Gypsum breccia, grayish-purple; 1-2 cm fragments of gypsum and broken claystone laminae; well indurated, calcite cement. |
| 339.8 - 350.0 | Gypsum rock, grayish-red, 5-cm crystals; abundant 5-cm patches of anhydrite; 1-mm grayish-red stylolites about 1 cm apart. |
| 350.0 - 360.2 | Anhydrite rock, olive-gray; upper part is gradational with unit above; lower 6 ft has 1-cm fibrous veins of gypsum approximately parallel to the bedding and 5 cm apart; lower 6 ft has alternating 5-cm bands that are grayish-red and greenish-gray; gradational with unit below. |
| 360.2 - 367.7 | Dolomite rock, greenish-gray with some grayish red-purple layers 1 cm thick; very fine grained; basal part has botryoidal or crossbedded texture; basal 1.5 ft porous with 1-mm solution cavities. (With next 2 units is Magenta member.) |

| Feet | |
|---|---|
| 367.7 - 369.5 | Siltstone, dolomitic; upper 0.6 ft greenish-gray, lower part grayish red-purple; slightly fissile. |
| 369.5 - 380.3 | Dolomite rock, silty, grayish red-purple with some 1-cm greenish-gray layers; has wavy botryoidal bedding; 1-cm fibrous gypsum veins parallel to bedding average 10 cm apart. |
| 380.3 - 441.5 | Anhydrite rock, grayish-red to greenish-gray; has a few 1-cm veins of gypsum parallel to bedding and some 5-cm masses of gypsum; 1-cm solution cavity at 432.9 ft; massive, microcrystalline. |
| 441.5 - 441.7 | Claystone, brownish-black; some 5-mm fragments of gypsum; plastic, slickensided. |
| 441.7 - 472.0 | Anhydrite rock, greenish-gray; 5-cm masses of gypsum abundant in upper 2 ft and lower 9 ft; massive. |
| 472.0 - 473.4 | Siltstone, greenish-gray; contains 1-5 cm breccia fragments of gypsum rock and claystone; fairly well indurated, some calcite cement. |
| 473.4 - 477.2 | Siltstone, grayish-red; has brecciated 1-cm gypsum beds about 5 cm apart; poorly indurated, plastic. |
| 477.2 - 482.6 | Gypsum rock, greenish-gray, 2-mm crystals (some larger); some clay-filled fractures; massive. |
| 482.6 - 482.8 | Claystone, olive-gray, slickensided; contains 2-mm breccia fragments of gypsum. |
| 482.8 - 497.4 | Gypsum rock, olive-gray, 1-mm crystals, massive; some 10-cm anhydrite layers; basal 0.4 ft has clay-filled solution cavities. |

| Feet | |
|---|---|
| 497.4 - 529.0 | Dolomite rock, light olive-gray, micro-crystalline; 3-mm cavities 5 mm apart; solution cavities; brecciated, water bearing. (Culebra dolomite member.) |
| 529.0 - 537.2 | Siltstone, clayey; upper 0.9 ft dark greenish-gray, lower part grayish-red; abundant 1-cm breccia fragments of gypsum; poorly consolidated, plastic. |
| 537.2 - 550.4 | Gypsum rock, olive-gray, 1-mm crystals with some patches having 10-cm crystals, massive. |
| 550.4 - 551.5 | Gypsum breccia, olive-gray; 2-cm angular fragments of gypsum in a matrix of greenish-gray clay. |
| 551.5 - 561.5 | Siltstone, clayey, moderate reddish-brown; a few 1-cm light greenish-gray spots; abundant 2-cm gypsum and siltstone breccia fragments; poorly consolidated, plastic. |
| 561.5 - 565.1 | Gypsum rock, olive-gray, 0.5-mm crystals, a few stylolites, massive. |
| 565.1 - 570.8 | Siltstone, clayey, moderate reddish-brown; 1-cm fragments of gypsum; poorly consolidated, plastic. |
| 570.8 - 576.2 | Gypsum rock, silty; alternating 5-cm layers of olive-gray gypsum rock and grayish-red siltstone; fairly well indurated. |
| 576.2 - 586.0 | Siltstone, sandy, grayish-red to greenish-gray, fairly well indurated in part, some dolomite cement; gradational with unit below. |
| 586.0 - 649.9 | Sandstone, very fine-grained, silty, greenish-gray, brecciated (fragments average 5 cm), friable; basal 3 ft well indurated with dolomite cement. |

| Feet | |
|---|---|
| 649.9 - 652.3 | Siltstone, grayish-red; abundant 1-cm breccia fragments of gypsum; 1-mm gypsum veins; poorly consolidated, plastic. (Top of Salado formation of Permian age.) |
| 652.3 - 652.5 | Gypsum rock, olive-gray, 2-mm crystals, massive. |
| 652.5 - 652.8 | Siltstone, grayish-red; abundant 2-mm gypsum fragments. |
| 652.8 - 653.4 | Gypsum rock, pale reddish-brown, 1-mm crystals, massive. (Alteration product of polyhalite rock.) |
| 653.4 - 654.1 | Siltstone, grayish-red; some 2-cm pale reddish-brown gypsum fragments. |
| 654.1 - 654.3 | Gypsum rock, pale reddish-brown. |
| 654.3 - 660.1 | Siltstone, clayey, grayish-red; abundant 1-cm gypsum fragments; very poorly indurated, plastic. |
| 660.1 - 660.4 | Gypsum rock, pale reddish-brown, 1-cm crystals. |
| 660.4 - 664.2 | Siltstone, grayish-red; abundant 1-5 cm fragments of gypsum rock and sandstone; poorly indurated, plastic. |
| 664.2 - 664.4 | Gypsum rock, moderate-red; bedding at 30°. |
| 664.4 - 667.7 | Siltstone, clayey, grayish-red; scattered 1-cm fragments of moderate-red gypsum; poorly indurated, plastic. |
| 667.7 - 668.5 | Gypsum rock, moderate-red, 1-cm crystals, brecciated in part. |
| 668.5 - 670.2 | Siltstone, clayey, grayish-red; some 3-cm fragments of moderate-red gypsum; plastic. |
| 670.2 - 672.6 | Sandstone, very fine grained, pale reddish-brown to greenish-gray, massive, friable, except basal 0.4 ft which is fairly well indurated. |

| Feet | |
|---|---|
| 672.6 - 684.5 | Siltstone, clayey, grayish-red; abundant 1-5 cm fragments of gypsum rock and sandstone; highly contorted; poorly indurated, plastic. |
| 684.5 - 685.2 | Gypsum rock, olive-gray, 2-mm crystals, bedding contorted. (Alteration product of anhydrite rock.) |
| 685.2 - 685.8 | Gypsum rock, moderate-red, 1-mm crystals. (Alteration product of polyhalite rock.) |
| 685.8 - 686.0 | Siltstone, clayey, grayish-red. |
| 686.0 - 687.3 | Gypsum rock, olive-gray with grayish-red stains. |
| 687.3 - 687.8 | Siltstone, clayey, grayish-red, contacts contorted. |
| 687.8 - 688.6 | Gypsum rock, olive-gray, massive. |
| 688.6 - 694.0 | Siltstone, clayey, grayish-red; 1-5 cm fragments and broken beds of sandstone and gypsum rock; poorly indurated, plastic. |
| 694.0 - 694.9 | Gypsum rock, olive-gray, 1-mm crystals, massive. |
| 694.9 - 706.8 | Anhydrite rock, greenish-gray, micro-crystalline; basal 0.6 ft silty; massive. |
| 706.8 - 708.1 | Siltstone, clayey, dark greenish-gray, poorly indurated, plastic; basal 0.2 ft grayish-red. |
| 708.1 - 709.7 | Anhydrite rock, upper 0.4 ft grayish red-purple, lower part greenish-gray; massive. |
| 709.7 - 725.0 | Halite rock, pale yellowish-brown, 1-cm crystals; 2 percent polyhalite in 1-10 mm blebs. |
| 725.0 - 726.9 | Halite rock, silty, grayish-red; 1 percent silt. |
| 726.9 - 731.6 | Halite rock, greenish-gray to yellowish-gray; 1 percent polyhalite in 2-mm blebs. |

| Feet | |
|---|---|
| 731.6 - 731.7 | Polyhalite rock, pale-red, contorted. |
| 731.7 - 732.5 | Halite rock, greenish-gray, 1-cm crystals; 2 percent polyhalite in 2-mm blebs. |
| 732.5 - 732.9 | Anhydrite rock, greenish-gray; 10 percent halite in 3-mm crystals. |
| 732.9 - 733.0 | Siltstone, clayey, grayish-red. |
| 733.0 - 742.4 | Halite rock, yellowish-gray, 1-cm crystals; 2 percent polyhalite. |
| 742.4 - 742.8 | Polyhalite rock, grayish orange-pink; 5 percent halite in 5-mm crystals and 3-mm layers. |
| 742.8 - 743.5 | Halite rock, moderate orange-pink, 2-cm crystals. |
| 743.5 - 748.8 | Halite rock, silty, grayish-red; 2 percent silt; 2 percent polyhalite. |
| 748.8 - 750.8 | Halite rock, silty, grayish-red; 10 percent silt; 1 percent polyhalite. |
| 750.8 - 752.2 | Halite rock, silty, grayish-red; 2 percent silt; 2 percent polyhalite. |
| 752.2 - 755.9 | Halite rock, pale-red; 2 percent polyhalite; 0.5 percent silt. |
| 755.9 - 759.0 | Halite rock, silty, grayish-red; 3 percent silt; 1 percent polyhalite. |
| 759.0 - 763.2 | Halite rock, moderate reddish-orange, 1-cm crystals; 2 percent polyhalite in 2-mm blebs and stringers. |
| 763.2 - 763.5 | Polyhalite rock, moderate reddish-orange. |
| 763.5 - 766.0 | Halite rock, silty, grayish-red; 5 percent silt; 0.5 percent polyhalite. |

| Feet | |
|---|---|
| 766.0 - 768.4 | Halite rock, grayish orange-pink; 2 percent polyhalite. |
| 768.4 - 768.6 | Polyhalite rock, moderate reddish-orange. |
| 768.6 - 773.2 | Halite rock, moderate orange-pink, 2-cm crystals; 1 percent polyhalite. |
| 773.2 - 773.3 | Polyhalite rock, moderate reddish-orange. |
| 773.3 - 774.1 | Halite rock, moderate orange-pink; 5 percent polyhalite in 2-cm masses. |
| 774.1 - 774.8 | Polyhalite rock, moderate reddish-orange, microcrystalline; 4 percent halite in 2-cm masses. |
| 774.8 - 775.2 | Halite rock, moderate orange-pink; 5 percent polyhalite. |
| 775.2 - 776.3 | Siltstone, clayey, grayish-red; 1-cm light greenish-gray layer at top; 30 percent halite in 2-mm blebs. |
| 776.3 - 777.9 | Halite rock, silty, pale-red, 1-cm crystals; 2 percent silt in 5-mm solution cavities. |
| 777.9 - 778.0 | Polyhalite rock, moderate reddish-orange. |
| 778.0 - 782.8 | Halite rock, silty, pale-red, 2-cm crystals; 2 percent silt; 1 percent polyhalite. |
| 782.8 - 787.3 | Halite rock, pale-red to moderate reddish-orange, 1-cm crystals; 2 percent polyhalite in 2-mm blebs; 0.5 percent silt. |
| 787.3 - 787.6 | Polyhalite rock, moderate reddish-orange, microcrystalline. |
| 787.6 - 796.8 | Halite rock, moderate orange-pink, 2-cm crystals; 2 percent polyhalite in 2-mm blebs. |
| 796.8 - 796.9 | Polyhalite rock, moderate reddish-orange. |
| 796.9 - 797.1 | Halite rock, moderate reddish-orange; 10 percent polyhalite. |

| Feet | |
|---|---|
| 797.1 - 798.3 | Polyhalite rock, moderate reddish-orange, microcrystalline; 10 percent halite in 1-mm crystals. |
| 798.3 - 808.2 | Halite rock, silty, pale-red, 2-cm crystals; 4 percent silt in 5-mm laminae and 3-mm solution cavities; 4 percent polyhalite in 1-cm masses. |
| 808.2 - 812.7 | Halite rock, greenish-gray to moderate reddish-orange, 5-mm crystals; 2 percent polyhalite in 3-mm blebs and stringers; 0.5 percent silt. |
| 812.7 - 814.1 | Halite rock, greenish-gray; 3 percent silt; 1 percent polyhalite. |
| 814.1 - 818.5 | Halite rock, moderate reddish-orange, 1-cm crystals; 3 percent polyhalite in 1-5 mm blebs and stringers. |
| 818.5 - 818.8 | Polyhalite rock, moderate reddish-orange; 20 percent halite in 1-cm masses. |
| 818.1 - 820.1 | Halite rock, yellowish-gray, 2-cm crystals; 0.5 percent polyhalite. |
| 820.1 - 821.8 | Halite rock, silty, greenish-gray; 10 percent silt; 1 percent polyhalite. |
| 821.8 - 823.8 | Halite rock, silty, light greenish-gray, 2-cm crystals; 2 percent silt; 2 percent polyhalite. |
| 823.8 - 824.8 | Halite rock, moderate orange-pink, 1-cm crystals; 5 percent polyhalite; 0.5 percent silt. |
| 824.8 - 829.4 | Anhydrite rock, light bluish-gray, microcrystalline; 40 percent halite in 2-mm crystals; basal 2 ft has well-developed anhydrite-halite layers about 5 mm thick; basal 0.2 ft is pure anhydrite. |

| Feet | |
|---|---|
| 829.4 - 829.7 | Claystone, light bluish-gray. |
| 829.7 - 830.8 | Halite rock, yellowish-gray, 3-cm crystals. |
| 830.8 - 831.3 | Halite rock, silty, greenish-gray; 3 percent silt. |
| 831.3 - 833.7 | Halite rock, grayish-orange; 3 percent polyhalite in 2-cm masses; 0.5 percent silt. |
| 833.7 - 833.9 | Polyhalite rock, moderate reddish-orange; 20 percent anhydrite; 20 percent halite; polyhalite has botryoidal replacement boundary with the anhydrite. |
| 833.9 - 835.3 | Halite rock, grayish-orange, 2-cm crystals; 5 percent polyhalite in 1-cm blebs. |
| 835.3 - 835.7 | Polyhalite rock, moderate reddish-orange, microcrystalline. |
| 835.7 - 836.2 | Halite rock, greenish-gray; 10 percent polyhalite; 10 percent anhydrite. |
| 836.2 - 837.4 | Anhydrite rock, light bluish-gray; 10 percent halite in 1-20 mm masses. |
| 837.4 - 837.7 | Halite rock, light greenish-gray. |
| 837.7 - 837.8 | Anhydrite rock, light bluish-gray; 40 percent halite. |
| 837.8 - 838.7 | Halite rock, grayish-orange; 2 percent polyhalite. |
| 838.7 - 839.0 | Anhydrite rock, light bluish-gray; 40 percent halite. |
| 839.0 - 840.0 | Halite rock, light-gray, 2-cm crystals. |
| 840.0 - 845.8 | Anhydrite rock, light bluish-gray; upper 0.5 ft has 40 percent halite in 1-cm crystals, remainder has about 10 percent halite in 2-mm crystals. |
| 845.8 - 846.1 | Halite rock, silty, greenish-gray; 10 percent anhydrite; 3 percent silt. |

| Feet | |
|---|---|
| 846.1 - 853.1 | Halite rock, yellowish-gray, 1-cm crystals; 1 percent polyhalite. |
| 853.1 - 854.0 | Halite rock, silty, greenish-gray; 4 percent silt; 2 percent polyhalite. |
| 854.0 - 855.3 | Halite rock, silty, greenish-gray; 25 percent silt; 1 percent polyhalite. |
| 855.3 - 857.4 | Halite rock, moderate reddish-orange; 5 percent polyhalite in 2-mm blebs. |
| 857.4 - 858.2 | Siltstone, pale reddish-brown; 30 percent halite. |
| 858.2 - 859.4 | Halite rock, silty, greenish-gray; 4 percent silt. |
| 859.4 - 878.7 | Halite rock, light greenish-gray to moderate orange-pink, 2-cm crystals; 2 percent polyhalite in 3-mm blebs. |
| 878.7 - 880.6 | Halite rock, moderate reddish-orange; 5 percent polyhalite. |
| 880.6 - 883.2 | Halite rock, silty, greenish-gray to pale-red; 10 percent silt; 2 percent polyhalite. |
| 883.2 - 883.6 | Siltstone, clayey, grayish-red; 10 percent halite; plastic. |
| 883.6 - 884.9 | Halite rock, silty, pale-red; 10 percent silt. |
| 884.9 - 887.9 | Halite rock, silty, pale-red; 3 percent silt; 3 percent polyhalite. |
| 887.9 - 888.5 | Halite rock, moderate orange-pink; 3 percent polyhalite. |
| 888.5 - 889.7 | Polyhalite rock, moderate reddish-orange, microcrystalline. |
| 889.7 - 897.0 | Halite rock, grayish-orange, 1-cm crystals. |
| 897.0 - 897.1 | Polyhalite rock, moderate orange-pink. |
| 897.1 - 899.0 | Halite rock, moderate orange-pink. |
| 899.0 - 899.5 | Polyhalite rock, moderate orange-pink. |

| Feet | |
|---|---|
| 899.5 - 903.0 | Halite rock, moderate orange-pink, 1-cm crystals; 0.5 percent polyhalite. |
| 903.0 - 904.1 | Halite rock, silty, greenish-gray; 2 percent silt. |
| 904.1 - 905.1 | Siltstone, clayey, grayish-red, plastic; 20 percent halite in 1-cm crystals. |
| 905.1 - 906.0 | Halite rock, moderate orange-pink; 2 percent polyhalite. |
| 906.0 - 907.4 | Halite rock, silty, pale-red; 5 percent silt; 2 percent polyhalite. |
| 907.4 - 914.6 | Halite rock, light greenish-gray, 1-cm crystals; 0.5 percent silt; 0.5 percent polyhalite. |
| 914.6 - 916.7 | Halite rock, moderate orange-pink; 1-cm crystals; 5 percent polyhalite. |
| 916.7 - 917.5 | Polyhalite rock, moderate reddish-orange, microcrystalline; 10 percent halite in 3-mm blebs. |
| 917.5 - 917.6 | Claystone, greenish-gray, plastic. |
| 917.6 - 931.7 | Halite rock, grayish-orange to greenish-gray, 2-cm crystals; 2 percent polyhalite. |
| 931.7 - 931.8 | Polyhalite rock, moderate reddish-orange. |
| 931.8 - 932.0 | Halite rock, grayish-orange. |
| 932.0 - 932.1 | Polyhalite rock, moderate reddish-orange. |
| 932.1 - 936.8 | Halite rock, silty, greenish-gray to pale-red, 2-cm crystals; 4 percent clay in 2-mm solution cavities; 2 percent polyhalite in 1-5 mm blebs and stringers. |
| 936.8 - 944.4 | Halite rock, very pale-orange, 2-cm crystals; 1 percent polyhalite. |

| Feet | |
|---|---|
| 944.4 - 946.2 | Polyhalite rock, moderate reddish-orange, microcrystalline; lower 1.4 ft has 30 percent halite in 1-mm crystals. |
| 946.2 - 956.3 | Halite rock, moderate orange-pink, 1-cm crystals; 3 percent polyhalite in 2-mm laminae and stringers. |
| 956.3 - 956.6 | Polyhalite rock, moderate-red. |
| 956.6 - 956.8 | Anhydrite rock, yellowish-gray, 2-mm laminae. |
| 956.8 - 957.1 | Polyhalite rock, moderate reddish-orange; 40 percent greenish-gray clay. |
| 957.1 - 959.5 | Halite rock, greenish-gray to moderate orange-pink; 1 percent polyhalite in 1-mm blebs. |
| 959.5 - 962.5 | Halite rock, silty, greenish-gray to pale-red; 10 percent silt. |
| 962.5 - 967.0 | Halite rock, greenish-gray to moderate orange-pink, 1-cm crystals; 2 percent polyhalite; 0.5 percent silt. |
| 967.0 - 968.4 | Anhydrite rock, light bluish-gray; 20 percent halite in 2-mm irregular layers; top 0.5 ft has 30 percent polyhalite. |
| 968.4 - 968.6 | Halite rock, grayish-orange. |
| 968.6 - 968.7 | Polyhalite rock, moderate reddish-orange. |
| 968.7 - 968.9 | Halite rock, grayish-orange. |
| 968.9 - 969.0 | Polyhalite rock, moderate reddish-orange. |
| 969.0 - 970.0 | Halite rock, grayish-orange; 2 percent polyhalite. |
| 970.0 - 970.2 | Polyhalite rock, pale-red. |
| 970.2 - 972.9 | Halite rock, grayish-orange, 1-cm crystals; 3 percent polyhalite. |
| 972.9 - 973.3 | Polyhalite rock, moderate reddish-orange, microcrystalline; 10 percent halite in 1-cm blebs. |

| Feet | |
|---|---|
| 973.3 - 974.7 | Anhydrite rock, light bluish-gray; 10 percent halite in 5-mm crystals. |
| 974.7 - 976.2 | Halite rock, grayish-orange; 0.5 percent polyhalite. |
| 976.2 - 976.3 | Polyhalite rock, moderate orange-pink. |
| 976.3 - 983.2 | Halite rock, grayish-orange to greenish-gray, 1-cm crystals; 1 percent polyhalite in 2-mm blebs. |
| 983.2 - 983.3 | Polyhalite rock, grayish-orange. |
| 983.3 - 984.3 | Halite rock, yellowish-gray; 0.5 percent polyhalite. |
| 984.3 - 984.4 | Polyhalite rock, moderate orange-pink; 50 percent halite in 1-cm masses. |
| 984.4 - 986.3 | Halite rock, yellowish-gray; 3 percent polyhalite in 3-mm blebs. |
| 986.3 - 986.6 | Polyhalite rock, moderate orange-pink; 40 percent halite in 1-cm masses. |
| 986.6 - 989.8 | Halite rock, silty, pale-red to greenish-gray; 10 percent silt in 3-mm blebs. |
| 989.8 - 993.8 | Halite rock, yellowish-gray to moderate orange-pink; 1 percent polyhalite; upper 2 ft has 1 percent silt. |
| 993.8 - 994.0 | Polyhalite rock, moderate reddish-orange. |
| 994.0 - 997.0 | Halite rock, silty, grayish-orange to greenish-gray; 2 percent silt in 2-mm blebs; 1 percent polyhalite; upper 0.6 ft has 20 percent clay, 5 percent polyhalite; unit grades into unit below. |
| 997.0 - 1005.8 | Halite rock, grayish-orange to white, 2-10 cm crystals; basal 0.8 ft has 5 percent polyhalite in stringers. |

| Feet | |
|---|---|
| 1005.8 - 1008.8 | Polyhalite rock, grayish orange-pink; upper 0.5 ft has 50 percent halite; basal 0.4 ft has 50 percent anhydrite. |
| 1008.8 - 1010.9 | Anhydrite rock, light bluish-gray; 1 percent halite in 2-mm crystals; basal 0.3 ft has 10 percent silt. |
| 1010.9 - 1011.0 | Polyhalite rock, very pale orange; 25 percent halite in 1-cm masses. |
| 1011.0 - 1014.1 | Halite rock, moderate reddish-orange; 1 percent polyhalite in 2-mm blebs. |
| 1014.1 - 1015.8 | Polyhalite rock, moderate reddish-orange; laminations 1 cm thick. |
| 1015.8 - 1023.6 | Halite rock, greenish-gray to grayish-orange; 1 percent polyhalite. |
| 1023.6 - 1026.5 | Halite rock, silty, light-brown; 5 percent silt. |
| 1026.5 - 1030.4 | Sandstone, very fine grained, silty, moderate-brown, friable; upper 0.7 ft has 20 percent halite; lower 1.6 ft has 50 percent halite. (Vaca Triste sandstone member.) |
| 1030.4 - 1032.5 | Halite rock, sandy, moderate-brown to greenish-gray; 10 percent sand; 2 percent polyhalite. |
| 1032.5 - 1046.9 | Halite rock, moderate reddish-orange to white, 2-10 cm crystals; 1 percent polyhalite. |
| 1046.9 - 1048.5 | Halite rock, silty, greenish-gray to pale-red; 4 percent silt. |
| 1048.5 - 1059.6 | Halite rock, yellowish-gray to moderate reddish-orange, 2-10 cm crystals; 1 percent polyhalite. |
| 1059.6 - 1061.0 | Halite rock, silty, pale-red; 10 percent clay. |

| Feet | |
|---|---|
| 1061.0 - 1061.1 | Siltstone, clayey, grayish-red, plastic. |
| 1061.1 - 1063.2 | Halite rock, moderate orange-pink; 2 percent polyhalite; 0.5 percent clay. |
| 1063.2 - 1065.3 | Halite rock, silty, pale-red to greenish-gray; 3 percent silt; 2 percent polyhalite. |
| 1065.3 - 1066.5 | Halite rock, moderate orange-pink; 1 percent polyhalite. |
| 1066.5 - 1066.8 | Polyhalite rock, moderate reddish-orange, microcrystalline; 10 percent halite in 3-mm blebs. |
| 1066.8 - 1067.3 | Halite rock, silty, greenish-gray; 5 percent silt. |
| 1067.3 - 1070.1 | Halite rock, moderate reddish-orange, 1-cm crystals; 1 percent polyhalite. |
| 1070.1 - 1072.0 | Siltstone, sandy, moderate-brown; 10 percent halite in 3-mm crystals. |
| 1072.0 - 1074.8 | Halite rock, silty, pale-brown; 4 percent silt. |
| 1074.8 - 1086.1 | Halite rock, greenish-gray to moderate reddish-orange, 1-2 cm crystals; 2 percent polyhalite in 1-4 mm blebs and stringers; 0.5 percent silt. |
| 1086.1 - 1091.2 | Halite rock, silty, pale-red, 2-cm crystals; 5 percent silt. |
| 1091.2 - 1098.2 | Halite rock, grayish-orange to greenish-gray, 1-2 cm crystals; 3 percent polyhalite; 0.5 percent silt. |
| 1098.2 - 1100.5 | Polyhalite rock, moderate reddish-orange, microcrystalline; upper 0.6 ft has 40 percent halite. |
| 1100.5 - 1111.9 | Halite rock, yllowish-gray to grayish-orange, 2-cm crystals; 0.5 percent polyhalite. |

| Feet | |
|---|---|
| 1111.9 - 1115.3 | Halite rock, silty, pale-red, 2-cm crystals; 5 percent silt. |
| 1115.3 - 1119.2 | Halite rock, moderate reddish-orange; 2 percent polyhalite. |
| 1119.2 - 1120.0 | Halite rock, silty, greenish-gray; 4 percent silt. |
| 1120.0 - 1122.0 | Halite rock, grayish-orange, 1-cm crystals; 0.5 percent polyhalite. |
| 1122.0 - 1122.4 | Polyhalite rock, moderate orange-pink; 40 percent halite in 5-mm blebs. |
| 1122.4 - 1123.3 | Halite rock, yellowish-gray; 20 percent anhydrite in 3-mm irregular laminae and blebs. |
| 1123.3 - 1125.5 | Anhydrite rock, light greenish-gray, microcrystalline; 20 percent polyhalite in 5-cm replacement masses; 10 percent halite in 3-mm crystals. |
| 1125.5 - 1125.9 | Polyhalite rock, moderate orange-pink. |
| 1125.9 - 1126.0 | Anhydrite rock, light greenish-gray. |
| 1126.0 - 1127.5 | Halite rock, grayish-orange; 1 percent polyhalite. |
| 1127.5 - 1127.7 | Polyhalite rock, moderate orange-pink. |
| 1127.7 - 1129.0 | Halite rock, grayish-orange, 5-mm crystals; 1 percent polyhalite. |
| 1129.0 - 1129.5 | Polyhalite rock, moderate orange-pink. |
| 1129.5 - 1132.7 | Halite rock, moderate reddish-orange, 1-cm crystals; 1 percent polyhalite. |
| 1132.7 - 1135.7 | Halite rock, silty, grayish-red; 10 percent silt. |
| 1135.7 - 1137.0 | Halite rock, silty, grayish-red to greenish-gray; 3 percent silt. |

| Feet | |
|---|---|
| 1137.0 - 1137.6 | Halite rock, moderate reddish-orange; 1 percent polyhalite in 1-mm blebs. |
| 1137.6 - 1138.5 | Halite rock, silty, light greenish-gray; 4 percent silt; 1 percent polyhalite. |
| 1138.5 - 1153.2 | Halite rock, grayish-orange, 1-cm crystals; 3 percent polyhalite in 2-mm layers 10 cm apart. |
| 1153.2 - 1153.3 | Polyhalite rock, grayish-orange. |
| 1153.3 - 1157.7 | Halite rock, grayish-orange to moderate reddish-orange; 1 percent polyhalite in 1-mm laminae. |
| 1157.7 - 1157.8 | Polyhalite rock, moderate reddish-orange. |
| 1157.8 - 1158.0 | Halite rock, moderate reddish-orange. |
| 1158.0 - 1158.4 | Polyhalite rock, moderate reddish-orange. |
| 1158.4 - 1158.6 | Siltstone clayey, dark greenish-gray. |
| 1158.6 - 1159.0 | Polyhalite rock, moderate reddish-orange; 30 percent greenish-gray silt. |
| 1159.0 - 1161.6 | Halite rock, moderate reddish-orange to greenish-gray; 2 percent polyhalite; 0.5 percent silt. |
| 1161.6 - 1167.6 | Halite rock, silty, mottled greenish-gray and grayish-orange; 5 percent silt; 5 percent polyhalite. |
| 1167.6 - 1178.0 | Halite rock, yellowish-gray, 2-cm crystals; 1 percent polyhalite. |
| 1178.0 - 1178.1 | Polyhalite rock, moderate orange-pink; 20 percent halite in 2-mm crystals. |
| 1178.1 - 1178.6 | Halite rock, moderate reddish-orange; 2 percent polyhalite. |
| 1178.6 - 1179.7 | Polyhalite rock, moderate orange-pink, microcrystalline. (Marker bed 120.) |

| Feet | |
|---|---|
| 1179.7 - 1180.5 | Halite rock, moderate reddish-orange; 1 percent polyhalite. |
| 1180.5 - 1181.0 | Halite rock, silty, greenish-gray; 5 percent silt; 1 percent polyhalite. |
| 1181.0 - 1187.1 | Halite rock, moderate reddish-orange to greenish-gray, 1-cm crystals; 1 percent polyhalite. |
| 1187.1 - 1189.7 | Halite rock, silty, greenish-gray, 1-cm crystals; 5 percent silt; 2 percent polyhalite. |
| 1189.7 - 1195.2 | Halite rock, grayish-orange; 2 percent polyhalite. |
| 1195.2 - 1195.9 | Polyhalite rock, pale reddish-brown. |
| 1195.9 - 1198.0 | Halite rock, silty pale-red; 2 percent silt; 1 percent polyhalite. |
| 1198.0 - 1208.2 | Halite rock, pale-red to moderate reddish-orange, 1-cm crystals; 2 percent polyhalite in 2-mm blebs and stringers. |
| 1208.2 - 1208.4 | Polyhalite rock, moderate reddish-orange; 20 percent halite in 1-cm blebs. |
| 1208.4 - 1208.7 | Halite rock, moderate reddish-orange. |
| 1208.7 - 1210.4 | Polyhalite rock, moderate reddish-orange, microcrystalline; 10 percent halite in 1-cm blebs. |
| 1210.4 - 1211.6 | Halite rock, silty, pale-red; 4 percent silt; 2 percent polyhalite. |
| 1211.6 - 1219.9 | Halite rock, pale-red, 1-cm crystals; 1 percent polyhalite; 1 percent silt. |
| 1219.9 - 1224.4 | Halite rock, grayish-orange, 3-cm crystals; 0.5 percent polyhalite. |

| Feet | |
|---|---|
| 1224.4 - 1233.6 | Halite rock, silty, pale-red, 1-cm crystals; 4 percent silt; 2 percent polyhalite. |
| 1233.6 - 1239.2 | Halite rock, greenish-gray to moderate reddish-orange; 2 percent polyhalite; 0.5 percent silt; natural gas show at 1239 ft. |
| 1239.2 - 1242.5 | Halite rock, grayish-orange; 2 percent polyhalite in 2-mm blebs. |
| 1242.5 - 1243.3 | Polyhalite rock, moderate orange-pink; 30 percent anhydrite. (With next 4 units is Union bed of local usage.) |
| 1243.3 - 1245.9 | Anhydrite rock, light olive-gray, microcrystalline, massive. |
| 1245.9 - 1246.3 | Polyhalite rock, pale yellowish-brown. |
| 1246.3 - 1258.1 | Anhydrite rock, light bluish-gray; basal 5 ft has 3-mm laminae; 2 percent halite in 5-mm crystals. |
| 1258.1 - 1261.3 | Polyhalite rock, pale reddish-brown, microcrystalline; upper contact gradational. (Base of Union bed of local usage.) |
| 1261.3 - 1261.5 | Siltstone, clayey, greenish-gray, plastic. |
| 1261.5 - 1264.7 | Halite rock, silty, greenish-gray to moderate reddish-orange; 2 percent silt; 3 percent polyhalite. |
| 1264.7 - 1264.8 | Siltstone, clayey, greenish-gray, plastic. |
| 1264.8 - 1266.4 | Halite rock, silty, pale-red; 5 percent silt. |
| 1266.4 - 1267.3 | Halite rock, silty, grayish-red; 25 percent silt. |
| 1267.3 - 1269.3 | Halite rock, pale-red; 2 percent polyhalite; 0.5 percent silt. |

| Feet | |
|---|---|
| 1269.3 - 1270.6 | Halite rock, silty, grayish-red; 4 percent silt; 2 percent polyhalite. |
| 1270.6 - 1285.9 | Halite rock, grayish-orange, 1-cm crystals; 1 percent polyhalite in 1-mm blebs and stringers. |
| 1285.9 - 1286.0 | Siltstone, grayish-red, plastic. |
| 1286.0 - 1287.6 | Halite rock, silty, greenish-gray; 1 percent silt; 1 percent polyhalite. |
| 1287.6 - 1290.7 | Halite rock, grayish-orange; 0.5 percent polyhalite. |
| 1290.7 - 1293.9 | Halite rock, silty, greenish-gray to moderate reddish-orange; 3 percent silt; 1 percent polyhalite. |
| 1293.9 - 1295.6 | Halite rock, moderate orange-pink; 1 percent polyhalite. |
| 1295.6 - 1295.7 | Polyhalite rock, moderate reddish-orange. |
| 1295.7 - 1297.7 | Halite rock, grayish-orange; 1 percent polyhalite. |
| 1297.7 - 1302.1 | Halite rock, silty, pale-red to yellowish-gray, 2-cm crystals; 2 percent silt; 1 percent polyhalite. |
| 1302.1 - 1309.6 | Halite rock, moderate orange-pink, 2-cm crystals; 3 percent anhydrite in 10-mm blebs; 2 percent polyhalite in 1-mm blebs. |
| 1309.6 - 1316.3 | Anhydrite rock, light greenish-gray, microcrystalline; 5 percent halite in 3-mm crystals. |
| 1317.3 - 1317.4 | Polyhalite rock, very pale orange. |
| 1317.4 - 1320.7 | Halite rock, grayish-orange, 1-cm crystals; 1 percent polyhalite. |
| 1320.7 - 1320.8 | Polyhalite rock, very pale orange. |
| 1320.8 - 1322.5 | Halite rock, grayish-orange; 2 percent polyhalite. |

| Feet | |
|---|---|
| 1322.5 - 1331.9 | Anhydrite rock, yellowish-gray; 20 percent polyhalite in irregular 1-cm masses; 5 percent halite in 3-mm crystals. |
| 1331.9 - 1332.5 | Siltstone, light greenish-gray; 40 percent polyhalite in 1-5 mm segregations. |
| 1332.5 - 1333.1 | Siltstone, greenish-gray; has 3-mm vertical halite vein. |
| 1333.1 - 1333.3 | Anhydrite rock, light greenish-gray. |
| 1333.3 - 1333.6 | Polyhalite rock, moderate orange-pink. |
| 1333.6 - 1333.7 | Siltstone, greenish-gray. |
| 1333.7 - 1338.7 | Halite rock, grayish-orange, 2-mm crystals; 0.5 percent polyhalite. |
| 1338.7 - 1341.1 | Halite rock, silty, greenish-gray; 1 percent silt; 1 percent polyhalite. |
| 1341.1 - 1347.3 | Halite rock, moderate orange-pink; 1 percent polyhalite; 0.5 percent silt; natural gas show at 1346 ft. |
| 1347.3 - 1356.5 | Halite rock, white, 1-cm crystals. |
| 1356.5 - 1359.5 | Halite rock, silty, greenish-gray to moderate reddish-orange; 5 percent silt; 1 percent polyhalite. |
| 1359.5 - 1360.1 | Halite rock, silty, pale-red; 5 percent leonite in 1-cm crystals; 3 percent polyhalite; 2 percent silt. |
| 1360.1 - 1362.4 | Halite rock, moderate reddish-orange, 1-cm crystals; 1 percent polyhalite. |
| 1362.4 - 1363.6 | Halite rock, pale-red; 5 percent langbeinite in 2-cm crystals; 1 percent polyhalite. |
| 1363.6 - 1366.9 | Halite rock, grayish-orange, 1-cm crystals; 0.5 percent polyhalite. |

| Feet | |
|---|---|
| 1366.9 - 1368.6 | Halite rock, grayish-orange to moderate reddish-orange, 1-cm crystals; 1 percent langbeinite in 1-mm blebs; 1 percent polyhalite in 1-mm blebs. |
| 1368.6 - 1369.2 | Polyhalite rock, moderate-red; 10 percent halite in 5-mm blebs. |
| 1369.2 - 1370.2 | Halite rock, silty, greenish-gray; 3 percent silt. |
| 1370.2 - 1371.0 | Halite rock, moderate reddish-orange; 3 percent polyhalite. |
| 1371.0 - 1371.1 | Polyhalite rock, moderate orange-pink. |
| 1371.1 - 1371.2 | Halite rock, moderate reddish-orange. |
| 1371.2 - 1371.3 | Polyhalite rock, moderate orange-pink. |
| 1371.3 - 1373.4 | Halite rock, grayish-orange to olive-gray; 2 percent polyhalite. |
| 1373.4 - 1377.7 | Halite rock, yellowish-gray to greenish-gray, 1-cm crystals; 1 percent langbeinite in widely scattered 1-cm crystals; 1 percent polyhalite. |
| 1377.7 - 1385.1 | Halite rock, moderate reddish-orange, 1-cm crystals; 2 percent polyhalite in 1-mm blebs and stringers. |
| 1385.1 - 1386.1 | Halite rock, olive-gray; 5 percent langbeinite in 1-cm crystals. |
| 1386.1 - 1395.7 | Halite rock, grayish-orange, 1-cm crystals; 1 percent polyhalite. |
| 1395.7 - 1397.6 | Halite rock, greenish-gray to moderate reddish-orange; 2 percent leonite in 1-mm blebs; 1 percent polyhalite; 0.5 percent silt; trace langbeinite. |
| 1397.6 - 1399.0 | Halite rock, pale-red; 30 percent leonite in 3-cm masses; 2 percent polyhalite; 0.5 percent silt. |

| Feet | |
|---|---|
| 1399.0 - 1401.2 | Halite rock, silty, pale-red; 3 percent silt; 2 percent leonite; 1 percent polyhalite. |
| 1401.1 - 1402.9 | Halite rock, grayish-orange; 1 percent polyhalite. |
| 1402.9 - 1403.0 | Polyhalite rock, moderate-red. |
| 1403.0 - 1408.4 | Halite rock, grayish-orange, 1-cm crystals; 1 percent polyhalite; 1-cm blebs of leonite at 1407.6 ft and at base. |
| 1408.4 - 1408.8 | Polyhalite rock, moderate reddish-brown. |
| 1408.8 - 1412.2 | Halite rock, grayish-orange; 4-cm bleb of leonite at top. |
| 1412.2 - 1412.6 | Halite rock, silty, pale-red; 10 percent silt; 1 percent polyhalite. |
| 1412.6 - 1415.5 | Halite rock, silty, greenish-gray; 2 percent polyhalite; 1 percent silt. |
| 1415.5 - 1422.2 | Halite rock, pale reddish-orange; 1 percent polyhalite. |
| 1422.2 - 1422.8 | Halite rock, silty, greenish-gray; 3 percent silt. |
| 1422.8 - 1429.6 | Halite rock, grayish-orange, 5-mm crystals. |
| 1429.6 - 1432.5 | Halite rock, moderate reddish-orange; 3 percent polyhalite. |
| 1432.5 - 1434.6 | Halite rock, pale yellowish-brown; 2 percent leonite in 5-mm blebs; 1 percent polyhalite. |
| 1434.6 - 1445.2 | Halite rock, moderate reddish-orange; 2 percent polyhalite. |
| 1445.2 - 1448.0 | Polyhalite rock, moderate-red; 2 percent halite in 1-mm crystals. |
| 1448.0 - 1448.2 | Siltstone, light greenish-gray. |
| 1448.2 - 1458.5 | Halite rock, grayish-orange, 5-mm crystals; 2 percent polyhalite. |

| Feet | |
|---|---|
| 1458.5 - 1461.0 | Halite rock, silty, pale-red; 2 percent silt; 0.5 percent polyhalite. |
| 1461.0 - 1475.2 | Halite rock, grayish-orange; 2 percent polyhalite in 1-4 mm blebs. |
| 1475.2 - 1475.4 | Anhydrite rock, yellowish-gray. |
| 1475.4 - 1476.7 | Halite rock, grayish-orange; 3 percent anhydrite; 1 percent polyhalite. |
| 1476.7 - 1477.6 | Anhydrite rock, yellowish-gray, microcrystalline, massive. |
| 1477.6 - 1477.7 | Siltstone, clayey, greenish-gray, plastic. |
| 1477.7 - 1481.7 | Halite rock, yellowish-gray. |
| 1481.7 - 1481.9 | Anhydrite rock, yellowish-gray; 40 percent halite in 3-mm blebs. |
| 1481.9 - 1482.9 | Halite rock, white. |
| 1482.9 - 1483.5 | Anhydrite rock, light-gray; 10 percent halite. |
| 1483.5 - 1484.5 | Halite rock, grayish-orange; 3 percent polyhalite. |
| 1484.5 - 1487.0 | Polyhalite rock, pale-red to moderate reddish-orange. |
| 1487.0 - 1495.4 | Halite rock, grayish-orange, 5-mm crystals. |
| 1495.4 - 1497.5 | Halite rock, silty, olive-gray; 4 percent silt. |
| 1497.5 - 1499.7 | Halite rock, moderate reddish-orange; 2 percent polyhalite in 2-mm blebs. |
| 1499.7 - 1500.0 | Halite rock, silty, dark greenish-gray; 1 percent silt; 1 percent polyhalite. |

## REFERENCES CITED


Adams, J. E., 1944, Upper Permian Ochoa series of Delaware Basin, West Texas and southeast New Mexico: Am. Assoc. Petroleum Geologists Bull., v. 28, p. 1596-1625.

Ahlen, J. L., and others, 1958, North-south stratigraphic cross-section, Delaware Basin-Northwest Shelf, southeastern New Mexico: Roswell, N. Mex., Roswell Geol. Soc.

Aleksandrov, G. P., and Levchenko, T. F., 1953, K voprosu o soderzkanii broma i ioda v kamennoi soli Zakarpatskogo mestorozhdeniia: Gigiena i Sanit., no. 1, p. 43.

Bates, R. L., 1942, Lateral gradation in the Seven Rivers formation, Rocky Arroyo, Eddy County, New Mexico: Am. Assoc. Petroleum Geologists Bull., v. 26, p. 80-99.

Berg, G., 1929, Vorkommen und Geochemie der mineralischen Rohstoffe: p. 128-129, Leipzig, Akad. Verlagsgesell.

Bischof, G., 1864, Lehrbuch der chemischen und physikalischen Geologie: Bonn, v. 2.

Born, H. J., 1934, Der Bleigehalt der Norddeutchen Salzlager und seine Beziehungen zu radioaktiven Fragen: Chemie der Erde, v. 9, p. 66-87.

Bramkamp, R. A., and Powers, R. W., 1955, Two Persian Gulf lagoons: Jour. Sedimentary Petrology, v. 25, p. 139-140.

Briggs, L. I., 1958, Evaporite facies: Jour. Sedimentary Petrology, v. 28, p. 46-56.

Carpelan, L. H., 1953, The hydrobiology of the Alviso salt ponds: Stanford Univ., PhD. dissert., 197 p.

Chave, K. E., 1960, Evidence on history of sea water from chemistry of deeper subsurface waters of ancient basins: Am. Assoc. Petroleum Geologists Bull., v. 44, p. 357-370.

Clarke, E. de C., and Teichert, C., 1946, Algal structures in a Western Australian salt lake: Am. Jour. Sci., v. 244, p. 271-276.

Clarke, F. W., 1924, The data of geochemistry (5th ed.): U. S. Geol. Survey Bull. 770, 841 p.

Dane, E. G., Jr., 1942, Density at high temperature; thermal expansion: Geol. Soc. America Special Papers, no. 36, p. 27-37.

D'Ans, J., 1933, Die Lösungsgleichgewichte der Systeme der Salze ocean-ischer Salzablagerungen: Berlin, Verlagsgesell. für Ackerbau, 254 p.

D'Ans, J., Bredtschneider, D., Eick, H., and Freund, H. E., 1955, Unter-suchungen über de Calciumsulfate: Kali u. Steinsalz, no. 9, p. 17-38.

D'Ans, J., and Kühn, R., 1940, Über den Bromgehalt von Salzgesteinen der Kalisalzlagerstatten: Kali, v. 34, p. 42-46, 59-64, 77-83.

Darton, N. H., 1899, Geology and water resources of Nebraska west of the one hundred and third meridian: U. S. Geol. Survey 19th Ann. Rept., pt. 4, p. 719-785.

Darwin, C., 1839, Journal of researches into the geology and natural history of the various countries visited by H. M. S. Beagle: London, Henry Colburn, 615 p.

DeFord, R. K., 1939, Discussion: Am. Assoc. Petroleum Geologists Bull., v. 23, p. 1550-1551.

DeFord, R. K., and Riggs, G. D., 1941, Tansill formation, West Texas and southeastern New Mexico: Am. Assoc. Petroleum Geologists Bull., v. 25, p. 1713-1728.

Dellwig, L. F., 1955, Origin of the Salina salt of Michigan: Jour. Sedimentary Petrology, v. 25, p. 83-110.

Gale, H. S., 1914, Prospecting for potash in Death Valley, California: U. S. Geol. Survey Bull. 540, p. 407-415.

Galley, J. E., 1958, Oil and geology in the Permian Basin of Texas and New Mexico: in Weeks, L. G., ed., Habitat of oil: Tulsa, Am. Assoc. Petroleum Geologists, p. 395-446.

Gester, G. C., and Hawley, H. J., 1929, Yates field, Pecos County, Texas: Am. Assoc. Petroleum Geologists, Structure Typical Am. Oil Fields, v. 2, p. 480-499.

Ginsburg, R. N., and Lloyd, R. M., 1956, A manual piston coring device for use in shallow water: Jour. Sedimentary Petrology, v. 26, p. 64-66.

Goldman, M. I., 1952, Deformation, metamorphism, and mineralization in gypsum-anhydrite cap rock, Sulphur Salt Dome, Louisiana: Geol. Soc. America Mem. 50, 169 p.

Goldschmidt, V. M., 1954, Geochemistry: Oxford, Clarendon Press, 730 p.

Goldschmidt, V. M., Krejci-Graf, K., and Wiite, H., 1948, Spuren-Metalle in Sedimenten: Akad. Wiss. Gottingen, Math. Physik. Kl., p. 35-52.

Grabau, A. W., 1920, Principles of salt deposition: New York, McGraw Hill Book Company, 435 p.

Green, J., 1959, Geochemical table of the elements for 1959: Geol. Soc. America Bull., v. 70, p. 1127-1183.

Harvey, H. W., 1955, The chemistry and fertility of sea waters: Cambridge, Cambridge Univ. Press.

Haslam, J., Allberry, E. C., and Moses, G., 1950, The analytical chemistry of bromine manufacture, Part II: The bromine content of the Cheshire salt deposit and of some borehole and other brines: Analyst, v. 75, p. 352-356.

Hayes, P. T., 1957, Geologic map of the Carlsbad Caverns East Quadrangle: U. S. Geol. Survey Geol. Quad. Map, GQ-98.

Herrmann, A. G., 1958, Geochemische Untersuchungen an Kalisalzlagerstätten im Südharz: Freiberger Forschungshefte, ser. C, no. 43, 111 p.

Jander, G., and Busch, F., 1930, Gewinnung von Rubidium- und Cäsium-Präparaten aus Carnallit, II: Zeitschr. anorg. allgem. Chem., v. 187, p. 165.

Jones, C. L., 1954, The occurrence and distribution of potassium minerals in southeastern New Mexico: New Mex. Geol. Soc. Guidebook, 5th Field Conf., p. 107-112.

_____, 1959, Potash deposits in the Carlsbad district, southeastern New Mexico: Geol. Soc. America Bull., v. 70, p. 1625.

Kemény, E., 1941, Uran- und Radiumgehalt von Steinsalz und Sylvin: Akad. Wiss. Wien Sitzungsber., v. 150, Abt. IIa, p. 193-207.

King, P. B., 1948, Geology of the southern Guadalupe Mountains, Texas: U. S. Geol. Survey Prof. Paper 215, 183 p.

_____, 1949, Regional geologic map of parts of Culberson and Hudspeth Counties, Texas: U. S. Geol. Survey Oil and Gas Inv., Prelim. Map 90.

King, R. H., 1947, Sedimentation in Permian Castile sea: Am. Assoc. Petroleum Geologists Bull., v. 31, p. 470-477.

Koritnig, S., 1951, Ein Beitrag zur Geochemie des Fluor (mit besonderer Berücksichtigung der Sedimente): Geochim. Cosmochim. Acta, v. 1, p. 89-116.

Krauskopf, K. B., 1955, Sedimentary deposits of rare metals: Econ. Geology, 50th anniversary volume, pt. 1, p. 411-463.

Krumbein, W. C., and Garrels, R. M., 1952, Origin and classification of chemical sediments in terms of pH and oxidation-reduction potentials: Jour. Geology, v. 60, p. 1-33.

Lane, A. C., 1908, Mine waters: Lake Superior Mining Inst. Proc. v. 13, p. 63-152.

_____, 1945, The evolution of the hydrosphere: Am. Jour. Sci., v. 243-A (Daly vol.), p. 393-398.

Lang, W. B., 1935, Upper Permian formation of Delaware Basin of Texas and New Mexico: Am. Assoc. Petroleum Geologists Bull., v. 19, p. 262-270.

_____, 1938, Geology of the Pecos River between Laguna Grande de la Sal and Pierce Canyon: N. Mex. State Engineer Bienn. Rept., v. 12-13, p. 80-86.

_____, 1942, Basal beds of Salado formation in Fletcher potash core test, near Carlsbad, New Mexico: Am. Assoc. Petroleum Geologists Bull., v. 26, p. 63-79.

_____, 1947, Occurrence of Comanche rocks in Black River Valley, New Mexico: Am. Assoc. Petroleum Geologists Bull., v. 25, p. 1472-1478.

Lietz, J., 1951, Sulfidische Klufterze im Deckgebirge des Salzstockes Reitbrook: Hamburg Geol. Staatsinst. Mitt., no. 20, p. 110-118.

Lloyd, E. R., 1929, Capitan limestone and associated formations of New Mexico and Texas: Am. Assoc. Petroleum Geologists Bull., v. 13, p. 645-658.

Lotze, F., 1957, Steinsalz und Kalisalze: Berlin, Gebrüder Borntraeger, 465 p.

Lowenstam, H. A., 1959, $O^{18}/O^{16}$ ratios and Sr and Mg contents of calcareous skeletons of recent and fossil brachiopods and their bearing on the history of the oceans: in Sears, M., ed., International Oceanographic Congress Preprints: Washington, Am. Assoc. Adv. Sci., p. 71-73.

Macallum, A. B., 1904, The paleochemistry of the ocean in relation to animal and vegetable protoplasm: Royal Canadian Inst. Trans., v. 7, p. 535-562.

Maley, V. C., and Huffington, R. M., 1953, Cenozoic fill and evaporite solution in the Delaware Basin, Texas and New Mexico: Geol. Soc. America Bull., v. 64, p. 539-546.

Marmer, H. A., 1949, Sea level change along the coasts of the United States in recent years: Am. Geophys. Union Trans., v. 30, p. 201-204.

Meinzer, O. E., Renick, B. C., and Bryan, K., 1926, Geology of No. 3 reservoir site of the Carlsbad irrigation project, New Mexico, with reference to water-tightness: U. S. Geol. Survey Water-Supply Paper 580, p. 1-39.

Miller, D. N., Jr., 1957, Authigenic biotite in spheroidal reduction spots, Pierce Canyon redbeds, Texas and New Mexico: Jour. Sedimentary Petrology, v. 27, p. 177-180.

Moore, G. W., and Hayes, P. T., 1958, Evaporite and blackmud deposition at Pupuri Salina, Mexico: Geol. Soc. America Bull., v. 69, p. 1616.

Moore, R. C., 1949, Classification and nomenclature of Permian(?) rocks in the Colorado River Valley, Texas: U. S. Geol. Survey Oil and Gas Inv. (Prelim.) map 80.

Moritz, C. A., 1951, Triassic and Jurassic stratigraphy of southwestern Montana: Am. Assoc. Petroleum Geologists Bull., v. 35, p. 1781-1814.

Morris, R. C., and Dickey, P. A., 1957, Modern evaporite deposition in Peru: Am. Assoc. Petroleum Geologists Bull., v. 41, p. 2467-2474.

Mortensen, H., 1930, Die Wüstenboden: in Blanck, E., ed., Handbuch der Bodenlehre: Berlin, Julius Springer, v. 3, p. 437-490.

Müller, A., and Schwartz, W., 1955, Über das Vorkommen von Mikroorganismen in Salzlagerstätten: Deutschen geol. Gesell. Zeitschr., v. 105, p. 789-802.

Müller, P., and Heymel, W., 1956, Determination of the gas concentration in the gas-occluding salts of the potash mines of the southern Harz and the Werra districts: Bergbautech., v. 6, p. 313-319.

Newell, N. D., Rigby, J. K., Fischer, A. G., Whiteman, A. J., Hickox, J. E., and Bradley, J. S., 1953, The Permian reef complex of the Guadalupe Mountains region, Texas and New Mexico: San Francisco, W. H. Freeman & Co., 236 p.

Ochsenius, C., 1877, Bildung der Steinsalzlager und ihrer Mitterlaugensalze: Halle.

Oriel, S. S., in press, The Ochoa Series and the base of the Triassic system: in McKee, E. D., and others, Paleotectonic maps, Triassic System: U. S. Geol. Survey Misc. Geol. Inv. map.

Page, L. R., and Adams, J. E., 1938, Stratigraphy, eastern Midland Basin, Texas: Am. Assoc. Petroleum Geologists Bull., v. 22, p. 1709.

Peirce, G. J., 1914, The behavior of certain micro-organisms in brine: Carnegie Inst. Washington Pub. 193, p. 49-69.

Phillips, F. C., 1947, Oceanic salt deposits: Quart. Reviews, v. 1, p. 91-111.

Quaide, W., 1958, Clay minerals from salt concentration ponds: Am. Jour. Sci., v. 256, p. 431-437.

Richards, F. A., 1957, Some current aspects of chemical oceanography: Phys. and Chem. of the Earth, v. 2, p. 77-128.

Richardson, G. B., 1904, Report of a reconnaissance in trans-Pecos Texas, north of the Texas and Pacific Railway: Univ. Texas Bull. 23, 119 p.

Rubey, W. W., 1951, Geologic history of sea water: Geol. Soc. America Bull., v. 62, p. 1111-1148.

Runnels, R. T., Reed, A. C., and Schleicher, J. A., 1952, Minor elements in Kansas salt: Kans. Geol. Survey Bull. 96, p. 185-200.

Santos Ruiz, A., Dean Gualbenzu, M., and Lopez de Azcona, J. M., 1952, La investigacion bioquimica de los oligoelementos mediante tecnica espectrografica: IV Cong. Intern. Patologia Comparada, p. 99-139.

Schenck, H. G., and others, 1941, Stratigraphic nomenclature: Am. Assoc. Petroleum Geologists Bull., v. 25, p. 2195-2202.

Scruton, P. C., 1953, Deposition of evaporites: Am. Assoc. Petroleum Geologists Bull., v. 37, p. 2498-2512.

Shaw, D. M., 1952, Geochemistry of thallium: Geochim. Cosmochim. Acta, v. 2, p. 118-154.

Sheldon, V. P., 1954, Oil production from the Guadalupe series in Eddy County, New Mexico: N. Mex. Geol. Soc. Guidebook, 5th Field Conf., p. 150-159.

Sloss, L. L., Krumbein, W. C., and Dapples, E. C., 1949, Integrated facies analysis: Geol. Soc. America Mem. 39, p. 91-123.

Spieker, E. M., 1956, Mountain-building chronology and nature of geologic time scale: Am. Assoc. Petroleum Geologists Bull., v. 40, p. 1769-1815.

Spiro, M. S., 1958, Über die Wege zur Erforschung der Evolution der Weltozeanzusammensetzung: Freiberger Forschungshefte, ser. A, no. 123, p. 236-242.

Taylor, R. E., 1957, Water-insoluble residue in rock salt of Louisiana salt plugs: Am. Assoc. Petroleum Geologists Bull., v. 21, p. 1268-1310.

Thomson, S. J., and Wardle, G., 1954, Coloured natural rock salt: a study of their helium content, colours, and impurities: Geochim. Cosmochim. Acta, v. 5, p. 169-184.

Udden, J. A., 1924, Laminated anhydrite in Texas: Geol. Soc. America Bull., v. 35, p. 347-354.

Usiglio, J., 1849, Analyse de l'eau de la Mediterranee sur les cotes de France: Annal. Chemie, v. 27, p. 92-107, 172-191.

Van't Hoff, J. H., 1912, Untersuchungen über die Bildungsverhältnisse der ozeanischen Salzablagerungen insbesondere des Stassfurter Salzlagers: Leipzig, Akad. Verlagsgesell.

Ver Plank, W. E., 1958, Salt in California: Calif. Div. Mines Bull. 175, 168 p.

Volkov, I. I., and Ostromov, E. A., 1957, Konkretsii sulfida zheleza v otlozheniyakh chernogo morya: Akad. Nauk S.S.S.R. Doklady, v. 116, p. 645-648.

Walter, J. C., 1953, Paleontology of the Rustler formation, Culberson County, Texas: Jour. Paleont., v. 27, p. 679-702.

Washburn, A. L., 1956, Classification of patterned ground and review of suggested origins: Geol. Soc. America Bull., v. 67, p. 823-865.

Yasui, E., and Suzuki, H., 1955, "Kaseisoda", shokuen "burain" narabi ni genryo shokuenchu ni fukumareru biryo fujunbun no bunko-kagakuteki teiryo ni tsuite: Jour. Chem. Soc. Japan, Ind. Chem. Sec., v. 58, p. 170-174.

Zenkevich, L. A., 1957, Caspian and Aral Seas: Geol. Soc. America Mem. 67, v. 1, p. 891-916.

Anonymous, 1956, Geochemistry of iodine: London, Chilean Iodine Educ. Bur., 150 p.

60-99

Figure 20

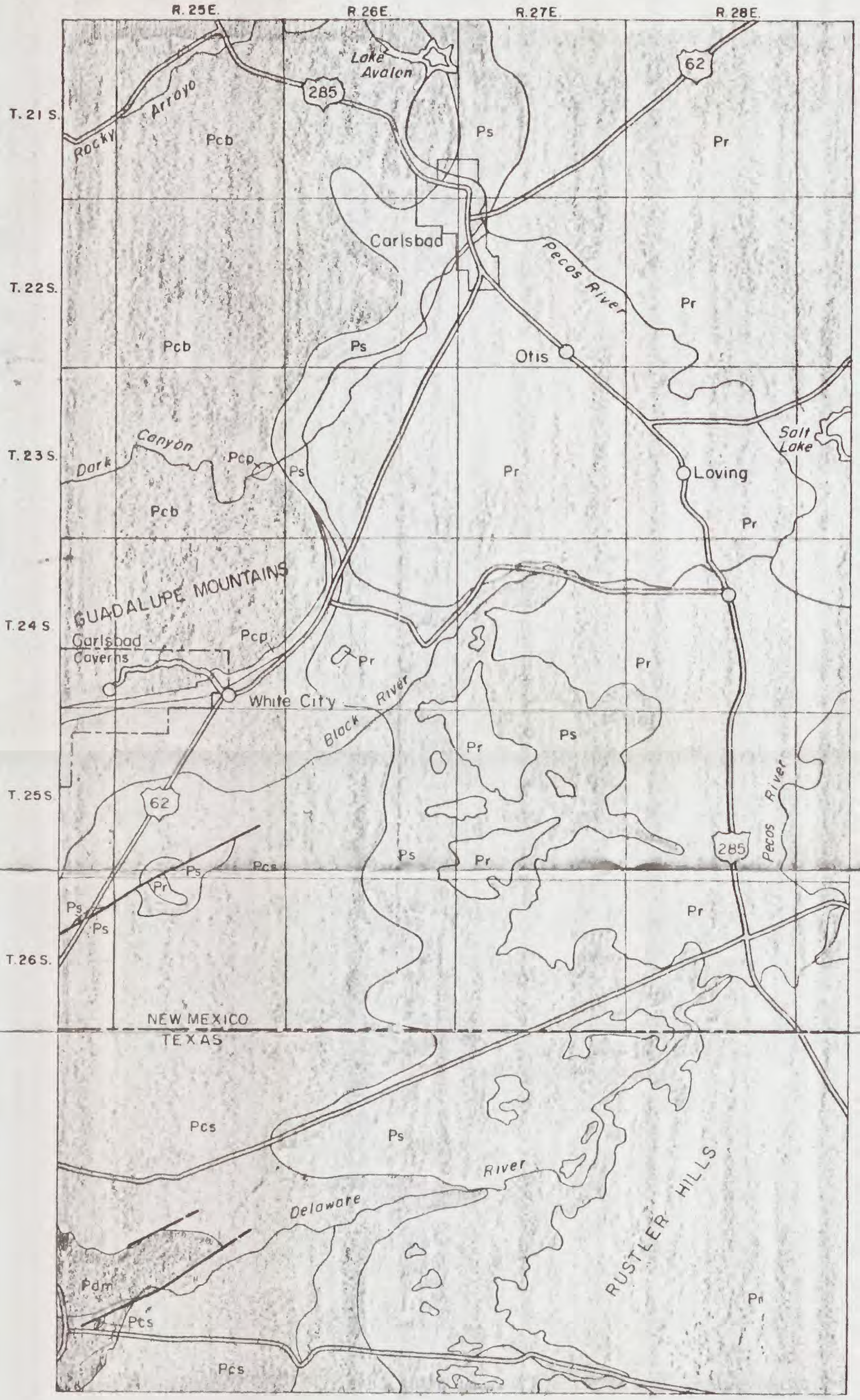


EXPLANATION

GUADALUPE MOUNTAINS AND NORTH

Pr — Rustler formation

Ps — Salado formation

Pcb / Pcp — Carlsbad group, Pcb; Capitan limestone, Pcp

PERMIAN

SOUTH OF GUADALUPE MOUNTAINS

Pr — Rustler formation

Ps — Salado formation

Pcs — Castile formation

Pdm — Delaware Mountain group

PERMIAN

Contact

Fault

0 6 Miles

0 5 10 Kilometers

BEDROCK GEOLOGY OF THE CARLSBAD AREA, NEW MEXICO AND TEXAS

This map is preliminary and has not been edited or reviewed for conformity with U. S. Geological Survey standards and nomenclature.

Figure 23

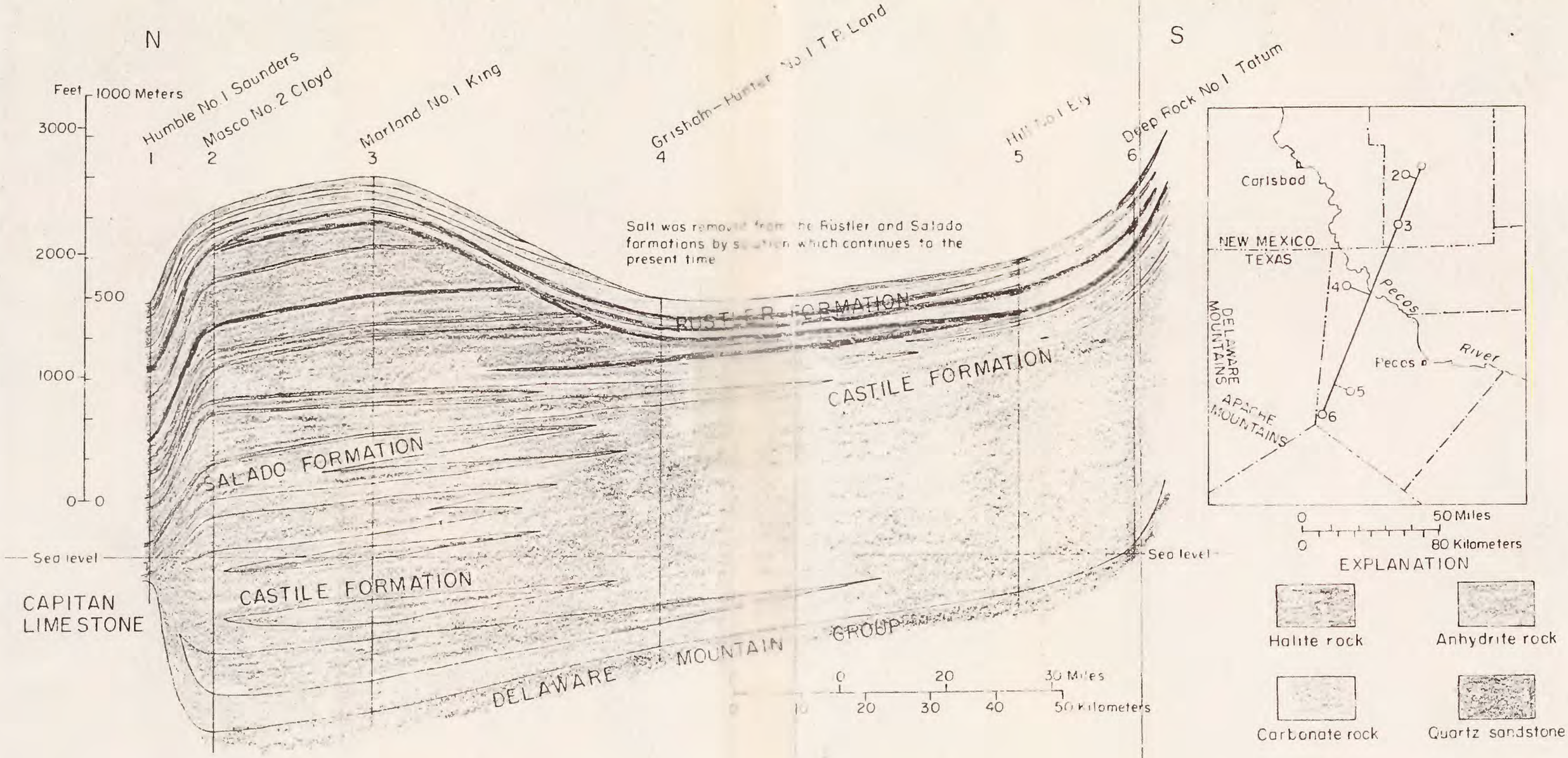


FACIES RELATIONS BETWEEN THE RUSTLER, SALADO, AND CASTILE FORMATIONS, NEW MEXICO AND TEXAS
(well logs from Adams, 1944)

60-99

Figure 9

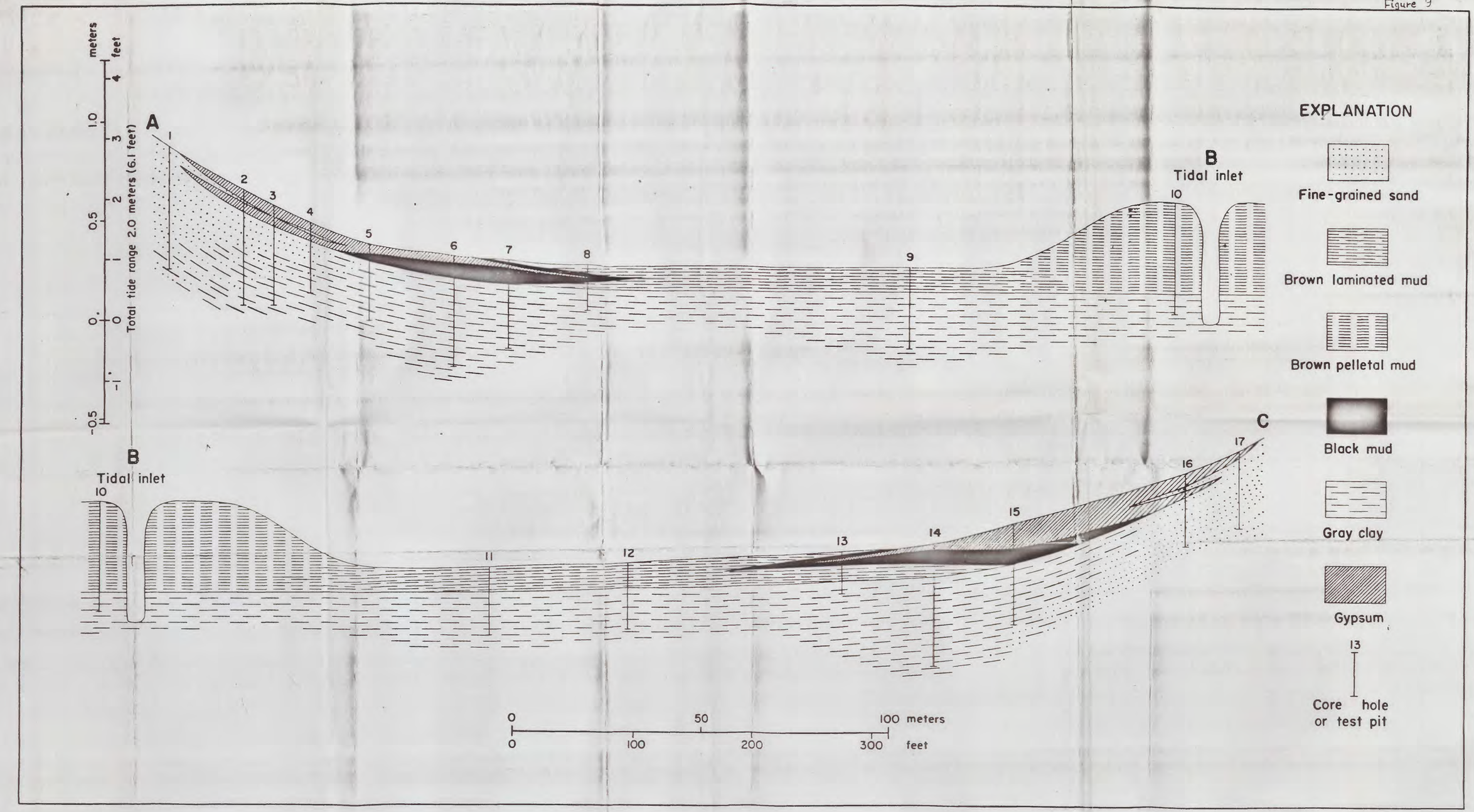


SECTION ACROSS PUPURI SALINA, SINALOA, SHOWING INTERTONGUING BETWEEN EVAPORITE AND CLASTIC DEPOSITS